NASA Technical Memorandum 81969

NASA-TM-81969 19810013510

ANALYTICAL STUDY OF THE CRUISE PERFORMANCE OF A CLASS OF REMOTELY PILOTED, MICROWAVE-POWERED, HIGH-ALTITUDE AIRPLANE PLATFORMS

Charles E. K. Morris, Jr.

April 1981

National Aeronautics and
Space Administration

Langley Research Center
Hampton, Virginia 23665

ANALYTICAL STUDY OF THE CRUISE PERFORMANCE OF A CLASS OF REMOTELY PILOTED, MICROWAVE-POWERED, HIGH-ALTITUDE AIRPLANE PLATFORMS

By

Charles E.K. Morris, Jr.

SUMMARY

The performance of a class of remotely piloted, microwave-powered, high-altitude airplane platforms was studied. Each cycle of the flight profile consists of climb while the vehicle is tracked and powered by a microwave beam, followed by gliding flight back to a minimum altitude. Parameter variations were used to define the effects of changes in the characteristics of the airplane aerodynamics, the power-transmission systems, the propulsion system, and winds.

Results show that wind effects limit the reduction of wing loading and increase of lift coefficient, two effective ways to obtain longer range and endurance for each flight cycle. Calculated climb performance showed strong sensitivity to some power and propulsion parameters. A simplified method of computing gliding endurance was developed.

INTRODUCTION

Remotely piloted vehicles operating at high altitude have been proposed to perform communication or observation tasks for various regions of the Earth's surface (refs. 1 and 2). A remote power supply, such as solar radiation or a microwave beam from a ground station, could give endurance limited only by systems reliability. Applications for such high-altitude aircraft platforms include mapping, resource monitoring, relaying communications, and conducting other tasks currently performed by satellites or manned aircraft.

Long-endurance aerial platforms offer advantages over alternate systems. Endurance of a manned aircraft is limited by fuel storage and human fatigue. Furthermore, the payload and equipment must include provisions for the pilot and his environmental control system. These factors adversely affect cost and complexity. A geosynchronous satellite has long endurance; however, it also has high cost, poor resolution for observation tasks, and constraints for communications tasks because of the extreme range. A satellite operating in a low orbit passes only infrequently and briefly over a given region. Compared to a platform in the upper atmosphere, a low-orbit satellite requires observation systems to have resolutions at least six times as great for equivalent quality of results.

Several types of high-altitude aircraft platforms have been proposed. Lighter-than-air concepts have been considered (ref. 3). Some of the difficulties of operating these vehicles at altitudes of 18 km (60,000 ft) and above

relate to the atmospheric environment. The airships would have to generate lift at air densities less than one-tenth that of sea level (ref. 4), and, according to reference 5, have the capability to fly against winds of up to approximately 50 m/s (100 kt). Airplane configurations using solar power have been discussed in references 6, 7, and 8. The study of reference 8 concludes that improved battery technology and extremely low wing loadings (down to 15 Pa (0.3 lb/ft^2)) would be required. Even so, a solar-powered configuration would be constrained to operate at low latitudes to obtain enough daylight hours and at locations and altitudes with modest wind velocities.

Studies of the design and operation of microwave-powered high-altitude airplane platforms (HAAP) have been reported in references 3 and 9 to 11. The HAAP configurations of all these reports were propeller-powered airplanes operating in the low-wind region near 20 kilometers (66,000 ft) altitude. Rectennae in the wing lower surface receive microwave energy and convert it to direct-current power for electric motors. These studies indicated that the designs were feasible based on the assumption of some extrapolation of existing microwave technology (such as that described in ref. 12).

This study provides predictions of cruise performance for the class of HAAP configurations that use a "linear" mode of flight. (These are described in the feasibility study of reference 10 and the design sensitivity study of reference 10.) In that mode, the flight profile consists of powered climb near a microwave ground station, followed by gliding flight that either returns the vehicle to the same microwave ground station or carries it to another station. Launch and recovery are not addressed in this study. Emphasis is placed on vehicle design and not power transmission.

Analyses of the results of this parametric study define trends that apply to HAAP vehicles within a wide range of sizes and weights. Performance is characterized as a function of altitude at the end of climb, excess energy stored in batteries, range, and endurance for each cycle of the flight profile. Parametric studies are conducted for variations in the aerodynamic characteristics, power-transmission system, propulsion system, flight profile, and winds. A minimum altitude of 18 kilometers (59,000 ft.) was selected for all cases as a probable constraint due to wind.

Operating characteristics of a microwave-powered airplane are sufficiently unconventional to require the development of a new computer program for performance prediction. The program used in this study is documented in Appendix A.

SYMBOLS

Positive senses of some angles, axes and forces are presented in figure 1.

A wing aspect ratio

A_p propeller disk area, m^2

a constant defined in equation (11)

b	wing span, m; also, constant defined in equation (11)
C_D	drag coefficient, D/qs
$C_{D,o}$	profile-drag coefficient
C_L	lift coefficient, L/qs
C_p	propeller-power coefficient, $P_p/\rho n^3 D_p^5$
D	drag, N
D_p	propeller diameter, m
E_s	stored energy, J
E_t	total energy received, J
e	Oswald efficiency factor; also, base of natural logarithms
g	acceleration of gravity, 9.80 m/sec^2 at sea level
h	altitude above sea level, km
h_i	altitude at initiation of glide, km
h_s	altitude at beam intercept point, km
J	propeller advance ratio, V/nD_p
k_a	acceleration correction factor (see eq. (4))
k_r	microwave-beam intensity factor (see eq. (12))
k_w	wind-profile scale factor
L	lift, N
n	propeller rotational speed, revolutions/second
P	maximum power available in beam, W
P_p	power absorbed by the propellers, W
P_r	power available at rectenna, W
q	dynamic pressure, $1/2\ \rho V^2$, N/m^2
R	reference value of radial distance from microwave ground station, km
r	actual radial distance from microwave ground station, km
S	wing area, m^2

T	propeller thrust, N
T_d	degraded propeller thrust, N
t	elapsed time, s
V	true airspeed, m/s
V_e	equivalent airspeed, $V\sqrt{\rho/\rho_o}$, m/s
V_g	ground speed, m/s
V_{tip}	propeller tip speed, m/s
V_w	local horizontal wind speed, m/s
W	vehicle gross weight, N
x	horizontal range, km
x_s	horizontal distance between ground station and beam intercept point, km
z	dummy variable of integration, km (see eq. (B3))
γ	flight path angle, deg
Δ	increment of parameter
η	propeller efficiency factor
θ	microwave-beam/evaluation angle, deg
μ	angle between wind vector and required ground-track vector
ρ	air density, kg/m^3
ρ_o	sea-level air density, 1.255 kg/m^3
	angle between airplane heading and required ground-track vector

Subscripts

c	end of climb
g	end of glide
max	maximum
t	total for one climb and glide cycle

A dot over a symbol denotes differentiation with respect to time. A bar over a symbol denotes an average value.

CONCEPT DESCRIPTION

The remotely piloted, microwave-powered HAAP of this study is based on the concept described in reference 9. Drawings of representative vehicles are shown in figure 2. A baseline configuration and microwave system are described in table I.

The linear mode of flight, used in this study (and those of references 9, 10, and 11) has a two-part cycle. The climb segment begins when a microwave beam begins to track the vehicle and transmit power to it. That power is used to climb and to store energy in batteries for use by the payload, guidance, and control systems. After power transmission terminates, the vehicle begins a long glide that either carries it to another ground station or back to the same station.

The transmission of microwave energy is modeled largely with the assumptions of reference 9. The multi-element retrodirective array or equivalent antenna (ref. 11) transmits a linearly polarized beam that is focused on the rectenna built into the HAAP. The two-dimensional tracking capability of the transmitter constrains the vehicle to fly in a predefined vertical plane over the ground station. The sum of all range-related phenomenon is assumed to attenuate beam intensity as an inverse function of range.

The conceptual design of the vehicle for this study is similar to a powered version of a high-performance sailplane. The payload fraction of 0.3 contains allocations for the observation or communications payload, batteries, and the guidance and control systems. The baseline configuration calls for high aerodynamic efficiency to be achieved with high-aspect-ratio wings and extensive amounts of natural laminar flow. The wing-mounted rectenna uses linear polarization unless otherwise noted. Rectenna-received power below a minimum level for motor starting, or above the power capacity of the motor, is stored in batteries. Power in the range required for propulsion is used by high-efficiency electric motors to drive variable-pitch, constant-speed propellers. During both flight segments, the vehicle remains trimmed at one lift coefficient. Although the propellers stop and fold streamwise when not in use to reduce drag, there is still a small increment in drag during gliding flight.

A more detailed study of HAAP should consider criteria for stability, control, aeroelasticity, reliability, and other factors. The design illustrated in figure 2(b) reflects some concern for reliability by minimizing the number of essential systems. Propulsion is provided by a single propeller. Aerodynamic control is achieved through control surfaces at the end of the tail booms; differential inputs of the horizontal surfaces produce wing twist. This design was examined briefly in an unpublished study which indicated that the two vehicles of figure 2 can have the same performance, control power, and weight. The generalized approach of this study is not constrained by choice of configuration.

ANALYSIS

The evaluation of vehicle performance for a microwave-powered airplane requires mathematical modeling of vehicle motion, atmospheric effects (including wind), power transmission, and propulsion-system characteristics. The development of the equations used in the microwave-HAAP performance program of Appendix A is given in the following sections.

Flight Mechanics

Equations for force balance along the body axes can be developed with the conventions shown in figure 1(a). The associated assumptions are that: thrust and drag act along the same axis; airspeed is adjusted by changing flight-path angle to obtain the required lift; configuration lift coefficient remains constant; and excess thrust is used to climb. The resulting equations are:

$$L - W \cos \gamma = 0 \tag{1}$$

$$T - D - W \sin \gamma - \frac{W}{g} \dot{V} = 0 \tag{2}$$

These equations can be modified to obtain the forms used in the performance program of Appendix A. First, thrust can be described in terms of propeller efficiency as:

$$T = \eta P_p / V \tag{3}$$

The term for the inertial acceleration force can be written as follows:

$$\frac{W}{g} \dot{V} = \frac{W}{g} \frac{dV}{dh} \frac{dh}{dt} = \frac{W}{g} \frac{dV}{dh} V \sin \gamma$$

For sufficiently small incremens of altitude, an acceleration correction factor k_a can be defined as:

$$k_a = \frac{V}{g} \frac{dV}{dh} \approx \frac{V}{g} \frac{\Delta V}{\Delta h} \tag{4}$$

Thus, equation (2) can be rewritten as

$$\eta P_p / V - D - (1 + k_a) W \sin \gamma = 0 \tag{5}$$

An expression for true airspeed, obtained from equation (1) may be written as:

$$V = \sqrt{\frac{W}{S} \frac{2 \cos \gamma}{\rho C_L}} \tag{6}$$

Except for the term $\cos \gamma$, equivalent airspeed is simply the equilibrium airspeed for a given configuration at sea level:

$$V_e = \sqrt{\frac{W}{S}\frac{2}{\rho_0 C_L}} = \sqrt{\frac{\rho}{\rho_0}}\,V \tag{7}$$

The equations for the vehicle trajectory above a flat earth are based on the conventions shown in parts (b) and (c) of figure 1:

$$V \cos\gamma \sin\phi - V_w \sin\mu = 0 \tag{8}$$

$$\dot{x} - V \cos\gamma \cos\phi + V_w \cos\mu = 0 \tag{9}$$

$$\dot{h} - V \sin\gamma = 0 \tag{10}$$

The use of these equations assumes that the airplane heading is automatically adjusted to compensate for the effects of wind. During climb, the resulting flight path must lie in the unique vertical plane swept out by the path of the microwave beam.

Several parameters are functions of altitude. Air density is modeled on the geometric standard atmosphere of reference 4. The ratio of local density to sea-level density is calculated as

$$\rho/\rho_0 = e^{-ah - bh^2} \tag{11}$$

where the exponential coefficients hold constant over a typical altitude increment of two kilometers. As in reference 10, it is assumed that L/D increases with altitude for the operating range of cruise altitudes because of the greater extent of laminar flow. The value of L/D is decremented (as a function of propeller size) for glide because of the drag of the folded propeller.

Power Transmission

The available power at the vehicle rectenna is assumed to be proportional to both range and the angular orientation of the rectenna surface with respect to the beam. Although the beam is considered to be focused, the effects of focusing precision and other factors are represented by a reciprocal relationship with range:

$$P_r \propto (R/r)^{k_r} \tag{12}$$

where R is a reference radial range from the ground station, r is the true radial range, and k_r has a nominal value of 1.0. The power available is assumed to be proportional to the projected area of the rectenna that can be observed from the microwave ground station (eq. 122, vol. 2 of ref. 13). This can be approximated as

$$P_r \propto S \sin(\theta+\gamma) \tag{13}$$

If both transmitter and rectenna use linear polarization, the power transfer can be conservatively approximated as a function of the phase angle between the two units (ref. 14 and eq. 25, vol. 1 of ref. 13):

$$P_r \propto \cos^2\phi \tag{14}$$

If the rectenna or antenna have circular polarization, then the transmission efficiency drops by a factor of one half but remains unaffected by relative ground angle between the antenna and rectenna axes.

All of these power-transmission relationships (expressions 12, 13, and 14) can be combined into one equation. It is convenient to describe power available for storage or propulsion in terms of power per unit weight as:

$$\frac{P}{W}r = \frac{P}{S}\left(\frac{S}{W}\right)\left(\frac{R}{r}\right)^{kr} \sin(\theta+\gamma)\cos^2\phi \tag{15}$$

where P/S is the maximum transmitted power per unit wing area available at the reference range R, W/S is wing loading, and both antenna and rectenna have linear polarization. As used in Appendix A, the equation, in addition, assumes an efficiency factor of 74 percent between the power reaching the rectenna surface and the power delivered to either the propeller shaft or the batteries.

Propulsion

Values of propulsive efficiency (eq. (3)) are determined from the tabulated values of reference 15 and are given as functions of advance ratio J and propeller-power coefficient C_p. These latter quantities can be determined as functions of both calculated and input parameters of the program of Appendix A:

$$J = \frac{\pi V}{V_{tip}} \tag{16}$$

$$C_p = \frac{\pi^4}{8}\left(\frac{P_p}{A_p}\right)\left(\frac{1}{V_{tip}}\right)^3 \tag{17}$$

$$\frac{P_p}{A_p} = \frac{P_p}{W}\left(\frac{W}{S}\right)\frac{S}{A_p} \tag{18}$$

where P_p/W is the power available to the propulsion system. It can be shown that net thrust for any number of propellers can be determined with this method if: A_p is total propeller-disk area; P_p is total power absorbed by the propellers; and all propellers have the same value of both tip speed and power loading (P_p/A_p).

The program of Appendix A imposes both an upper and lower limit on the power-to-weight ratio of equation (18). As shown in the sketch below all energy not used for propulsion is stored.

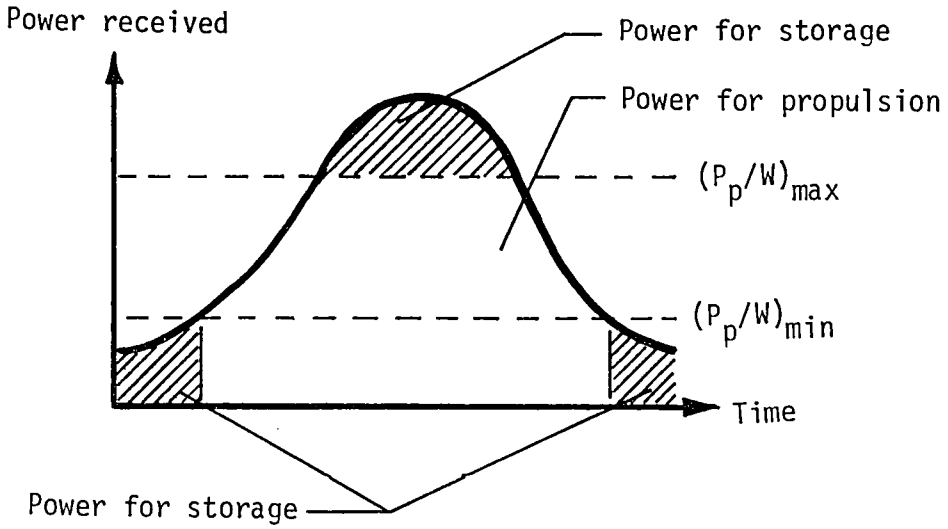

Winds

The model of the wind aloft is based on one set of wind data. This data is the 99 percent profile of reference 5 in figure 3 which describes a wind profile that is exceeded only one percent of the time at five sites in the United States. Figure 3 shows that the profile shifts substantially when the probability of including all winds is decreased from 99 to 95 percent. The second 99 percent profile of figure 3 is based on data from a world-wide set of sites (ref. 16) and indicates that the reference wind profile is reasonable but generally conservative. In the computer program of Appendix A, the magnitude of the wind at a given altitude is the product of the associated value from the reference profile and an amplitude factor k_W. In the program, the direction of the wind vector at any altitude is assumed to remain constant at the same azimuth throughout an entire climb-glide cycle.

DISCUSSION OF RESULTS

The results of calculations of HAAP system performance are presented to show the effect of variations in aerodynamic, power-system, and other parameters. Although not all of the combinations of values represent reasonable systems, the more extreme sets help to define trends. In most cases, the results are compared with the performance of the baseline HAAP system described in Table I. (This baseline system is similar to, but not indentical with, that of reference 9.)

The variety of potential uses for a HAAP system has led to the use of several measures of performance to define results for most sections of this study. Requirements for a nominal ground-track pattern and the availability of sites for ground stations could produce emphasis on long endurance (total time per flight cycle) and zero-wind range. The need for high resolution in

observation tasks and wide-area coverage in communications tasks may produce some differences in the specifications for maximum altitude capability. Wide variations may also occur in the level of stored energy required to operate each payload as well as guidance and control systems. Therefore, the results presented for each parametric variation usually include range, endurance, final climb altitude, and stored energy.

Typical Flights

One cycle of flight is presented in figures 4 and 5 for each of three HAAP configurations with differing wing loadings. The essentially linear flight profile for gliding flight in figure 4 is a direct function of L/D. As shown in figure 5, the climb segment is affected by numerous parameters. The low wing-loading case of $W/S = 50$ Pa (1.0 lbf/ft^2) has a fairly simple calculated history. During climb, the flight path is fairly linear, the rate of climb nearly constant, and the propeller provides thrust all of the time. The highest wing-loading case of $W/S = 250$ Pa (5.2 lbf/ft^2) has an "s-shaped" climb profile (fig. 4) and climb history (fig. 5). Initially, the relatively smaller wing for $W/S = 250$ Pa does not receive enough power to start the motors. The airplane continues to store the received energy and to lose altitude as it glides nearer to the ground station (fig. 5(b)). When it is close enough to receive adequate power, the airplane uses all available power to climb. Near the end of the nominal climb period, the power received again drops below the minimum level. The airplane then glides and stores the received energy again. This latter glide segment illustrates the reasons that h_c can be less than the maximum altitude achieved in climb.

Figure 5 indicates that there are strong relationships between performance, power available, and the flight path (defined with respect to the ground station). Consequently, the flight profile could be changed to maximize stored energy or some other parameter. All subsequent sets of results, however, are obtained for the simple, nominal type of flight at constant lift coefficient.

Equivalent Airspeed

The design value of V_e is important for a HAAP vehicle. As shown in equation (7) and figure 6, V_e is a function of both C_L and W/S. Maximizing L/D to improve range leads to the selection of the highest value of C_L that allows some margin of safety against stall. Requirements for adequate rectenna area and for long endurance (i.e., slow descent rate) can produce design emphasis on low values of W/S. Figure 6 shows that these design trends lead to low values of V_e.

The effect of winds produce constraints on the minimum acceptable level of V_e. Figure 7 presents a wind profile that is exceeded only one-percent of the time at five sites (ref. 5). As indicated in a subsequent discussion on wind effects, this profile can provide a reasonable design criteria for HAAP vehicles that must avoid being blown away from a given site. The data suggests that V_e above 16.6 m/s (32.2 knots) is required if flight profiles extend to

as low as 18 kilometers in altitude. Application of this criteria to the data of figure 6 limits C_L as a function of W/S.

Airplane Aerodynamic Characteristics

The effect of W/S and L/D on HAAP performance are evaluated in figure 8. The parameter W/S also affects the power and propulsion system, since the rectenna is assumed to cover all the wing area S. Thus, decreasing W/S increases available power per unit weight. Large propulsion systems can then operate the propeller continuously at full power during climb. As shown in figure 5, this effect can result in a sustained high rate of climb. Figure 8 shows that reductions in W/S produce substantial improvements in attainable altitude and, below about W/S = 100 Pa, large increases in stored energy. Variations in L/D have relatively less effect on altitude and energy performance than variations in W/S. Range and endurance are both increased by reduced W/S or by increased L/D. (In the case of the baseline HAAP, Reynolds number effects change L/D as a function of altitude; however, the performance in that case can be shown to vary less than one percent from the performance for L/D = 45 and W/S = 100 Pa (2.1 lbf/ft^2).)

The effect of L/D can also be considered in light of the independent effects of C_L and C_D (fig. 9). The value of C_D is assumed to be calculated as

$$C_D = C_{D,o} + C_L^2/\pi Ae$$

The set of $C_{D,o}$ values used provides reasonable agreement between the maximum values of calculated L/D and those obtained from references 17 and 18. The effect of induced drag reduces the level of L/D that results from simply increasing C_L (fig. 9(a)). Both C_L and $C_{D,o}$ appear to have significant effects on range and endurance. All of the trends for changes aerodynamic are in agreement with those determined in reference 11.

Gliding Flight

A simplfied analysis of gliding-flight endurance can be accomplished with an approximate solution to the expression of reference 8 for glide time between specified altitudes. Appendix B presents the development of an expression for a glide-time parameter $t_g V_e$ (D/L) which is independent of configuration.

An approximation for air density as a function of altitude allows the glide-endurance equation to assume integrable form. Figures 10 and 11 provide a means of comparing that the appropriate function with the values given in reference 4. Figure 11 shows that the two density models are in good agreement between 18 and 23 kilometers (59,000 and 75,000 ft), which the is altitude range of interest.

The glide-time parameter can be used to determine the relative endurance achieved by gliding between different sets of initial and final altitudes. Figure 12 presents the glide-time parameter as a function of initial altitude

and altitude decrements. The computed results show that a given decrement of altitude yields a larger glide time at lower altitudes. This occurs because the vehicle travels more slowly through the denser atmosphere at lower altitudes.

Results of gliding-endurance calculations are compared in figures 13 and 14 for the computer program of Appendix A and the closed-form solution of Appendix B. The computer program has the advantage of accounting for acceleration effects and of using a more detailed model of density variation with altitude. The figures show that agreement between the methods is best at low values of W/S, L/D, and h_c. If the acceleration correction factor is removed from the computer program, the computer yields glide times which are virtually identical to those given by the closed-form method of Appendix B.

Power Transmission System

Climb performance is strongly affected by numerous interrelated parameters that characterize the power transmission system. As shown in equation (15) these include P/S, R, and k_r. Parametric variations are considered here even though further development of microwave technology may lead to revisions of equation (15). The review of the present results is simplified by presenting only climb performance since gliding flight has already been treated.

The character of beam-range effects is controlled by the exponent k_r in equation (15). As shown in figure 15, focused power is independent of range at $k_r = 1$. For any value of $k_r > 0$, the equation requires that received power increases indefinitely as r/R approaches 0. In the present study, the values of r/R range from about 0.4 to 1.0, and the effect of k_r does not reach physically implausible proportions for $k_r = 1$. In an real system the transmitter would have a finite value of beam intensity at zero range; beyond a given range some value of k_r would model the beam attentuation. Thus, increases in only k_r imply a disproportionately large increase in actual transmitter power. Due to the large value of R, $r/R \leq 1$ during climb; since the effect of k_r is amplification at those regions, power intensity is always equal to or greater than the reference value P/S.

Climb performance is presented as a function of k_r in figure 16 and several climb histories are presented in figure 17. Increasing k_r appears to allow the value of final climb altitude to increase asymptotically to a maximum and stored energy to increase exponentially. Since $r/R \leq 1$, increasing k_r simply increases available power at the vehicle. The calculated results appear to be opposite to the effects that would be anticipated from an increasing decay of beam intensity with distance; however, the short ranges and the implied large increase in transmitted power overcome the effects of decay rate.

Climb performance is also sensitive to reference range R and the power density at that range P/S. Increasing P/S leads to large increases in stored energy (fig. 18) and allows the vehicle to climb higher. However, as in the case of $(P_p/W)_{max} = 4$ W/N in figure 18, motor size can limit altitude, no matter how much power is received. Similar trends are shown for increasing R in figure 19. Increases in R or P/S are also associated with large increases in transmitted power.

The initial range and altitude for beam intercept also affects climb performance. Figure 20 shows that beam interceptions at longer range permit higher altitudes to be attained. However, the trajectories of these higher flying vehicles can reduce the amount of stored energy per flight cycle due to the attenuation of received power with range. This attenuation and the decrease of density with altitude combine to determine vehicle ceiling. As shown in figure 21, both the rate of climb and the energy storage for the baseline configuration can be estimated to be negligible at an altitude of about 29 km (95,000 ft.).

Propulsion System

The effects of variations in overall propulsion-system efficiency are shown in figure 22. The computer program of Appendix A determines η as a function of J and C_p from a conventional propeller-performance table (ref. 15). This tabulated data does not reflect any effects of high-altitude, low Reynolds number phenomena on propeller aerodynamics. This omission, and other simplifications, may lead to optimistic predictions of propeller performance. The result of operating with degraded thrust T_d is a nearly linear decrease in attainable altitude (fig. 23). This indicates that even a small degradation in propulsion-system efficiency translates into noticeable performance decreases.

The effect of relative motor size is shown in figure 23. The parameter $(P_p/W)_{max}$ reflects not only the maximum power that the propulsion system can absorb, it also indicates the ratio of motor size to total vehicle weight. The largest value of $(P_p/W)_{max}$ considered here is twice that of the baseline configuration. The computed results show that increasing the relative size of the motor generally leads to decreases in stored energy and to increases in attainable altitude until a maximum performance level is achieved. Beyond that point, increasing $(P_p/W)_{max}$ is detrimental to performance. This variation indicates that the optimization of propulsion parameters is a function of wing loading (and rectenna size).

A review of the calculated flight histories leading to the results of figure 23 reveals that the variation in performance is related to both trajectory characteristics and limits on the minimum power required. The vehicle with the larger motor may have to glide closer to the ground station before receiving enough power to overcome starting loads and other constraints. The more powerful vehicle climbs faster and generally flys a higher trajectory as it passes over the ground station. The more powerful vehicle then reaches the minimum (P_p/W) condition and begins its glide phase sooner. Detailed design of a HAAP will apparently be sensitive to constraints on minimum and maximum motor power.

The effect of two propeller parameters on climb performance is shown in figure 23 and 24. The baseline value of tip speed (172 m/s) appears to be a good selection (fig. 24), although performance appears to be fairly insensitive to small variations in that parameter until the tip speed encounteres compressibility effects. The area ratio S/A_p is a somewhat artificial parameter that is a convenient element in equation (18). That measure of relative propeller size is also set at a good value in the baseline configuration ($S/Ap = 2.65$).

Winds Aloft

Although winds aloft can greatly influence the success of any given mission, wind effects on HAAP design are difficult to quantify. The statistical nature of basic wind data (refs. 5, 16, and 19) must be properly evaluated to avoid developing excessively stringent design criteria. Wind profiles that are exceeded only one percent of the time probably provide adequate design guidelines. The winds that exceed those limits tend to be associated with large storms occurring at lower altitudes. These more detectible, lower-altitude phenomon may provide enough warning to make appropriate changes in the flight program, such as maintaining as much altitude as possible. In addition, the relationships of wind direction at different altitudes are not considered in most sources of data. Nonuniformity of wind direction at different altitudes may make HAAP operations easier than predicted for uniform wind direction.

Operational limits imposed by winds tend to affect HAAP operations at lower altitudes. Figure 7 shows that for $V_e \geq 10$ m/s (19 kt), the selection of a design value of V_e for lower altitudes will ensure an adequate margin of true airspeed V at higher altitudes. Thus, operations need not be restricted to the nominal low-wind region of about 20 kilometers (66,000 ft).

HAAP operations with actual real-time wind profiles will be more complex than for the flight trajectories considered in this study. Profiles for mean wind values from reference 19 show consistent trends with altitude of different seasons in figure 26(a); however, the associated data of figure 26(b) show there is a considerable variation possible between the mean and instantaneous values. Below 18 kilometers altitude, the mean winds blow predominately from west to east, although the instantaneous value appears to vary considerably (fig. 26(b)). Data from references 16 and 19 clearly indicate that winds at 18 kilometers and above are typically much stronger in winter. Despite the evidence of complexity, this study models winds on the basis of the profile shown in figure 7 and on the assumption of uniform wind direction. The wind-profile scale factor k_W affects only the magnitude of the nominal profile (ref. 5); k_W does not directly reflect the probability level of encountering that profile.

Studies were conducted of the effect of wind-profile magnitude and wind direction relative to required ground track. The first cases to be considered are those for the baseline HAAP configuration with a headwind or tailwind over the nominal ground track (fig. 27). Increases in wind-profile magnitude for a headwind ($\mu = 0^o$) reduce groundspeed and increase the amount of time spent in passing over the ground station. The additional energy available through the extended climb period produces substantial increases in attainable altitude; however, the headwinds affect the glide for a longer period of time and can substantially reduce total range. The reverse relationships appear true for tailwinds. The data for $\mu = 0^o$ terminates at $k_W = 0.97$ because headwinds at 18 kilometers, the initial altitude, can become no stronger without blowing the vehicles away from the ground station.

As shown in figure 1(c), adjustments to vehicle heading can cause the vector summation of wind and airspeed velocities to produce the desired ground track

for the HAAP (for sufficiently low wind speeds). However, if the vehicle rectenna is not exactly aligned with the transmitting antenna, the use of linear polarization will result in a reduction in power-transmission efficiency (eq. (14)). The effect of parametric variations in wind conditions is shown in figure 28. As in figure 27, the absence of calculated results for a given condition indicates that the baseline HAAP configuration could not fly in those winds. Typical performance near to limiting conditions is shown in figure 28(a) for $\mu = 45^0$ and $k_w = 0.74$. As winds approach limiting conditions, the vehicle spends a large part of its climb time in slowly making headway at the lowest altitudes (near 18 kilometers); power storage increases significantly, but final altitude decreases. Figure 28 shows that as amplitude of the wind profile increases, only tailwinds permit flight. In all cases, the unsuccessful attempts at flight were terminated by winds at 18 kilometers blowing the vehicle away from the ground station.

Flight with more severe wind profiles would be possible for all wind directions if the baseline configuration or flight plan were modified. Previously discussed results show that increasing the design value of equivalent airspeed could allow the vehicle to operate in the presence of stronger winds. Another solution would be to increase the value of minimum altitude. As shown in figure 7, the nominal wind profile for this study is more severe at the lower altitudes. Figure 26 shows that such data is representative. An alterante solution would be to accept the cost and complexity of circular polarization, at least for the transmitter. The relative benefits of the last two methods are suggested in figure 29. If stored energy is not a limiting factor, the restriction of the flight profile to higher altitudes appears to offer a simple, viable solution.

Although turbulence and wind shear affect the development on HAAP design criteria, these effects are not considered herein. Some limited data on these phenomena at high altitude are availabe in references 20 and 21.

CONCLUDING REMARKS

A parametric study of performance has been conducted for remotely-piloted, microwave-powered, high-altitude airplane platforms. The nominal flight plan consists of climb and glide cycles: while receiving power, the vehicle climbs and stores excess energy; it then glides back down to a minimum altitude above a microwave ground station.

Calculated results identifed several basic trends. Low values of wing loading and high values of lift coefficient were shown to result in long range, long endurance, and low equivalent airspeed. Wind effects constrain the lower limits of both equivalent airspeed and operating altitude. Calculations also showed that power-transmission and propulsion-system characteristics could strongly affect climb performance. An approximate, closed-form solution was developed to predict gliding endurance.

APPENDIX A

COMPUTER PROGRAM FOR HAAP PERFORMANCE

A computer program has been developed to calculate the performance of a HAAP vehicle. This appendix contains a listing of the program, a sample input file and the corresponding sample set of output listing. The results presented in the output listing can be interpreted with the description of variable names given in Tables II and III.

The program calculations and logic are based on the HAAP operating procedures as described in the main report. The program calculates the flight trajectory and system performance at specified intervals of time. These intervals are 10 seconds for climb and 20 seconds for glide unless the end of climb or glide is approached; at that point, the intervals are adjusted to be one-tenth their previous value. The only configuration change allowed during a given flight is the folding or unfolding of the propellers.

The program yields results for parametric studies. The first set of output information describes initial conditions in terms of the characteristics of the airplane aerodynamics, propeller and power-system variables, wind and trajectory parameters. The listings presented in columns provide histories of performance and flight mechanics. For each run, the input parameter being varied is listed in the first column on the left. Each set of parametric variations may be conducted for performance at a single point (with respect to the ground station), during climb or glide only, or throughout an entire climb and glide cycle.

The sample case included in this appendix illustrates the effect of wind magnitude. Performance is calculated for the baseline configuration HAAP with winds at right angles to the nominal ground ($\mu = 90^{0}$). The required inputs are: N1 = 3, N2 = 10, AMU = 90., SI = 0., SF = 1.0, and SS = 0.2. Results indicate that a full strength wind profile does not allow the vehicle to initiate climb at 18 kilometers.

```
      PROGRAM HAAP (INPUT,OUTPUT,TAPE5=INPUT,TAPE6=OUTPUT)
C
      DIMENSION A(5), BDN(17), BD(17) ,Z(8,20)
C     A- ALPHANUMERIC LABEL, BDN- NAMES OF ELEMENTS OF BASELINE DATA ARRAY
C     BD- BASEINE DATA ARRAY, Z- FINAL OUTPUT ARRAY
C
      COMMON /PAAH/ WOS,CL, BLOD,HLOD, TS,SOAP, POS,RR, POWL,WK, AMU,
     1      XS,HS, POWR,TDOT,HI,RKR, AK,ETA, GAMMA,POW, POWP,POWS, PSID,
     2      R,RLOD, ROC,THETA, VE,VG, VT,PCP, PJ,N4,N5,X,H
      EQUIVALENCE (BD(1),WOS)
C
      NAMELIST/DD/ WOS,CL,BLOD,HLOD,TS,SOAP,POS,RR,POWL,WK,AMU,XS,HS,
     1             SI,SF,SS,N1,N2,N3,N4,TDOT,POWR,HI,RKR
C
      DATA         WOS,CL,BLOD,HLOD,TS,SOAP,POS,RR,POWL,WK,AMU,XS,HS,
     1             SI,SF,SS,N1,N2,N3,N4,TDOT,POWR,HI,RKR/
     2             144.,0.9,36.6,.418,172.,2.653,1.1,50.,8.62,0.0,0.0,
     3             40.,18.0,0.,0.,0.,2,2,50,1,1.0,0.25,25.,1./
C
      DATA BDN/7H    W/S, 6H    CL, 8H   L/D-B, 8H   L/D-H,6H    TS,
     1         8H   S/A-P, 7H    P/S, 6H    RR, 8H   P/W-L, 6H    WK,
     2         6H    MU, 5H   XS, 5H   HS, 9H  P/W M-M, 7H   TDOT,
     3         6H    HI, 6H   PKR/
C
C     BASELINE DATA ARRAY   1.W/S  2.CL  3.L/D-B  4.L/D-H 5.TS  6.S/A-P
C
C                           7.P/S  8.RR  9.P/W-L  10.WK  11.MU  12.XS
C
C                           13.HS   14.POWR   15.TDOT   16.HI   17.RKR
C
C     PARAMETER VARIATION CODE  SI- INITIAL VALUE
C                               SF- FINAL VALUE
C                               SS- STEP INCREMENT (POSITIVE OR NEGATIVE)
C
C     CONTROL CODE  N1-(SINGLE POINT, CLIMB, TOTAL FLIGHT, GLIDE ONLY)
C                   N2-(ELEMENT IN ARRAY BD TO BE VARIED)
C                   N3-(NUMBER OF CALCULATION POINTS PER LISTED LINE)
C                   N4-(RECTENNA POLARIZATION- LINEAR OR CIRCULAR)
C                   N5-(CODE=1 WHEN VG< 0)
C
  100 FORMAT (1H1,5X,5A10// 5X, 14HAIRCRAFT AERO., 7X,9HPROPELLER, 11X,
     1  5HPOWER, 14X,5HWINDS, 9X,11HSTART POINT, 4X,12HVARIABLE SET,
```

```
     2  9X,4HCODE// 5X,4HW/S=,F6.1, 5H N/M2, 6X, 3HTS=,F6.1, 4H M/S,7X,
     3 4HP/S=,F5.2, 6H KW/M2, 4X, 3HWK=,F5.2, 6X, 3HXS=,F6.2, 3H KM, 4X,
     4 6HFIRST=,F8.3, 5X, 3HN1=,I3/  114X,3HN2=,I3/  6X,3HCL=,F5.2, 9X,
     5 6HS/A-P=,F6.3, 12X,3HRR=,F5.1, 3H KM, 7X, 3HMU=,F5.1, 4H DEG, 2X,
     6 3HHS=,F6.2, 3H KM, 4X, 6HFINAL=,F8.3, 5X, 3HN3=,13/ 114X, 3HN4=,
     7 I3/5X,4HL/D=,F5.1, 29X, 8HMAX P/W=,F5.2, 6H KW/KN, 18X, 3HHI=,
     8 F6.2, 3H KM, 4X, 5HSTEP=, F8.3, 6X, // 2X, 7HL/D(H)=,
     9 F6.3,27X,8HMIN P/W=, F4.2, 10H X MAX P/W ///)
 101 FORMAT (5A10)
 111 FORMAT (2X,A10,4X,1HX,6X,1HH,5X,3HR/C,3X,5HP/W-P,2X,5HP/W-S,2X,
    1         5HGAMMA,2X,5HTHETA,4X,1HR,6X,2HVG, 4X,2HVT,5X,3HVEC,5X,
    2         1HT,6X,2HAK,4X, 3HETA, 3X, 2HCP, 4X, 1HJ ,5X, 3HPSI//
    3         16X,2HKM, 5X,2HKM,4X,3HM/S, 4X,3HW/N,4X, 3HW/N,4X,
    4         3HDEG, 4X,3HDEG, 5X,2HKM,4X,3HM/S, 4X,3HM/S, 4X,3HM/S,
    5         4X,3HSEC,29X, 3HDEG //)
 113 FORMAT (2X,F9.5,1X,,6F7.2,F7.1,F7.2,3F7.1,F8.0,2F6.3,2F6.3,F6.1)
 114 FORMAT (5X/)
 115 FORMAT (2X,F9.5,1X, 3F7.2, F21.2, 14X, 3F7.1, F8.0, F8.4)
 200 FORMAT (//2X,A10, 4X,2HXC, 5X,2HHC, 4X,2HTC, 4X,5HE/W-S, 3X,
    1         5HE/W-T, 4X,2HXT, 7X,2HTT// 16X, 2HKM, 5X,2HKM, 4X,2HHR,
    2         4X,4HKJ/N, 4X,4HKJ/N, 5X,2HKM, 7X,2HHR/)
 201 FORMAT (110X,3HTG=, F6.3, 3H HR //)
 202 FORMAT (3X,F8.3,1X,2F7.2,F6.3,2F8.3,2F8.2)
C
C
      GO TO 3
   2  X= 0.0
      H= HS
      IF (N1.EQ.1.OR.N1.EQ.4) GO TO 3
      WRITE (6,200) BDN(N2)
      DO 300 I=1,N
      WRITE (6,202) Z(1,I),Z(2,I),Z(3,I),Z(4,I),Z(5,I),Z(6,I),Z(7,I),
    1               Z(8,I)
 300 CONTINUE
   3  READ (5,101) A
      IF (EOF(5)) 199,4
   4  READ (5,DD)
      WRITE (6,100) A,WDS,TS,PDS,WK,XS,SI,N1, N2, CL,SOAP,RR,AMU,HS,SF,
     2              N3,N4, BLDD,POWL,HI,SS, HLDD,POWR
      N= 0
C
C     N2- PARAMETER FOR VARIATION, CHOSEN FROM ARRAY BD
```

```
      7 WRITE (6,111) BDN(N2)
C       INITIALIZE PARAMETER ---  NEW STARTING POINT IS NEW X OR Y
        N5= 0
        BD(N2)= SI
        GO TO 17
C
     13 Z (2,N)= X
        Z (3,N)= H
        Z (4,N)= TT
        Z (5,N)= EOWS
        Z (6,N)= EOWT
        IF (N1.EQ.3) GO TO 40
C
C       INCREMENT PARAMETER
     14 CONTINUE
        N5= 0
        IF (N1.EQ.3) Z(7,N)= X
        IF (N1.EQ.3) Z(8,N)= TG
        IF (N1.EQ.4) WRITE (6,201) TG
C
C
     16 BD(N2)= BD(N2) +SS
        DELTA= SF -BD(N2)
        IF (SS.GT.0..AND.DELTA.GE.0.) GO TO 17
        IF (SS.LT.0..AND.DELTA.LE.0.) GO TO 17
        GO TO 2
     17 N= N+1
        Z(1,N)= BD(N2)
        GO TO (20,30,30,39) ,N1
C
C       CALCULATE VALUES AT ONE POINT
     20 T= 0.
        X= 0.
        H= HS
        EOWS= 0.
        EOWT= 0.
        GAMMA= 0.
        CALL RCLIMB
        WRITE (6,113) BD(N2), X,H, ROC,POWP, POWS,GAMMA, THETA,R, VG,VT,
       1               VE,T, AK,ETA, PCP,PJ, PSID
        WRITE (6,114)
        GO TO 14
```

```
C
C     CALCULATE TOTAL CLIMB PHASE
   30 NK= 0
      POW1= 0.0
      POWS1= 0.
      GAMMA= 0.
      THETA= 0.0
      T= 0.
      EOWS= 0.
      EOWT= 0.
      RR95= RR* .95
      TT= 0.
      X= 0.0
      H= HS
      TDEL= 10.
      WRITE (6,114)
C
C     N3 - PRINTOUT INCREMENT FOR COMPLETE CLIMB
   31 IF (NK.EQ.N3) NK= 0
      GAMMA= GAMMA/57.2957
   32 CALL RCLIMB
      IF (N5.GE.1) GO TO 14
      IF (R.GT.RR95.AND.THETA.LT.50.) TDEL= 1.
      IF (T.EQ.0.) GO TO 35
      NK= NK+1
C
C     X AND H GIVEN IN KM
   33 X= X +VG*TDEL/1000.
      H= H +ROC*TDEL/1000.
C
C     SPECIFIC-ENERGY INCREMENTS FROM AVERAGED POWER FOR TIME INCREMENT
C     STORED SPECIFIC ENERGY (E/W-S) AND TOTAL UTILIZED SPECIFIC
C     ENERGY (E/W-T) ARE GIVEN IN KJ/N
      EOWS= EOWS +(POWS+POWS1)*TDEL/2000.
      POWS1= POWS
      EOWT= EOWT +(POW +POW1)*TDEL/2000.
      POW1= POW
      IF (R.GT.RR.AND.THETA.LT.90) GO TO 35
      IF (X.LT.0.) GO TO 35
      IF (NK.EQ.N4) GO TO 35
      T= T+TDEL
      GO TO 31
```

```
C     WRITE DATA FOR ONE INCREMENT OF CLIMB OR FINAL CLIMB POINT
   35 CONTINUE
      WRITE (6,113) BD(N2), X,H, ROC,POWP, POWS,GAMMA, THETA,R, VG,VT,
     1                VE,T, AK,ETA, PCP,PJ, PSID
      TT= T/3600.
      T= T+TDEL
      IF (X.LT.0.) GO TO 13
      IF (R.GT.RR.AND.THETA.LT.90) GO TO 13
      GO TO 31
C
C
C     CALCULATE GLIDE PHASE
C
   39 T= 20.
      TDEL= 20.
      X= 0.
      H= HI
   40 NG = 0
      HS101= 1.01* HS
      T= T -TDEL
      PDF= 2.653/SOAP
C     PDF IS PROP DRAG FACTOR-PROPORTIONAL TO RATIO OF DISK AREA TO WING AREA
      TDEL = 20.
      GAMMA= 0.0
   41 GAMMA= GAMMA/57.2957
C
C     BEGIN CALCULATION FOR NEW GAMMA AT NEW ALTITUDE
   42 RLOD= BLOD +HLOD*H
      IF (NG.EQ.N3) NG= 0
C     DECREMENT L/D DUE TO DRAG OF FOLDED PROPELLER
      IF (N1.LT.4) RLOD= RLOD -1.5*PDF
      KK= 0
C
C     ITERATE FOR GAMMA
   43 KK= KK +1
      IF (KK.EQ. 10) GO TO 50
      VE= 1.27775*SQRT (WOS*COS(GAMMA)/CL)
      CALL ALTF (AMU, VE, WK, H, PSI, VT, VG, N5)
      VY= -VT*COS(GAMMA) /RLOD
      CALL ACCEL(VY,H,VG,AMU,VE,WK,GAMMA,AK)
      ROC= VY/(1. +AK)
C     CALCULATE RESULTING CLIMB ANGLE
```

```
                GAMMAC= ASIN(ROC/VT)
                DELG= ABS(GAMMAC-GAMMA)
                IF (DELG.LT..0002) GO TO 50
          C     AJUST CLIMB ANGLE AND REPEAT
  215           GAMMA= GAMMAC
                GO TO 43
             50 NG = NG + 1
          C
          C     X AND H GIVEN IN KM
  220        54 X= X +VG*TDEL/1000.
                H= H +ROC*TDEL/1000.
                T= T + TDEL
                IF (H.LT.HS101) TDEL= 2.
                IF (NG.EQ.N3) GO TO 55
  225           IF (H.GT.HS) GO TO 42
             55 GAMMA= GAMMA*57.2957
          C     WRITE DATA FOR ONE INCREMENT OF GLIDE OR FINAL POINT
                WRITE (6,115) BD(N2),X,H, ROC, GAMMA, VG, VT, VE, T, AK
                IF (H.GT.HS) GO TO 41
  230           TG= T/3600.
                Z(7,N)= X
                Z(8,N)= TG
                GO TO 14
          C
  235      199 STOP
                END
```

```
      C
      C
            SUBROUTINE DENSITY (CH, SIGMA)
      C
      C     CURVE FIT TO 62 ATMOS. FOR CALCULATION OF DENSITY RATIO
      C
      C     INPUT: ALTITUDE IN KM; OUTPUT: DIMENSIONESS DENSITY RATIO (SIGMA)
            DIMENSION DC1(15),DC2(15)
      C
      C     SIGMA= E **(CC1*H +CC2*H**2) WHERE H IS IN KM
      C
            DATA (DC1(I),I=1,15)/.0958554,.0948554,.0955529,.0950089,.0942258,      DC1
           1                     .0942258,.0770834,.0879373,.0962238,.1027082,      DC1
           2                     .1045655,.1107329,.1160101,.1204581,.1243220/      DC1
            DATA (DC2(J),J=1,15)/.117337,.117337,.124898,.133965,.143754,           DC2
           1                     .143754,.307572,.230044,.178253,.142229,           DC2
           2                     .132942,.104908,.082920,.065812,.052013/           DC2
      C
            ICH= 1+ IFIX(CH/2.)
      C
            CC1= DC1(ICH)
            CC2= DC2(ICH)
      C
            IF (CH.LE.11..OR.CH.GE.12.) GO TO 20
            CC1= .0675418
            CC2= .387085
      C
         20 SIGMA= EXP(-CC1*CH -CC2*CH*CH/100.)
            RETURN
            END
```

```
      C
      C
            SUBROUTINE ALTF(AMU,VE,WK,H,PSI,VT,VG,N5)
      C     CALCULATE TRUE AIRSPEED, WINDSPEED, AND GROUNDSPEED - SI UNITS
      C     INPUTS: WIND AZIMUTH, EQUIVALENT AIRSPEED, WIND SCALE FACTOR, AND
      C     ALTITUDE; OUTPUT: GROUND-TRACK OFFSET ANGLE, TRUE AIRSPEED, AND
      C     GROUND SPEED. (ALL SPEEDS IN M/S; ALL ANGLES IN DEGREES.)
      C         FOR WK= 1., RESULTING WIND PROFILE IS FOR 99% INCLUSIVE
      C         PROFILE FOR 5 LAUNCH SITES FROM NASA TM 78118.
      C
        300 FORMAT (4X, 24HWIND SPEED TOO LARGE AT ,F4.1, 4H KM.)
      C
            CALL DENSITY (H,SIGMA)
            VT= VE*(SIGMA)**(-.5)
            IF (H.GE.14.) GO TO 50
            VW= WK*88.
            GO TO 62
         50 IF (H.GE.15.) GO TO 51
            VW= WK* (88. -18.*(H -14.))
            GO TO 62
         51 IF (H.GE.20.) GO TO 52
            VW= WK* (70. -5.8*(H -15.))
            GO TO 62
         52 IF (H.GE.23.) GO TO 53
            VW= WK*41.
            GO TO 62
         53 VW= WK* (41. +4.7778*(H -23.))
         62 SPSI= VW*SIND(AMU)/VT
            IF (SPSI.GE.1.) GO TO 64
            PSI= ASIN(SPSI)
            VG= VT*COS(PSI) -VW*COSD(AMU)
            GO TO 65
         64 WRITE (6,300) H
            N5= 1
         65 CONTINUE
            RETURN
            END
```

```
C
C
      SUBROUTINE PROPCAL (PCP,PJ,ETA)
      DIMENSION PT(15,41)
C     INPUT: PROPELLER POWER COEFFICIENT AND ADVANCE RATIO
C     OUTPUT: PROPELLER EFFICIENCY FACTOR
C     DATA SOURCE: HAM. STD. CHARTS FOR CL-I= 0.3, AF= 80., AND THREE BLADES
C                                                                        J
C     EACH DATA STATEMENT GIVES VALUES OF ETA AS CP, RANGES FROM .0 TO .35
C
      DATA (PT(I, 1),I=1,15)/.0,.74,.66,.57,.48,.42,.37,.33,.28,.24,.22,      .40
     1.19,.17,.16,.14/                                                        .40
      DATA (PT(I, 2),I=1,15)/.0,.78,.71,.61,.54,.47,.41,.36,.32,.28,.24,      .45
     1.22,.19,.175,.16/                                                       .45
      DATA (PT(I, 3),I=1,15)/.0,.80,.76,.66,.58,.52,.45,.41,.35,.31,.27,      .50
     1.24,.22,.19,.18/                                                        .50
      DATA (PT(I, 4),I=1,15)/.0,.83,.80,.71,.62,.56,.49,.45,.39,.35,.30,      .55
     1.27,.24,.22,.19/                                                        .55
      DATA (PT(I, 5),I=1,15)/.0,.84,.82,.75,.67,.60,.54,.48,.43,.38,.33,      .60
     1.29,.26,.24,.22/                                                        .60
      DATA (PT(I, 6),I=1,15)/.0,.85,.84,.78,.70,.63,.57,.52,.46,.41,.37,      .65
     1.32,.28,.25,.24/                                                        .65
      DATA (PT(I, 7),I=1,15)/.0,.87,.86,.80,.73,.67,.61,.55,.50,.44,.40,      .70
     1.35,.31,.28,.25/                                                        .70
      DATA (PT(I, 8),I=1,15)/.0,.88,.87,.82,.76,.70,.64,.59,.53,.47,.43,      .75
     1.38,.34,.30,.28/                                                        .75
      DATA (PT(I, 9),I=1,15)/.0,.88,.88,.84,.78,.73,.67,.62,.57,.52,.46,      .80
     1.40,.37,.34,.29/                                                        .80
      DATA (PT(I,10),I=1,15)/.0,.88,.89,.86,.81,.75,.70,.65,.60,.55,.49,      .85
     1.44,.39,.36,.33/                                                        .85
      DATA (PT(I,11),I=1,15)/.0,.88,.90,.87,.82,.78,.72,.68,.63,.58,.52,      .90
     1.47,.42,.39,.34/                                                        .90
      DATA (PT(I,12),I=1,15)/.0,.87,.90,.88,.84,.80,.75,.70,.65,.61,.56,      .95
     1.5,.45,.41,.38/                                                         .95
      DATA (PT(I,13),I=1,15)/.0,.87,.914,.89,.85,.81,.77,.72,.68,.63,.6,     1.00
     1.54,.48,.45,.40/                                                       1.00
      DATA (PT(I,14),I=1,15)/.0,.86,.913,.9,.87,.83,.78,.74,.7,.66,.62 ,     1.05
     1.56,.51,.47,.44/                                                       1.05
      DATA (PT(I,15),I=1,15)/.0,.85,.915,.901,.88,.84,.8,.76,.72,.68,        1.10
     1 .64,.60,.55,.50,.475/                                                 1.10
      DATA (PT(I,16),I=1,15)/.0,.84,.916,.91,.89,.85,.82,.78,.74,.7,.67,     1.15
     1.62,.575,.54,.49/                                                      1.15
```

```
      DATA (PT(I,17),I=1,15)/.0,.84,.917,.912,.895,.86,.83,.79,.75,.73,
     1 .69,.65,.60,.55,.53/
      DATA (PT(I,18),I=1,15)/.0,.83,.918,.915,.9,.87,.84,.81,.77,.74,.7,
     1.67,.63,.58,.55/
      DATA (PT(I,19),I=1,15)/.0,.82,.917,.916,.902,.88,.85,.82,.79,.75,
     1 .73,.69,.66,.61,.58/
      DATA (PT(I,20),I=1,15)/.0,.8,.916,.92,.91,.89,.86,.83,.8,.77,.74 ,
     1.71,.675,.64,.60/
      DATA (PT(I,21),I=1,15)/.0,.8,.915,.92,.912,.895,.87,.84,.81,.78,
     1 .75,.72,.70,.67,.63/
      DATA (PT(I,22),I=1,15)/.0,.8,.915,.92,.914,.9,.88,.85,.82,.8,.77 ,
     1.74,.71,.68,.65/
      DATA (PT(I,23),I=1,15)/.0,.8,.915,.92,.916,.905,.885,.86,.83,.81,
     1 .78,.75,.73,.70,.67/
      DATA (PT(I,24),I=1,15)/.0,.8,.912,.92,.918,.91,.89,.87,.84,.82,.8,
     1.77,.74,.72,.69/
      DATA (PT(I,25),I=1,15)/.0,.8,.91,.92,.92,.911,.90,.88,.85,.83,.8 ,
     1.78,.755,.73,.70/
      DATA (PT(I,26),I=1,15)/.0,.8,.91,.92,.92,.914,.9,.885,.86,.84,.81,
     1.79,.77,.74,.72/
      DATA (PT(I,27),I=1,15)/.0,.79,.905,.92,.92,.915,.905,.89,.87,.845,
     1 .82,.80,.78,.755,.735/
      DATA (PT(I,28),I=1,15)/.0,.78,.902,.92,.92,.917,.909,.895,.875,
     1 .85,.83,.81,.79,.77,.75/
      DATA (PT(I,29),I=1,15)/.0,.77,.9,.92,.92,.917,.91,.90,.88,.86,.84,
     1.82,.80,.78,.76/
      DATA (PT(I,30),I=1,15)/.0,.77,.9,.917,.92,.92,.913,.903,.89,.87,
     1 .85,.83,.81,.79,.77/
      DATA (PT(I,31),I=1,15)/.0,.76,.89,.915,.92,.92,.915,.907,.893,.88,
     1 .86,.84,.82,.80,.78/
      DATA (PT(I,32),I=1,15)/.0,.75,.88,.914,.92,.92,.916,.909,.895,.88,
     1 .86,.85,.83,.81,.79/
      DATA (PT(I,33),I=1,15)/.0,.74,.87,.911,.92,.92,.917,.912,.9,.89,
     1 .87,.855,.835,.82,.80/
      DATA (PT(I,34),I=1,15)/.0,.72,.86,.91,.92,.92,.919,.914,.903,.89,
     1 .87,.86,.845,.825,.81/
      DATA (PT(I,35),I=1,15)/.0,.7,.86,.905,.919,.92,.92,.915,.908,.9,
     1 .88,.865,.85,.83,.82/
      DATA (PT(I,36),I=1,15)/.0,.7,.85,.9,.917,.92,.92,.917,.91,.9,.89 ,
     1.87,.86,.84,.825/
      DATA (PT(I,37),I=1,15)/.0,.7,.85,.9,.915,.92,.92,.918,.912,.902,
     1 .89,.88,.865,.85,.83/
```

```
      DATA (PT(I,38),I=1,15)/.0,.7,.85,.89,.913,.92,.92,.918,.913,.907,      2.25
     1 .895,.885,.87,.855,.84/                                               2.25
      DATA (PT(I,39),I=1,15)/.0,.7,.84,.88,.911,.92,.92,.918,.915,.908,      2.30
     1 .9 ,.89,.875,.86,.845/                                                2.30
      DATA (PT(I,40),I=1,15)/.0,.7,.83,.88,.91,.918,.92,.918,.915,.91,       2.35
     1 .902,.89,.88,.865,.85/                                                2.35
      DATA (PT(I,41),I=1,15)/.0,.7,.82,.87,.907,.916,.918,.918,.916,         2.40
     1 .912,.905,.895,.885,.87,.86/                                          2.40
C
C     INTERPOLATION OF ETA FROM HAM.-STD TABLES FOR AF=80,B=3,CLI=.3
      RCP= 40.*PCP +1.
      ICP= IFIX(RCP)
      DCP= RCP -FLOAT(ICP)
      RJ= 20.*PJ -7.
      IJ= IFIX(RJ)
      DIJ= RJ -FLOAT(IJ)
C     POINTS A & B AT GIVEN CP VALUE; POINT A AT LOWER J VALUE THAN POINT B
      PTA= (1.-DCP)*PT(ICP,IJ) +PT(ICP+1,IJ)*DCP
      PTB= (1.-DCP)*PT(ICP,IJ+1) +PT(ICP+1,IJ+1)*DCP
      ETA= PTA +(PTB-PTA)*DIJ
      RETURN
      END
```

```
      C
      C
            SUBROUTINE ACCEL (VY,H,VG,AMU,VE,WK,GAMMA,AK,N5)
      C     INPUT: VERTICAL VELOCITY IN M/S, ALTITUDE IN KM, GROUND SPEED
      C     IN M/S, WIND AZIMUTH IN DEG, EQUIVALENT AIRSPEED IN M/S, WIND SCALE
      C     FACTOR, AND FLIGHT PATH ANGLE IN DEG; OUTPUT: ACCELERATION CORRECTION
      C     FACTOR
            IF (VY.LT.0) GO TO 84
            Y1= H+.1
            Y2= H-.1
            GO TO 85
         84 Y1= H-.1
            Y2= H+.1
         85 VAV= SQRT (VY*VY +VG*VG)
            CALL ALTF (AMU,VE,WK,Y1,PSI1,VT1,VG1,N5)
            IF (N5.EQ.1) GO TO 87
            CALL ALTF (AMU,VE,WK,Y2,PSI2,VT2,VG2,N5)
            IF (N5.EQ.1) GO TO 87
            V1= SQRT (VG1**2 +(VT1*SIN(GAMMA))**2)
            V2= SQRT (VG2**2 +(VT2*SIN(GAMMA))**2)
            DELV= V1-V2
            AK= DELV*VAV/1950.
         87 CONTINUE
            RETURN
            END
```

```
      C
      C
            SUBROUTINE RCLIMB
            COMMON /PAAH/ WOS,CL, BLOD,HLOD, TS,SOAP, POS,RR, POWL,WK, AMU,
     1           XS,HS, POWR,TDOT, H1,RKR, AK,ETA, GAMMA,POW, POWP,POWS, PSID,
     2           R,RLOD, ROC,THETA, VE,VG, VT,PCP, PJ,N4,N5,X,H
            DATA C1/ 9.9397/
      C     C1 EQUALS (PI**4 )/(8.(S.L. DENSITY))
      C
      C     BASIC PARAMETERS
            XR= X -XS
            R= SQRT (XR*XR +H*H)
            THETA= ATAN2(H,XR)
            RLOD= BLOD +HLOD*H
            KODE= 1
            KK= 0.0
         60 VE= 1.27775*SQRT(WOS*COS(GAMMA)/CL)
      C     NOTE: VE IS CORRECTED FOR FLIGHT PATH ANGLE, GAMMA
            CALL ALTF (AMU,VE,WK,H,PSI,VT,VG,N5)
            IF (N5.EQ.1) GO TO 90
            CALL DENSITY(H,SIGMA)
      C
      C     CALCULATION OF POWER - RECEIVED,AVAILABLE AND STORED
      C     740 FACTOR IS 1000 W/KW X .74 EFFICIENCY FACTOR
            ANGLE= 3.1415926 -THETA +GAMMA
         70 POW=((RR/R)**RKR)* 740.*(POS/WOS)*SIN(ANGLE)
            IF (N4.EQ.1) POW= POW* (COS(PSI))**2
            KK= KK+1
            IF (KK.GT.10) GO TO 90
            POWERL= POW/POWL
            IF (POWERL.GT.POWR) GO TO 75
      C     KEEP PROP FOLDED AND STORE ALL INCOMING ENERGY
            ETA= 0.0
            POWP= 0.0
            PJ= 0.0
            PCP= 0.0
      C     DECREMENT L/D TO ACCOUNT FOR DRAG OF FOLDED PROPELLERS
            RLOD= RLOD -1.5
            KODE= -1
            POWS= POW
            GO TO 83
         75 DPOW= POW -POWL
```

```
      IF (DPOW)  76,76,77
C     ALL POWER TO PROP
   76 POWP= POW
      POWS= 0.0
      GO TO 78
C     POWER TO PROP AND REMAINDER TO STORAGE
   77 POWP= POWL
      POWS= DPOW
   78 IF (KODE) 79,79,82
   79 RLOD= RLOD +1.5
C
C     CALCULATION OF NONDIMENSIONAL CHARACTERITICS OF PROPELLER
   82 PJ= 3.14159*VT/TS
      POAP=  POWP*WOS* SOAP
      PCP= C1*POAP/(SIGMA*TS**3)
      CALL PROPCAL (PCP,PJ,ETA)
C
C     CALCULATION OF RATE OF CLIMB - THRUST AND DRAG COMPONENTS
C     TDOT IS RATIO OF ACTUAL, DEGRADED THRUST TO THRUST FROM TABLE LOOK-UP
      ETA= ETA*TDOT
   83 VYT= ETA*POWP
      VYD= VT*COS(GAMMA)/RLOD
      VY= VYT-VYD
      CALL ACCEL(VY,H,VG,AMU,VE,WK,GAMMA,AK)
      IF (N5.GE.5) GO TO 90
      ROC= VY/(1.+AK)
C
C     CALCULATE RESULTING CLIMB ANGLE
      GAMMAC= ASIN(ROC/VT)
      DELG= ABS(GAMMAC-GAMMA)
      IF (DELG.LT..001) GO TO 90
C
C     AJUST CLIMB ANGLE AND REPEAT
      GAMMA= GAMMAC
      GO TO 60
C
C     CALCULATION FOR GAMMA (FLIGHT PATH ANGLE) HAS CONVERGED
   90 THETA= THETA*57.2957
      GAMMA= GAMMA*57.2957
      PSID= PSI*57.2958
      RETURN
      END
```

SAMPLE CASE: VARIATION OF WIND-PROFILE MAGNITUDE

AIRCRAFT AERO.	PROPELLER	POWER	WINDS	START POINT	VARIABLE SET		CODE
W/S= 144.0 N/M2	TS= 172.0 M/S	P/S= 1.10 KW/M2	WK= 0.00	XS= 40.00 KM	FIRST=	0.000	N1= 3
CL= .90	S/A-P= 2.653	RR= 50.0 KM	MU= 90.0 DEG	HS= 18.00 KM	FINAL=	1.000	N2= 10
L/D= 36.6		MAX P/W= 8.62 KW/KN		HI= 25.00 KM	STEP=	.200	N3= 50
L/D(H)= .418		MIN P/W= .25 X MAX P/W					N4= 1

WK	X	H	R/C	P/W-P	P/W-S	GAMMA	THETA	R	VG	VT	VEC	T	AK	ETA	CP	J	PSI
	KM	KM	M/S	W/N	W/N	DEG	DEG	KM	M/S	M/S	M/S	SEC					DEG
0.00000	0.00	18.00	.78	2.73	0.00	.85	155.8	43.86	51.3	51.3	16.2	0.	.021	.716	.021	.937	0.0
0.00000	.51	18.01	.78	2.73	0.00	.85	155.8	43.86	51.3	51.3	16.2	10.	.021	.716	.021	.937	0.0
0.00000	27.52	19.89	6.18	8.62	1.95	6.01	123.4	23.75	59.0	59.0	16.1	510.	.029	.889	.086	1.078	0.0
0.00000	60.98	22.79	4.16	6.58	0.00	3.19	48.3	30.44	74.6	74.6	16.1	1010.	.045	.907	.105	1.363	0.0
0.00000	83.61	23.41	.67	2.66	0.00	.54	28.3	49.43	78.7	78.7	16.2	1312.	.051	.902	.047	1.438	0.0
0.00000	84.32	23.41	.60	2.60	0.00	.48	27.9	50.05	78.8	78.8	16.2	1321.	.051	.897	.046	1.439	0.0
0.00000	157.90	21.68	-1.62			-1.35			68.8	68.8	16.2	2321.	-.0394				
0.00000	222.49	20.16	-1.44			-1.36			60.9	60.9	16.2	3321.	-.0301				
0.00000	280.07	18.79	-1.30			-1.36			54.6	54.6	16.2	4321.	-.0239				
0.00000	309.28	18.09	-1.24			-1.37			51.7	51.7	16.2	4871.	-.0211				
0.00000	313.19	18.00	-1.23			-1.37			51.3	51.3	16.2	4947.	-.0212				
.20000	0.00	18.00	.59	2.60	0.00	.65	155.8	43.86	50.2	51.3	16.2	0.	.022	.681	.020	.937	11.8
.20000	.50	18.01	.59	2.60	0.00	.65	155.8	43.86	50.2	51.3	16.2	10.	.022	.681	.020	.937	11.8
.20000	26.93	19.78	6.19	8.62	1.51	6.08	124.7	23.98	57.9	58.5	16.1	510.	.029	.890	.085	1.068	8.4
.20000	59.85	22.70	4.37	6.83	0.00	3.37	49.8	29.64	73.6	74.1	16.1	1010.	.045	.904	.107	1.353	6.4
.20000	83.64	23.38	.63	2.63	0.00	.51	28.2	49.44	78.1	78.5	16.2	1330.	.050	.898	.046	1.435	6.3
.20000	84.34	23.38	.57	2.57	0.00	.45	27.8	50.06	78.1	78.6	16.2	1339.	.050	.893	.045	1.435	6.3
.20000	157.30	21.66	-1.62			-1.34			68.2	68.7	16.2	2339.	-.0393				
.20000	221.25	20.14	-1.44			-1.36			60.2	60.8	16.2	3339.	-.0300				
.20000	278.04	18.77	-1.30			-1.37			53.7	54.5	16.2	4339.	-.0250				
.20000	305.76	18.09	-1.24			-1.37			50.6	51.7	16.2	4871.	-.0224				
.20000	309.69	18.00	-1.23			-1.37			50.2	51.3	16.2	4949.	-.0225				

.40000	0.00	18.00	.11	2.21	0.00	.12	155.8	43.86	46.8	51.3	16.2	0.	.026	.579	.017	.937	24.2
.40000	.47	18.00	.11	2.21	0.00	.12	155.8	43.86	46.8	51.3	16.2	10.	.026	.579	.017	.937	24.2
.40000	24.96	19.37	6.23	8.62	.01	6.31	128.9	24.81	53.7	56.6	16.1	510.	.031	.891	.079	1.034	18.5
.40000	56.01	22.36	5.13	7.75	0.00	4.07	55.5	27.06	70.2	72.1	16.1	1010.	.042	.892	.115	1.317	13.1
.40000	83.02	23.26	.60	2.59	0.00	.45	28.4	46.84	76.0	77.8	16.2	1384.	.046	.891	.045	1.422	12.5
.40000	84.39	23.27	.47	2.47	0.00	.39	27.7	50.05	76.0	77.9	16.2	1402.	.046	.882	.043	1.423	12.5
.40000	155.32	21.56	-1.61			-1.34			66.1	68.1	16.2	2402.	-.0386				
.40000	217.19	20.05	-1.43			-1.35			58.1	60.4	16.2	3402.	-.0300				
.40000	271.40	18.69	-1.30			-1.36			50.6	54.2	16.2	4402.	-.0281				
.40000	293.92	18.10	-1.24			-1.38			47.3	51.7	16.2	4862.	-.0261				
.40000	297.87	18.00	-1.24			-1.38			46.8	51.3	16.2	4946.	-.0262				
.60000	0.00	18.00	-1.29	0.00	1.55	-1.39	155.8	43.86	40.4	51.3	16.2	0.	-.032	0.000	0.000	0.000	38.0
.60000	.40	17.99	-1.24	0.00	1.55	-1.39	155.8	43.86	40.4	51.3	16.2	10.	-.032	0.000	0.000	0.000	38.0
.60000	20.00	18.11	2.81	4.60	0.00	3.11	138.5	27.27	41.0	51.6	16.2	510.	.032	.883	.035	.942	37.4
.60000	44.80	20.84	6.08	8.62	2.23	5.52	78.5	21.20	58.7	63.7	16.1	1010.	.034	.891	.100	1.163	22.7
.60000	77.76	22.69	1.00	2.96	0.00	.77	31.5	43.45	70.1	74.3	16.2	1510.	.045	.900	.047	1.357	19.3
.60000	84.66	22.75	.30	2.27	0.00	.26	27.0	50.06	70.6	74.7	16.2	1617.	.045	.852	.036	1.365	19.2
.60000	150.21	21.10	-1.55			-1.35			60.9	65.7	16.2	2617.	-.0356				
.60000	206.85	19.64	-1.40			-1.37			52.4	58.4	16.2	3617.	-.0370				
.60000	254.42	18.31	-1.27			-1.38			42.9	52.6	16.2	4617.	-.0328				
.60000	262.37	18.07	-1.25			-1.38			40.9	51.6	16.2	4807.	-.0323				
.60000	264.57	18.00	-1.24			-1.38			40.4	51.3	16.2	4861.	-.0325				
.80000	0.00	18.00	-1.30	0.00	.82	-1.40	155.8	43.86	29.3	51.3	16.2	0.	-.041	0.000	0.000	0.000	55.1
.80000	.29	17.99	-1.25	0.00	.82	-1.40	155.8	43.86	29.3	51.3	16.2	10.	-.041	0.000	0.000	0.000	55.1
.80000	12.50	17.37	-1.20	0.00	.68	-1.40	147.9	32.69	19.1	48.8	16.2	510.	-.041	0.000	0.000	0.000	66.9

WIND SPEED TOO LARGE AT 16.9 KM.
WIND SPEED TOO LARGE AT 16.9 KM.
WIND SPEED TOO LARGE AT 16.9 KM.
WIND SPEED TOO LARGE AT 16.9 KM.
WIND SPEED TOO LARGE AT 16.9 KM.
WIND SPEED TOO LARGE AT 16.9 KM.
WIND SPEED TOO LARGE AT 16.8 KM.
WIND SPEED TOO LARGE AT 16.8 KM.
WIND SPEED TOO LARGE AT 16.8 KM.
WIND SPEED TOO LARGE AT 16.9 KM.

WIND SPEED TOO LARGE AT 18.0 KM.

WK	XC	HC	TC	E/W-S	E/W-T	XT	TT
	KM	KM	HR	KJ/N	KJ/N	KM	HR
0.000	84.32	23.41	.367	1.452	9.803	313.19	1.37
.200	84.34	23.38	.372	1.377	9.730	309.69	1.37
.400	84.39	23.27	.389	1.154	9.509	297.87	1.37
.600	84.66	22.75	.449	1.197	9.203	264.57	1.35
.800	-I	-I	-I	-I	-I	17.38	1.35
1.000	-I	-I	-I	-I	-I	0.00	1.35

APPENDIX B

GLIDE-TIME PARAMETER

An expression for the time required to glide between two altitudes is given as equation 29 of reference 8. The development of that equation assumes that the aerodynamic characteristics (C_L and C_D) remain constant and that acceleration effects (eq. (4)) are negligible. That endurance equation for gliding flight is written as:

$$t_g = \frac{L}{D}\sqrt{\frac{C_L}{W/S\ (\cos\ )^{-3/2}}} \int_{h_1}^{h_2} \sqrt{\frac{\rho}{2}}\, dh \tag{B1}$$

where h_1 and h_2 are the final and initial altitudes, respectively. Equation (B1) can be simplified in two ways. First, since γ is a small angle, the cosine term can be approximated as 1.0. Second, if the range of altitudes lies between about 16 and 26 kilomters, equation (11) can be used to approximate density variation by choosing $a = 0.105$ and $b = 0.0013$ throughout that altitude range.

Substituting equation (11) into equation (B1) yields an integrable expression:

$$t_g = \frac{L}{D}\sqrt{\frac{C_L \rho_o}{2\ W/S}}\ e^{(a^2/8b)} \int_{h_1}^{h_2} e^{-(b/2)(h\ +\ (a/2b))^2}\ dh \tag{B2}$$

$$= \frac{L}{D}\ \frac{1}{V_e}\ e^{(a^2/8b)}\ \sqrt{\frac{2}{b}} \int_{z_1}^{z_2} e^{-z^2}\ dz$$

$$= \frac{L}{D}\ \frac{1}{Ve}\ e^{(a^2/8b)}\ \sqrt{\frac{\pi}{2b}}\ (\text{erf}\ (z_2) - \text{erf}\ (z_1)) \tag{B3}$$

where $z = \sqrt{b/2}\ \ (h + (a/2b))$

Equation (B3) may be rearranged to produce an expression independent of vehicle aerodynamic characteristics. After substituting the values of a and b, the equation becomes:

$$t_g V_e \frac{D}{L} = 27.873\ (\text{erf}\ (z_2) - \text{erf}\ (z_1)) \tag{B4}$$

where $z = 1.0296 + 0.025495h$

where h is expressed in kilometers, V_e in meters per second, and t_g in hours. As in equation (B1), h_1 is the final altitude because of the negative rate of climb.

Glide time can be determined for a specific vehicle where L/D and V_e are given. For the class of vehicles considered in this study, the values of $L/(DV_e)$ lie approximately between 10 and 0.1. The largest value yields the longest glide time and is produced by low W/S and high L/D.

REFERENCES

1. Kuhner, M. B.; and McDowell, J. R.: User Definition and Mission Requirements for Unmanned Airborne Platforms. NASA CR 156861, 1979.

2. Youngblood, James, W.: Darnell, Wayne L.; Johnson, Robert W.; and Harriss, Robert C.: Airborne Spacecraft - A Remotely Powered, High-Altitude RPV for Environmental Applications. NASA paper presented at Electronics and Aerospace Systems Conference (Arlington, Virginia), Oct. 9-11, 1979.

3. Sinko, J.W.: High Altitude Powered Platform Cost and Feasibility Study. NASA CR 150285, 1977.

4. Anon.: U.S. Standard Atmosphere, 1962. NASA, U.S. Air Force, and U.S. Weather Bur., Dec. 1962.

5. Kaufman, John W., ed.: Terrestrial Envronment (Climatic) Criteria Guidelines for Use in Aerospace Vehicle Development, 1977 Revision. NASA TM 78118, 1977.

6. Irving, F. G.; and Morgan, D.: The Feasibility of an Aircraft Propelled by Solar Energy. AIAA Paper No. 74-1042, 1974.

7. Boucher, R. J.: Project Sunrise. AIAA Paper 79-1264, 1979.

8. Phillips, William H.: Some Design Considerations for Solar-Powered Aircraft. NASA TP 1675, 1980.

9. Heyson, Harry H.: Initial Feasibility Study of a Microwave-Powered Sailplane as a High-Altitude Observation Platform. NASA TM 78809, 1978.

10. Turriziani, R. Victor: Sensitivity Study for a Remotely Piloted Microwave-Powered Sailplane Used as a High-Altitude Observation Platform. NASA CR 159089, 1979.

11. Fordyce, Samuel W.; and Brown, William C.: Applications of Free-Space Microwave Power Transmission. Aeronautics & Astronautics, vol. 17, no. 9. Sept. 1979, pp. 54-61.

12. Brown, William C.: A Profile of Power Transmission by Microwaves. Aeronautics & Astronautics, vol. 17, no. 5, May 1979, pp 50-55.

13. Hansen, R. C.: Microwave Scanning Antennas, Academic Press, 1964.

14. Dickinson, Richard M.: Beamed Microwave Power Transmitting and Receiving Subsystems Radiation Characteristics. JPL Publication 80-11, June 1980.

15. Anon.: Generalized Method of Propeller Performance Estimation, Report PDB 6101, Revision A. Hamilton Standard, June 1963.

16. Strganac, Thomas W.: Wind Study for High Altitude Platform Design, NASA RP-1044, 1979.

17. Hoerner, Sighard F.: Fluid-Dynamic Drag. S. F. Hoerner, 1958.

18. Taylor, John W. R., ed.: Jane's All the World's Aircraft, 1979-1980, Franklin Watts, Inc., N. Y., 1979.

19. Cochrane, James A.; Henry, Robert M.; and Weaver, William L.: Revised Upper-Air Wind Data for Wallops Island Based on Serially Completed Data for the Years 1956 to 1964. NASA TN D-4570, 1968.

20. Tolefson, H. B.: An Investigation of Vertical-Wind Shear Intensities from Balloon Soundings for Application to Airplane- and Missile-Response Problems. NACA TN 3732, 1956.

21. Coleman, Thomas L.; and Steiner, Roy: Atmospheric Turbulence Measurements Obtained form Airplane Operations at Altitudes Between 20,000 and 75,000 Feet for Several Areas in the Northern Hemisphere. NASA TN D-548, 1960.

TABLE I.- DESCRIPTION OF BASELINE CONFIGURATION OF HIGH-ALTITUDE AIRPLANE PLATFORM

Airplane aerodynamics:	
Aspect ratio, A	30
Lift coefficient, C_L	0.9
Lift-to-drag ratio	
Altitude function, L/D	36.6 + 0.418 h
Folded propeller decrement, L/D	1.5
Oswald efficiency factor, e	0.96
Wing loading, W/S	144 N/m^2
Propellers(s):	
Activity factor	80.
Design lift coefficient	0.3
Ratio of wing area to propeller-disk area, S/A_p	2.653
Tip speed, V_{tip}	172. m/s
Motors(s):	
Maximum specific power (available), $(P/W)_{max}$	8.62 W/N
Minimum specific power (required), $(P/W)_{min}$	2.16 W/N
Power transmission:	
Power intensity at reference range, P/S	1.10 kW/m^2
Reference range, R	50 km
Range-power attenuation factor	R/r
Transmission initiation point	
Altitude, h_s	18 km
Horizontal range, x_s	40 km
Transmission-termination slant range	50 km

TABLE II.- INPUT PARAMETERS FOR PERFORMANCE PROGRAM OF APPENDIX A

Array number	Program name	Description
1	WOS	W/S
2	C_L	C_L
3	BLOD	L/D component independent of altitude of altitude
4	HLOD	coefficient of altitude-dependent term in L/D equation, km^{-1}
5	TS	V_{tip}
6	SOAP	S/A_p
7	POS	P/S
8	RR	R
9	POWL	maximum P/W used by propulsion system
10	WK	k_w
11	AMU	μ
12	XS	x_s
13	HS	h_s
14	POWR	ratio of minimum P/W to maximum P/W for propulsion system
15	TDOT	T_d/T
16	HI	h_i
17	RKR	k_r
	N1	code for flight mode calculation (1- single, 2- climb, 3- climb plus glide, or, 4- glide only)
	N2	element in input array to be varied
	N3	number of calculation points per listed line
	N4	transmitter polarization code (1- linear; 2- circular)
	SF	final value of variation set
	SI	initial value of variation set
	SS	step size of variation set

TABLE III.- OUTPUT PARAMETERS FOR PERFORMANCE PROGRAM OF APPENDIX A

Output listing name*	Parameter
X	x
H	h
R/C	$\dot{h}$
P/W-P	P/W available for propulsion
P/W-S	P/W available for storage
GAMMA	γ
THETA	θ
R	r
VG	V_g
VT	V
VE	$V_e \sqrt{\cos \gamma}$
T	t
AK	k_a
ETA	η
CP	C_p
J	J
PSI	ϕ
XC	x_c
HC	h_c
TC	t_c
E/W-S	E_s/W
E/W-T	E_t/W
XT	x_t
TT	t_t

* given in listing sequence

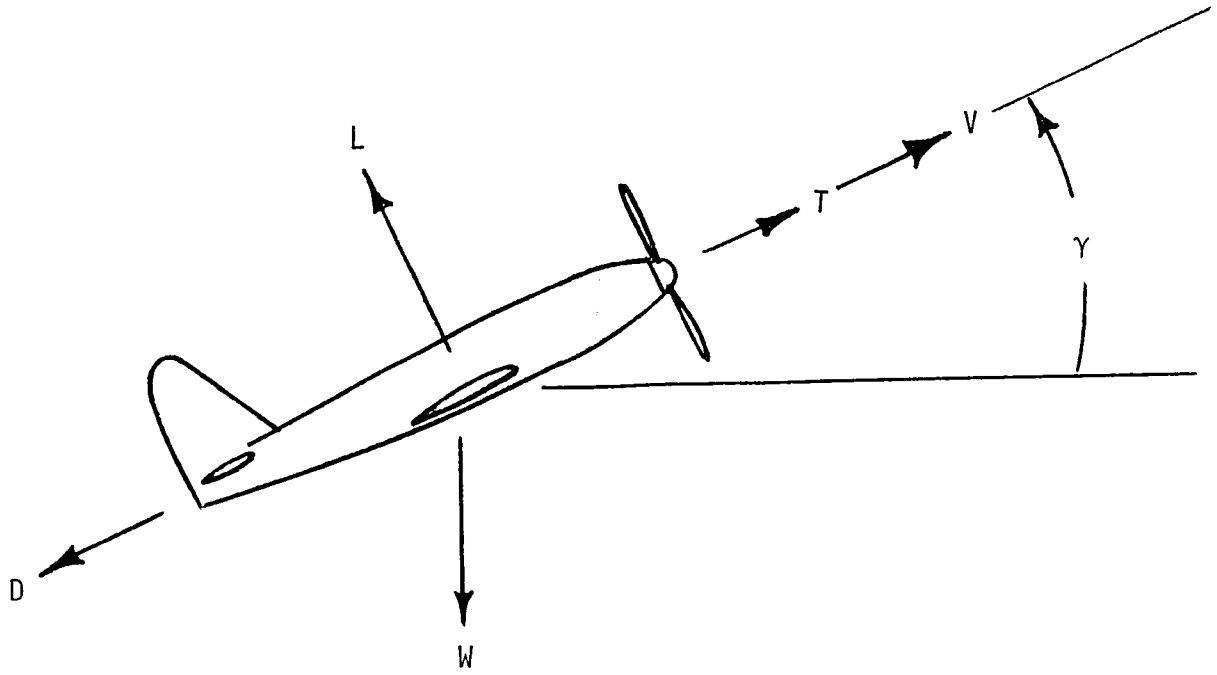

(a) Forces in longitudinal plane.

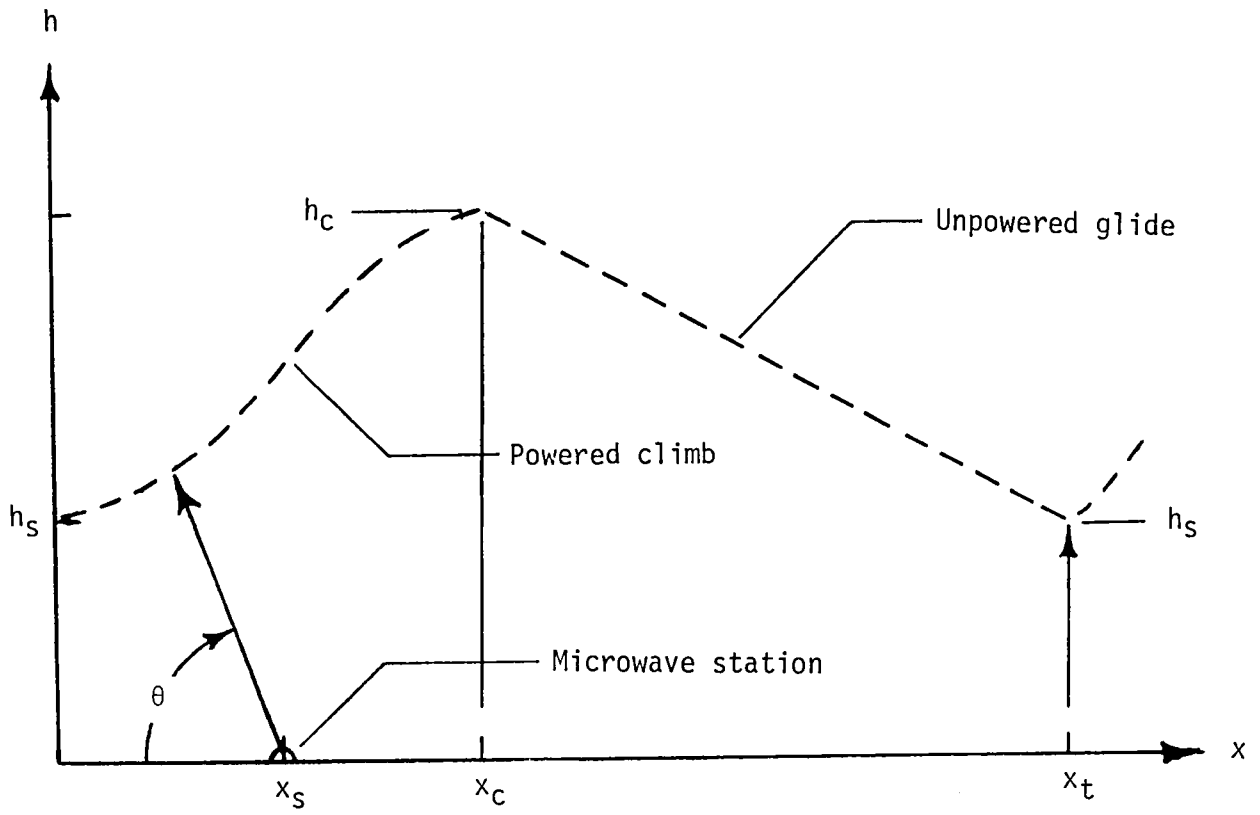

(b) Flight path profile

Figure 1. - Conventions used to define senses of displacements, forces, angles and velocities.

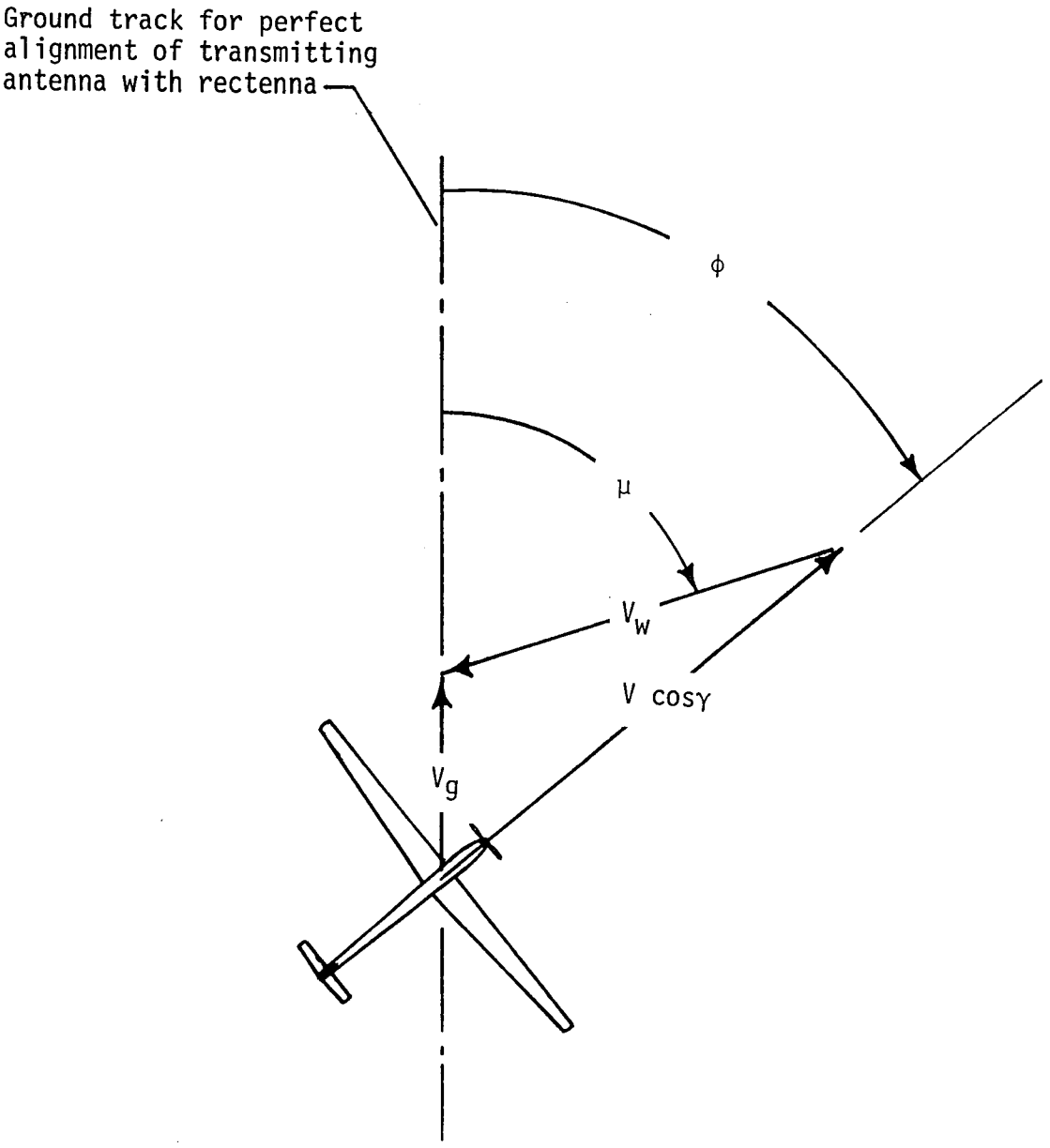

(c) Velocities in lateral plane.

Figure 1. - Concluded

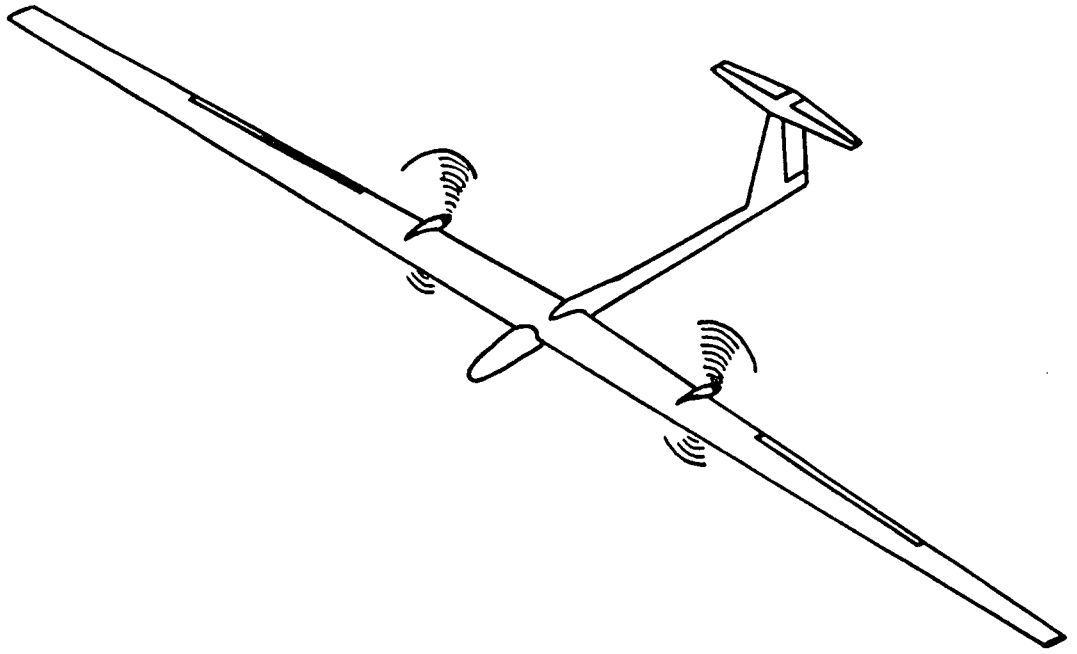

(a) configuration of reference 9

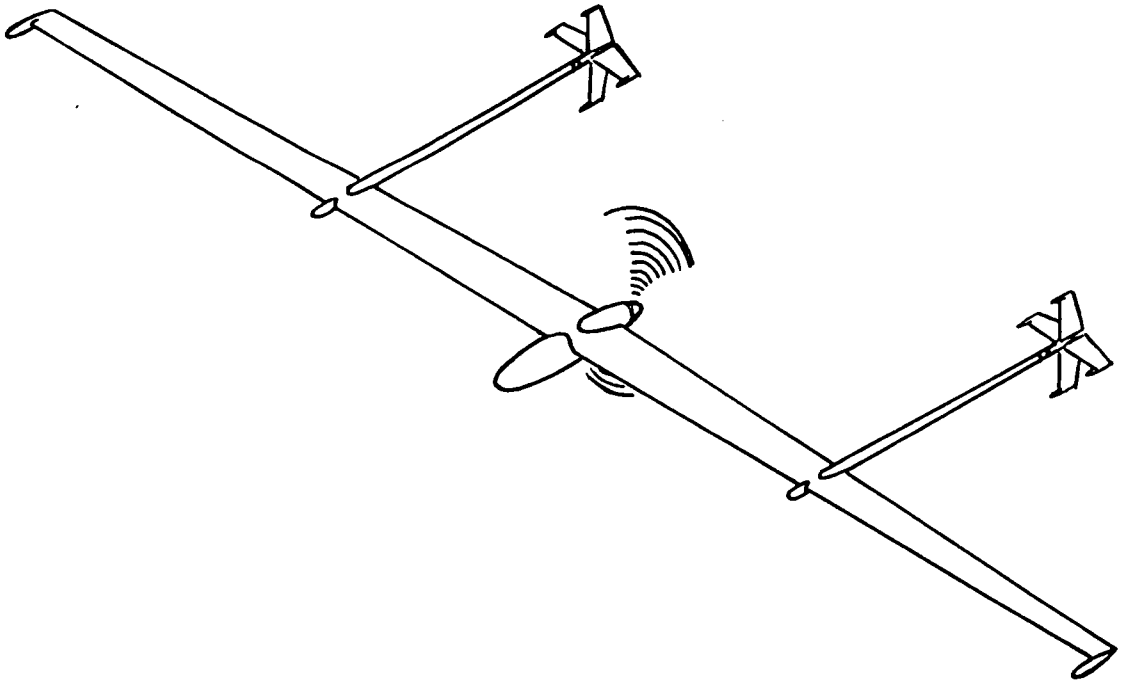

(b) alternate configuration

Figure 2. - Conceptual HAAP designs.

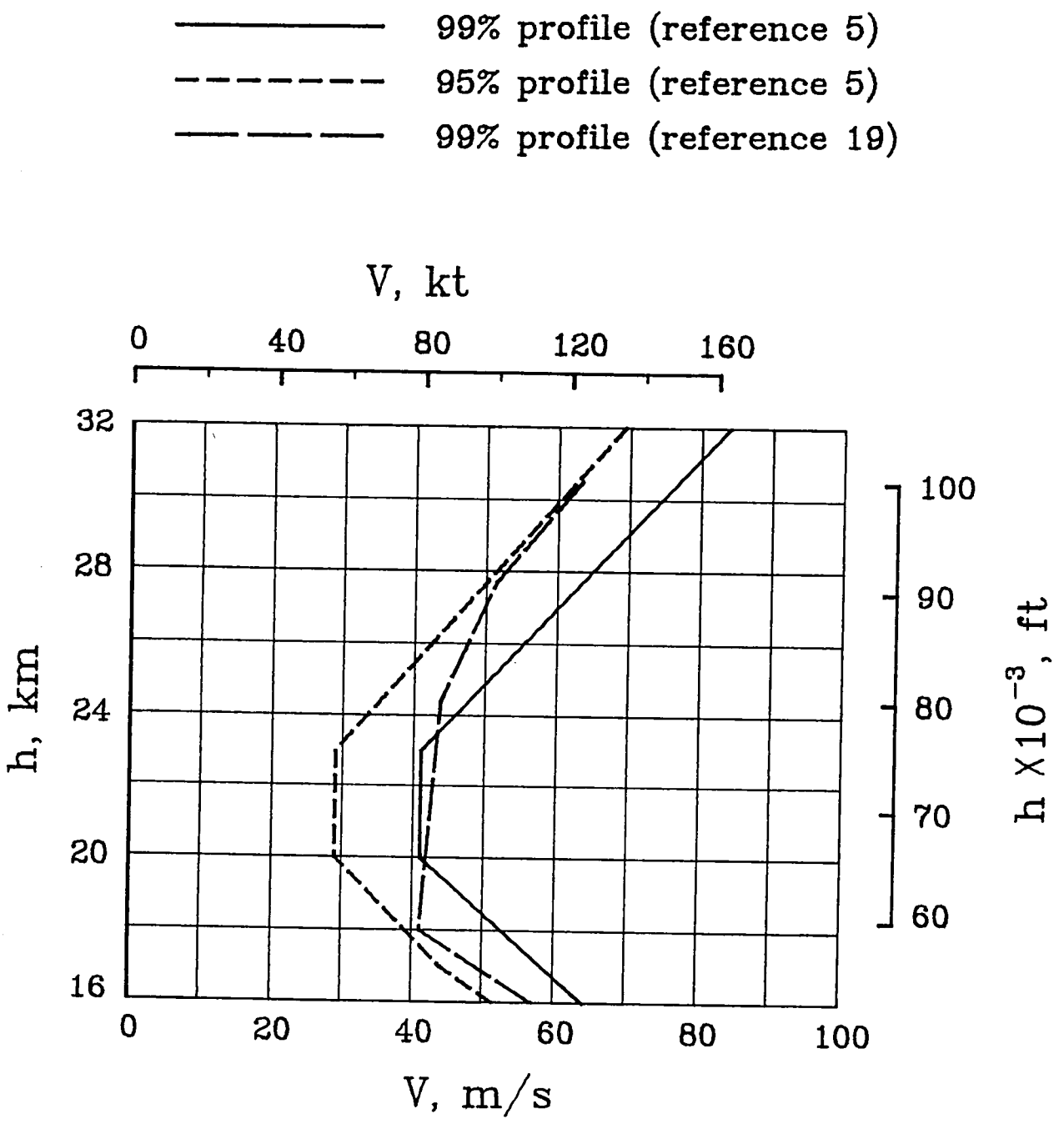

Figure 3. - Wind profile data.

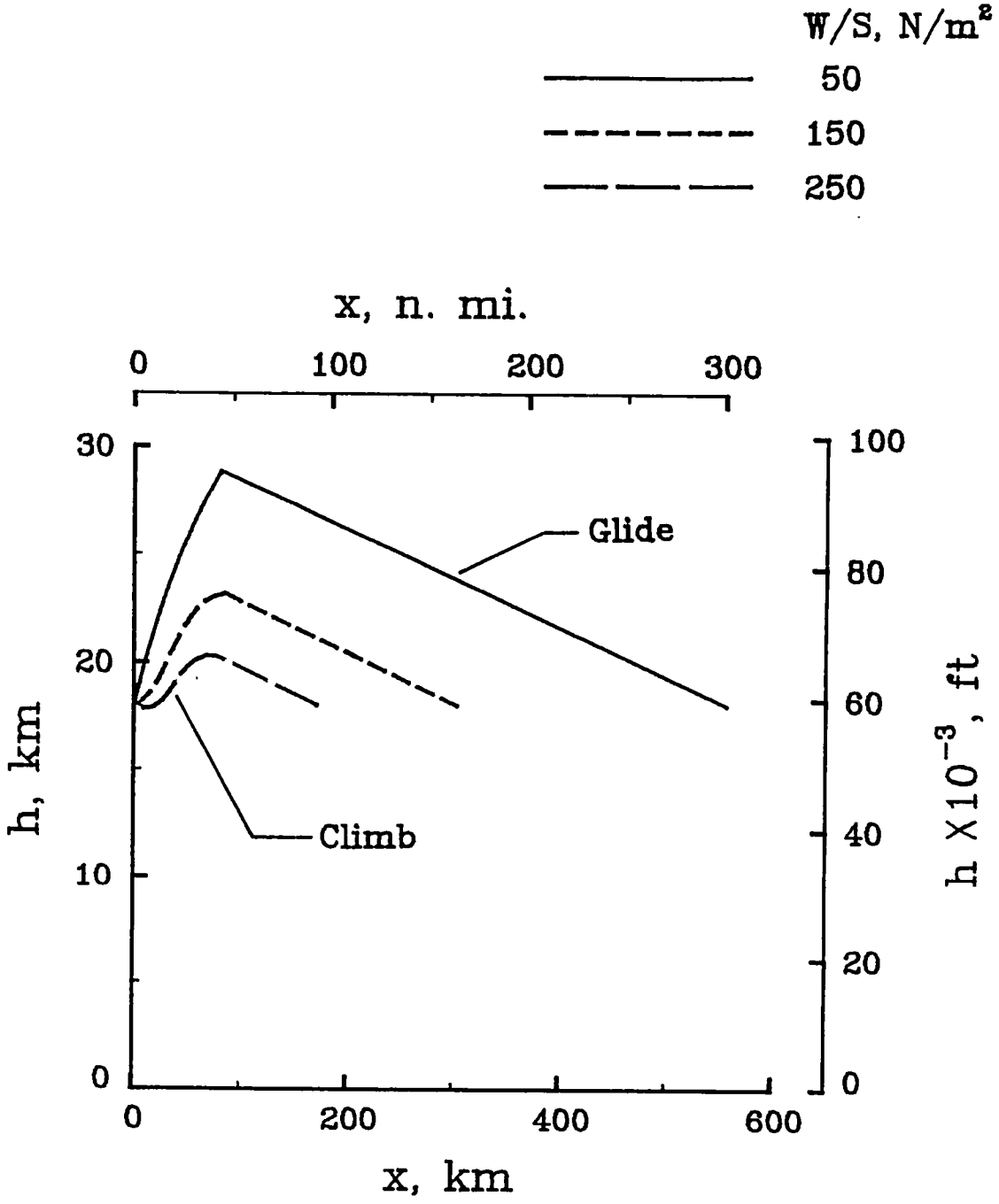

Figure 4. - Flight profiles.

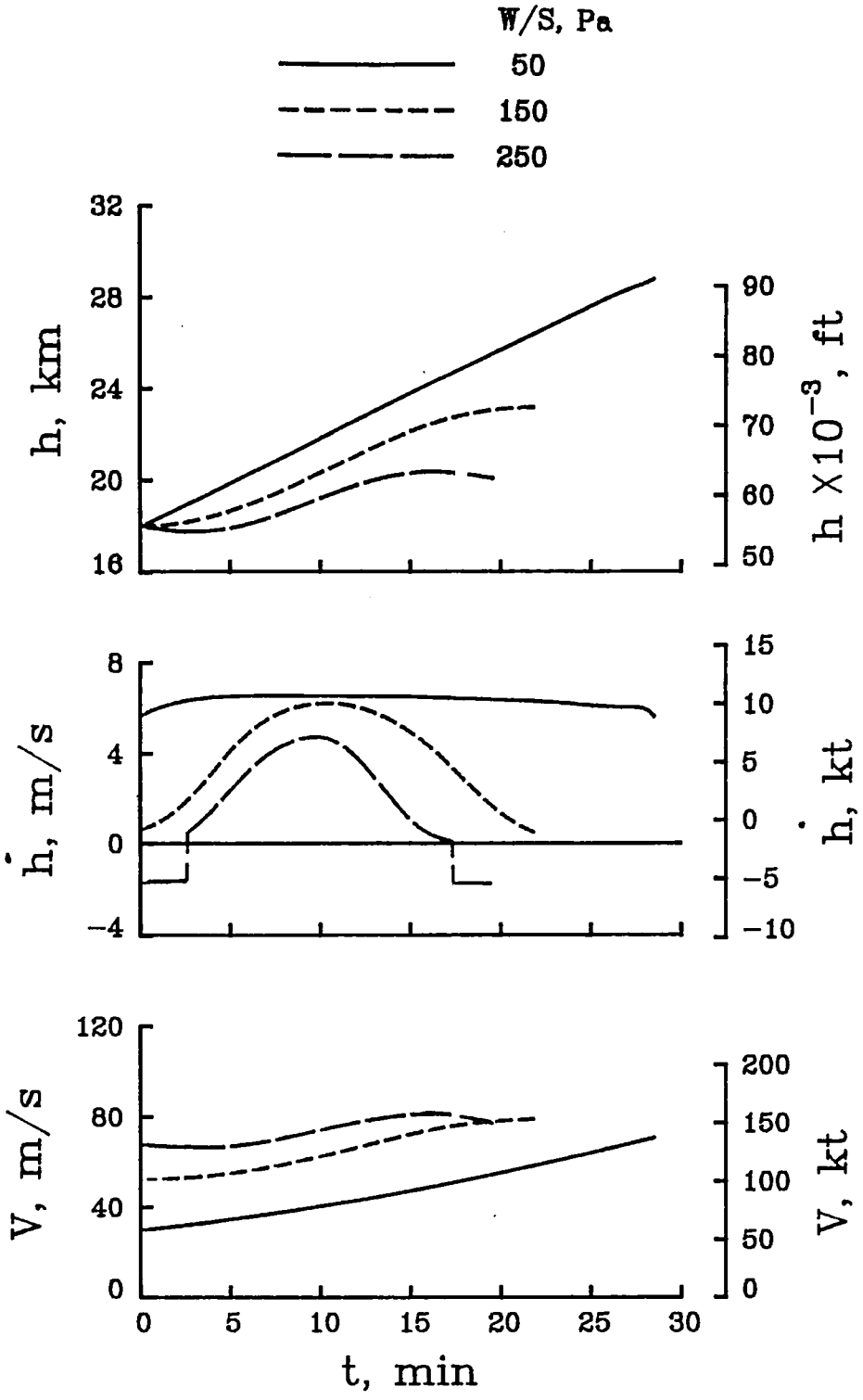

(a) Trajectory.

Figure 5. - History of flight parameters for representative variations in baseline configurations.

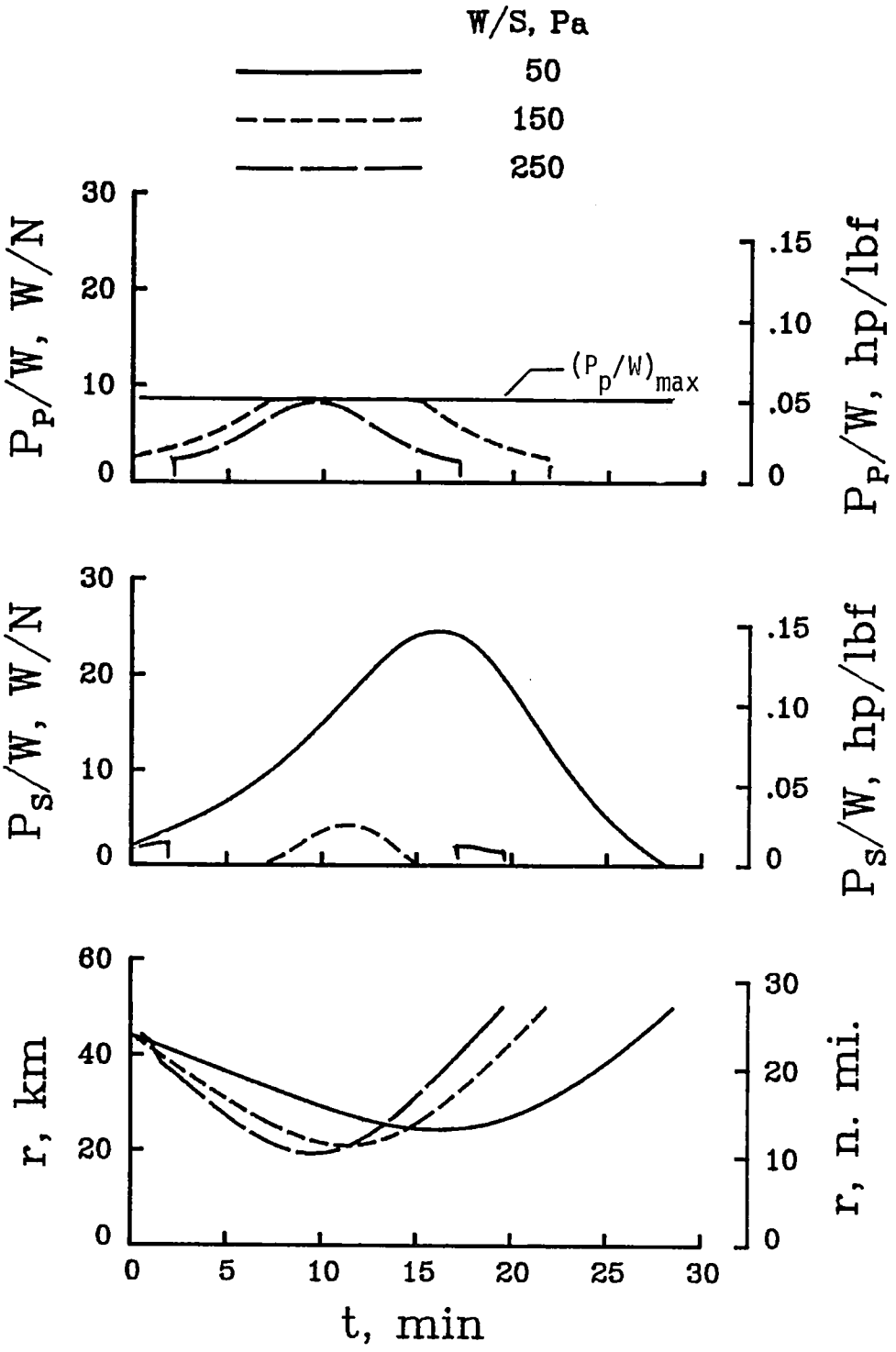

(b) Power and range parameters.

Figure 5. - Continued.

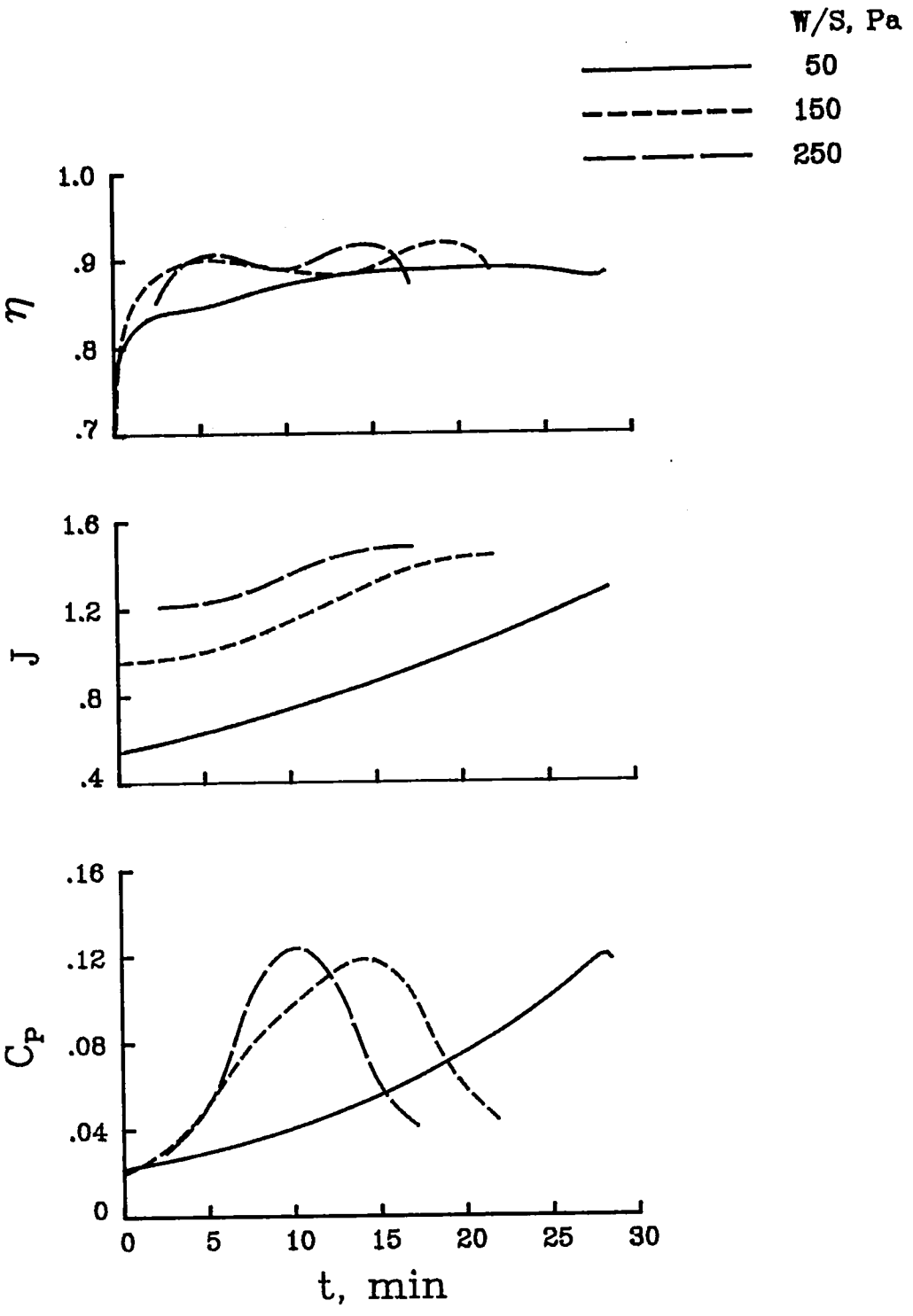

(c) Propeller parameters.

Figure 5. - Concluded.

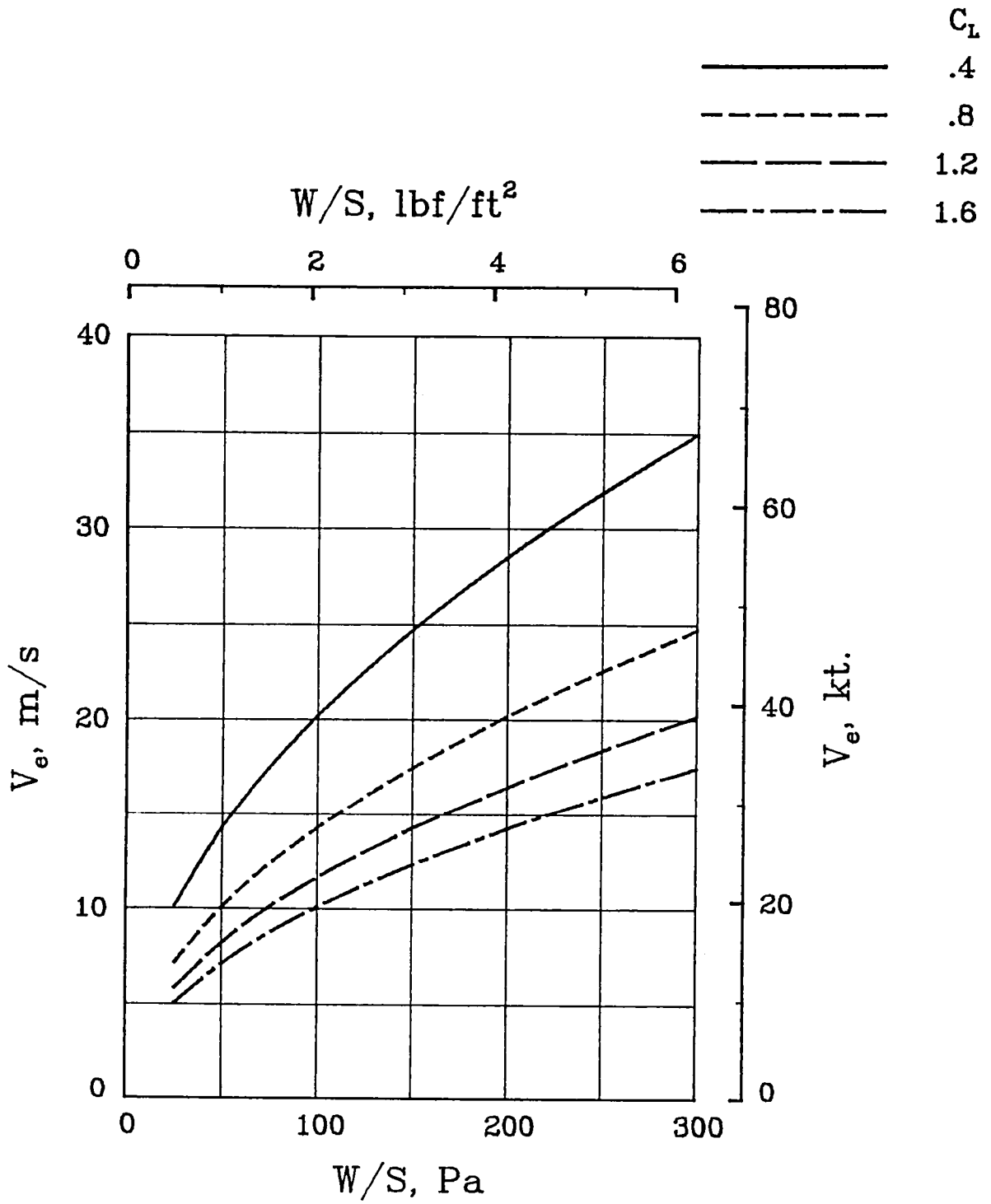

Figure 6. - Variation of equivalent airspeed with wing loading and lift coefficient.

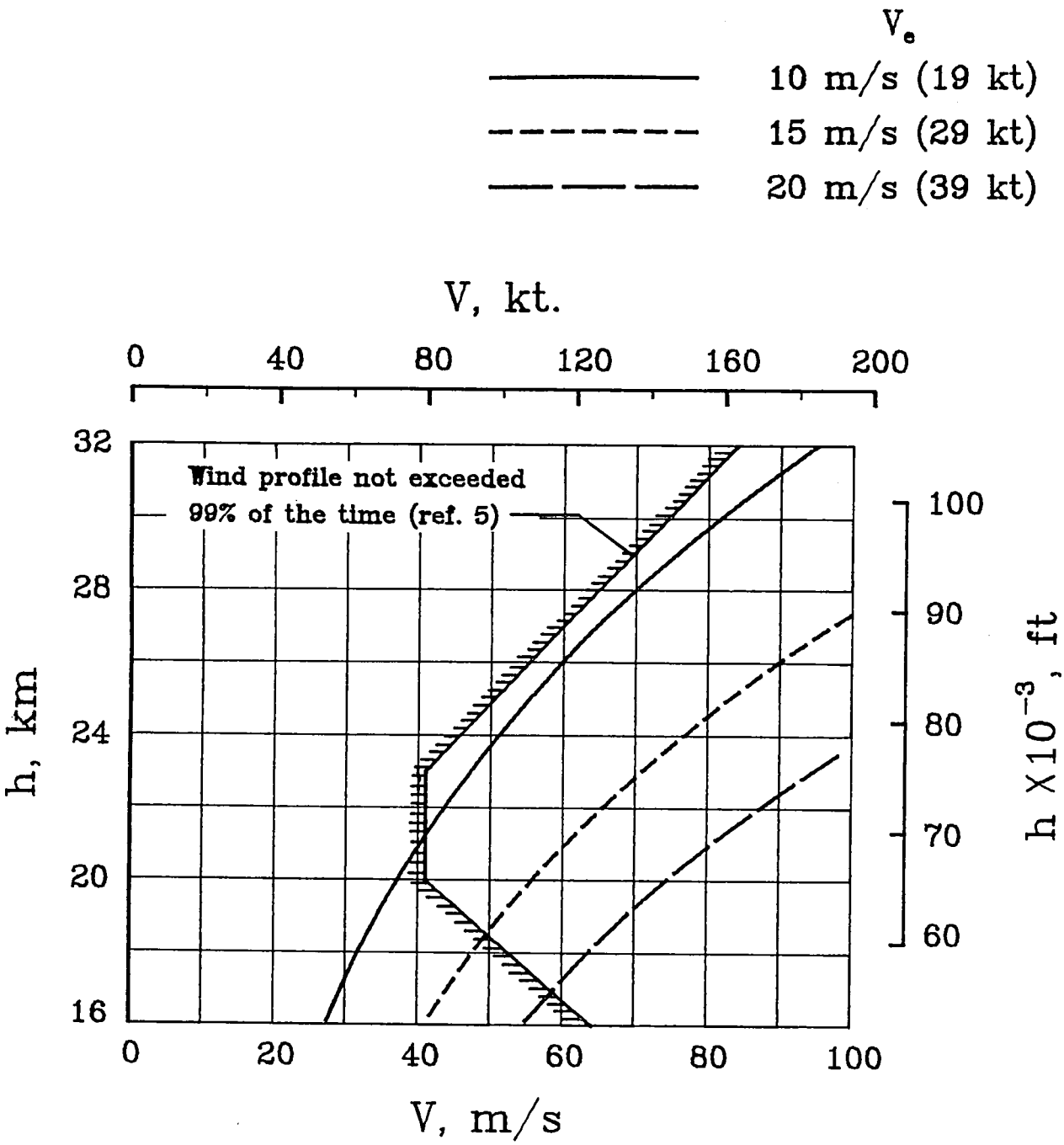

(a) True airspeed profile.

Figure 7. - Comparison of limiting wind profile and vehicle airspeed.

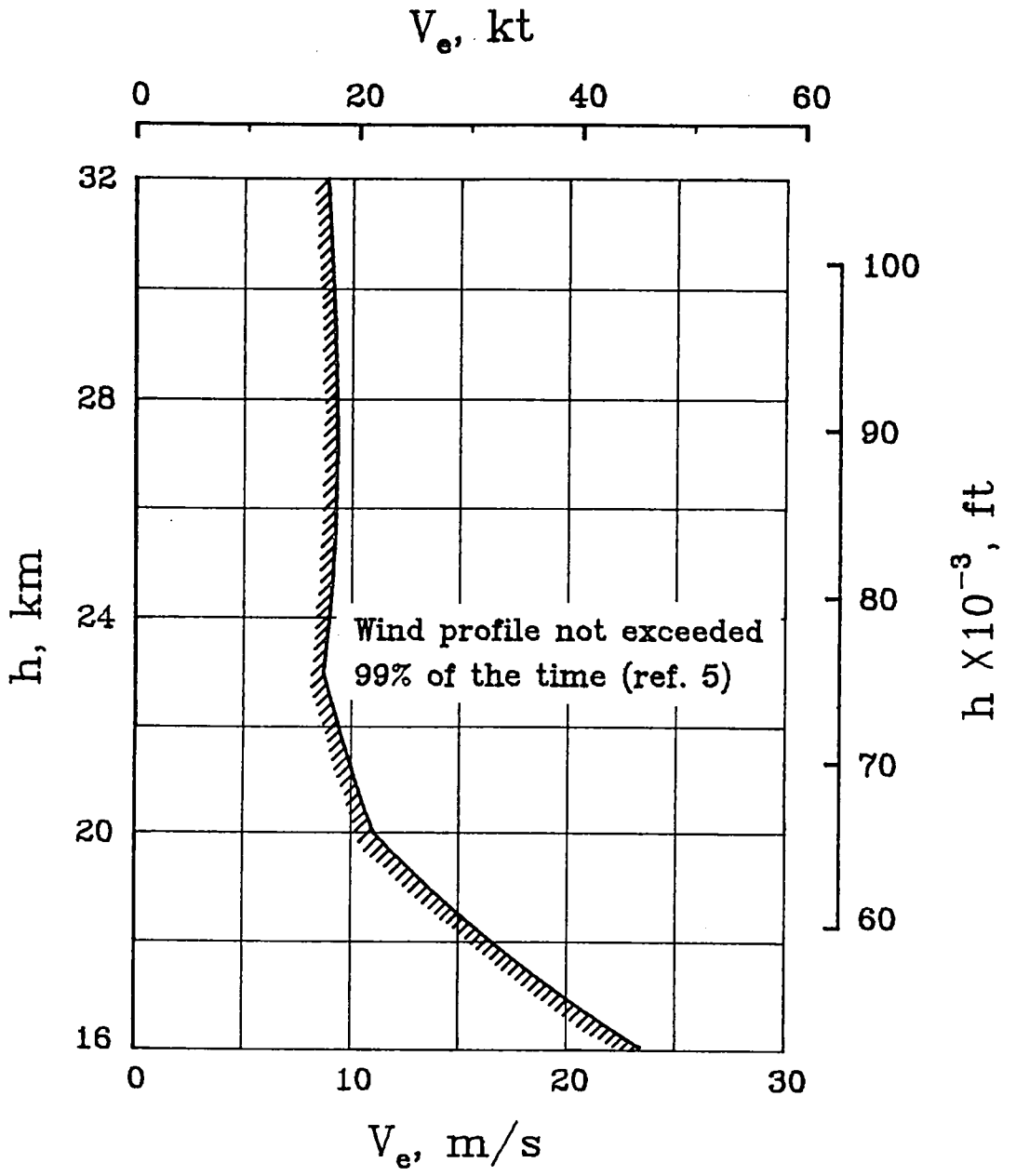

(b) Equivalent airspeed profile.

Figure 7. - Concluded.

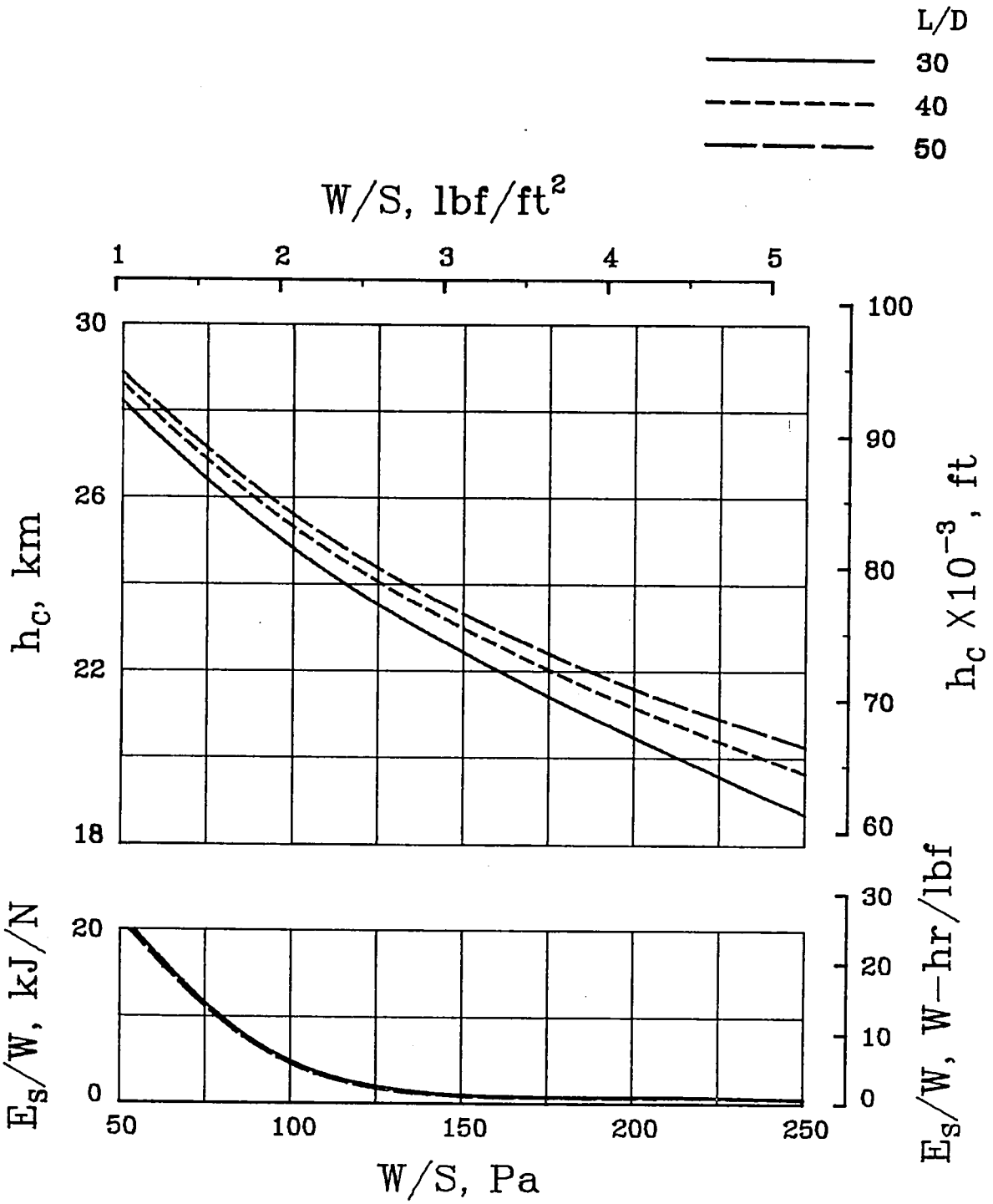

Figure 8. - Effect of wing loading and lift-to-drag ratio on the performance of the baseline configuration.

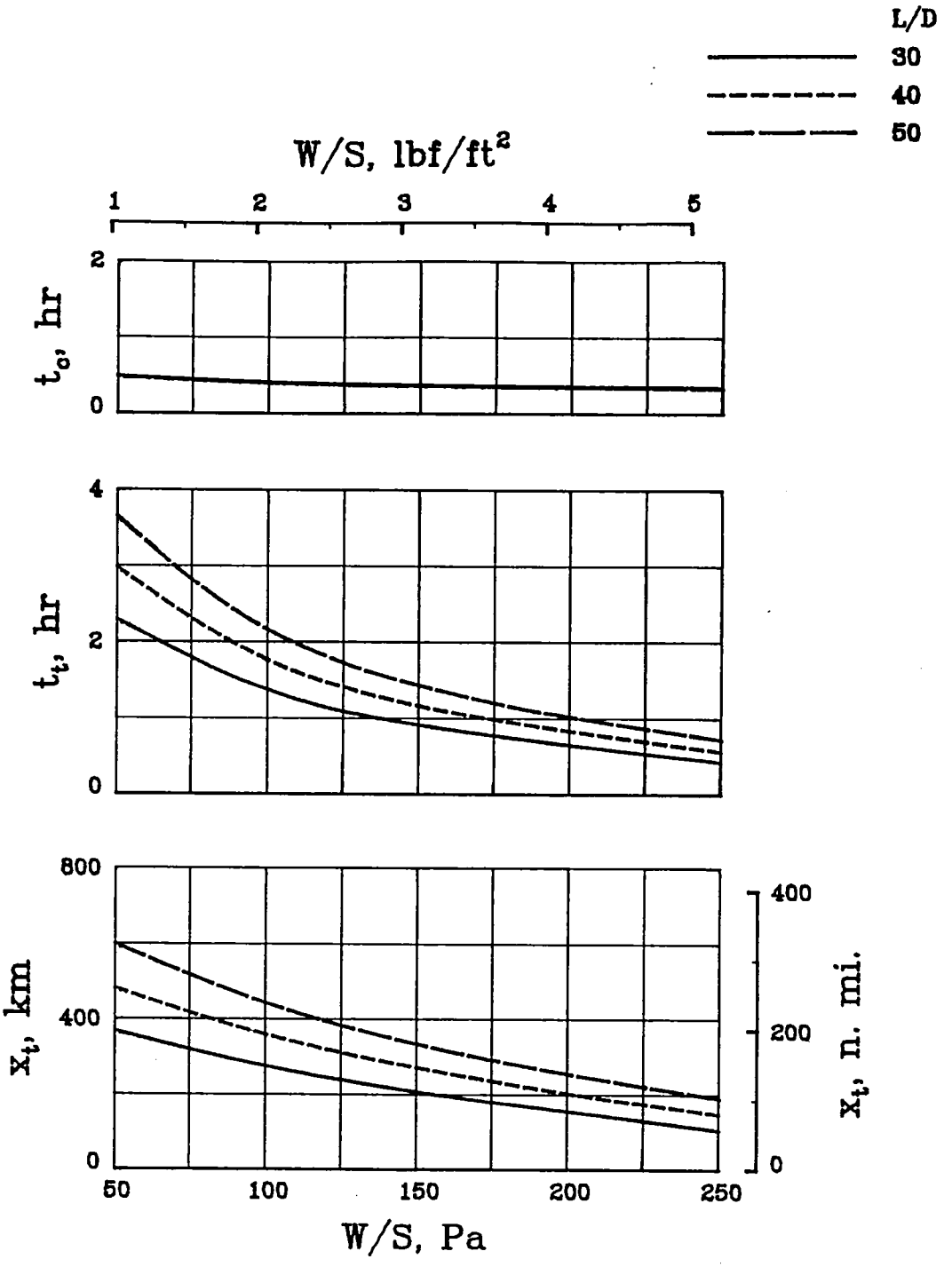

Figure 8. - Concluded.

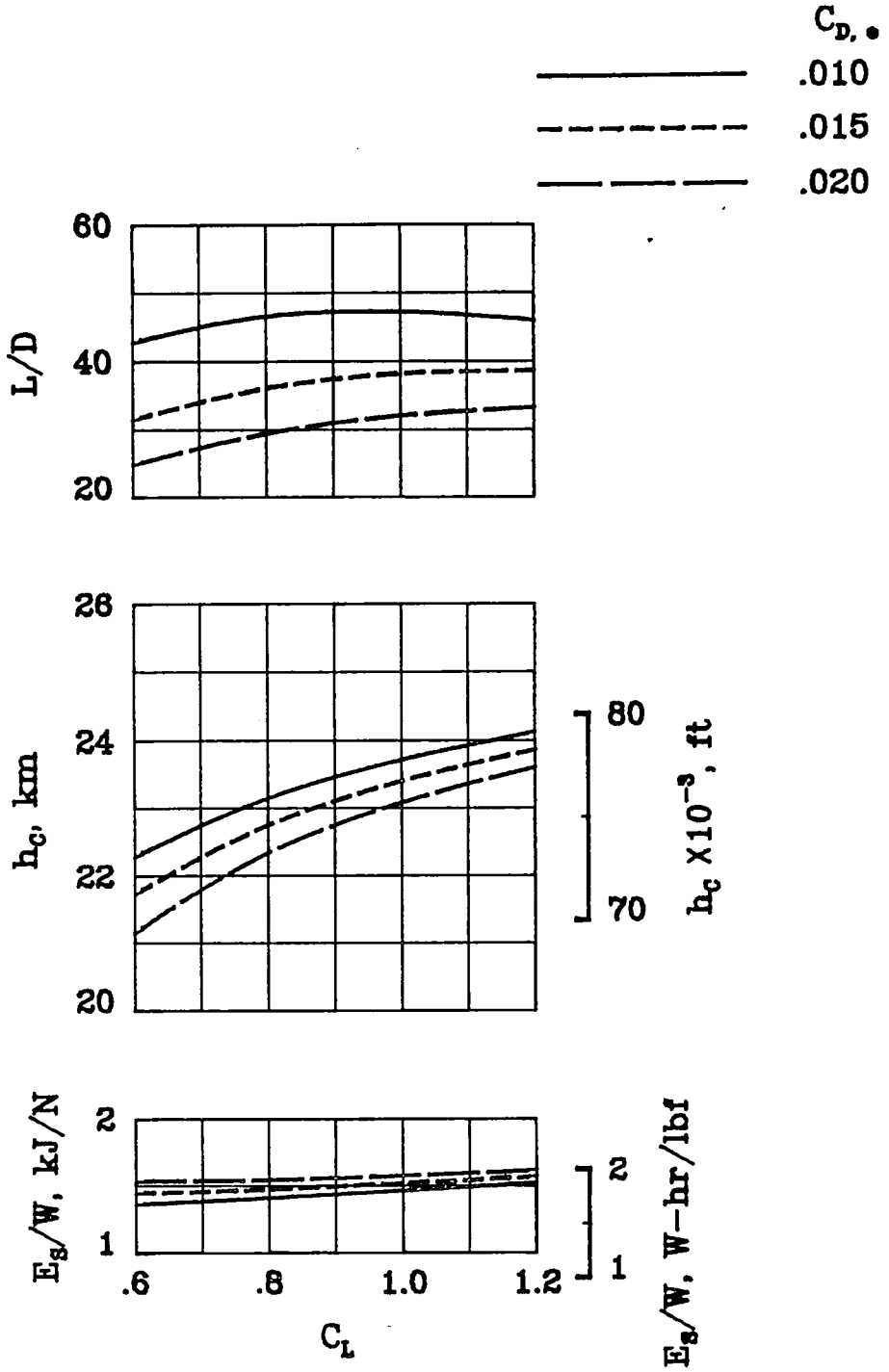

Figure 9. - Effect of airplane lift and drag coefficients on performance.

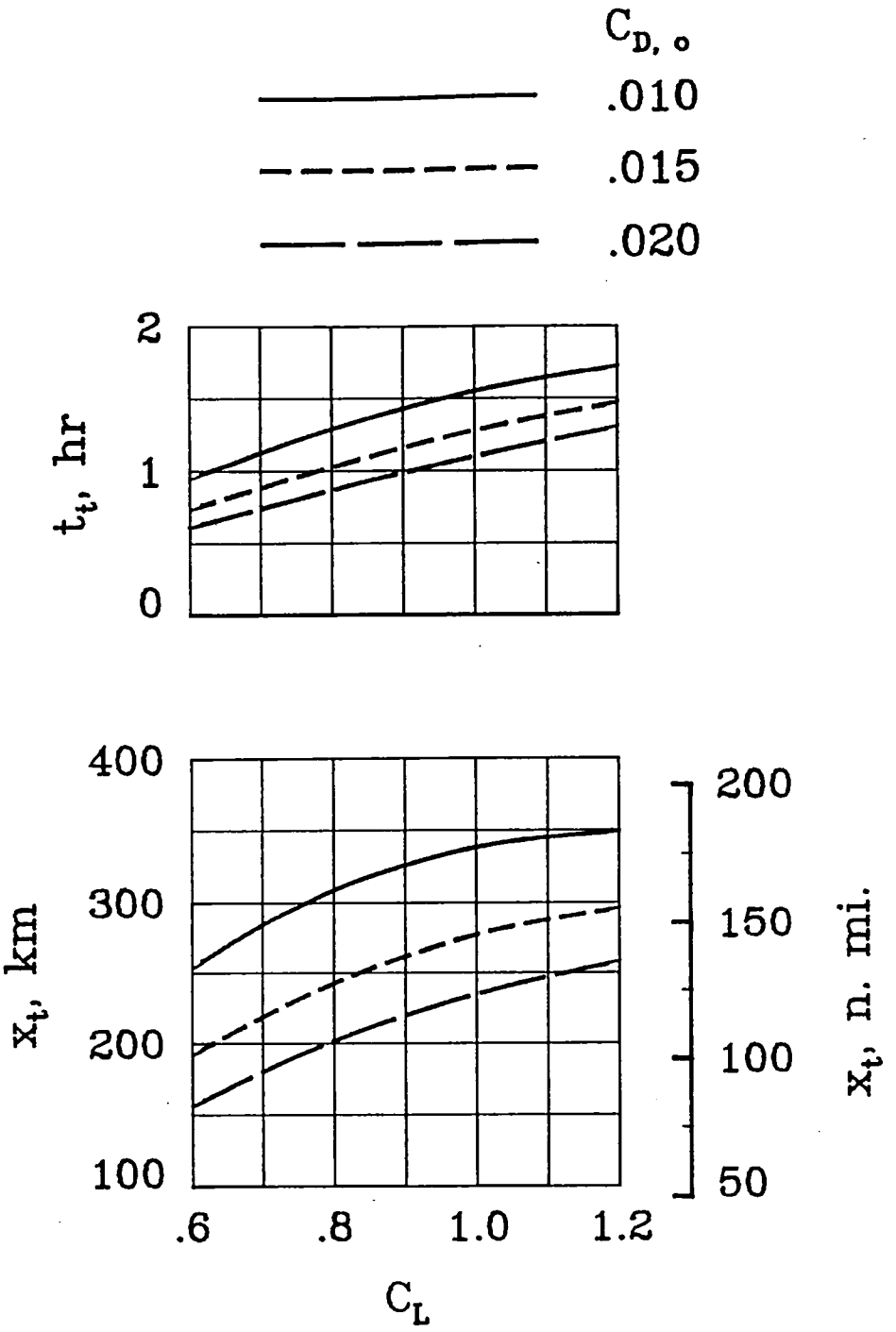

Figure 9. - Concluded.

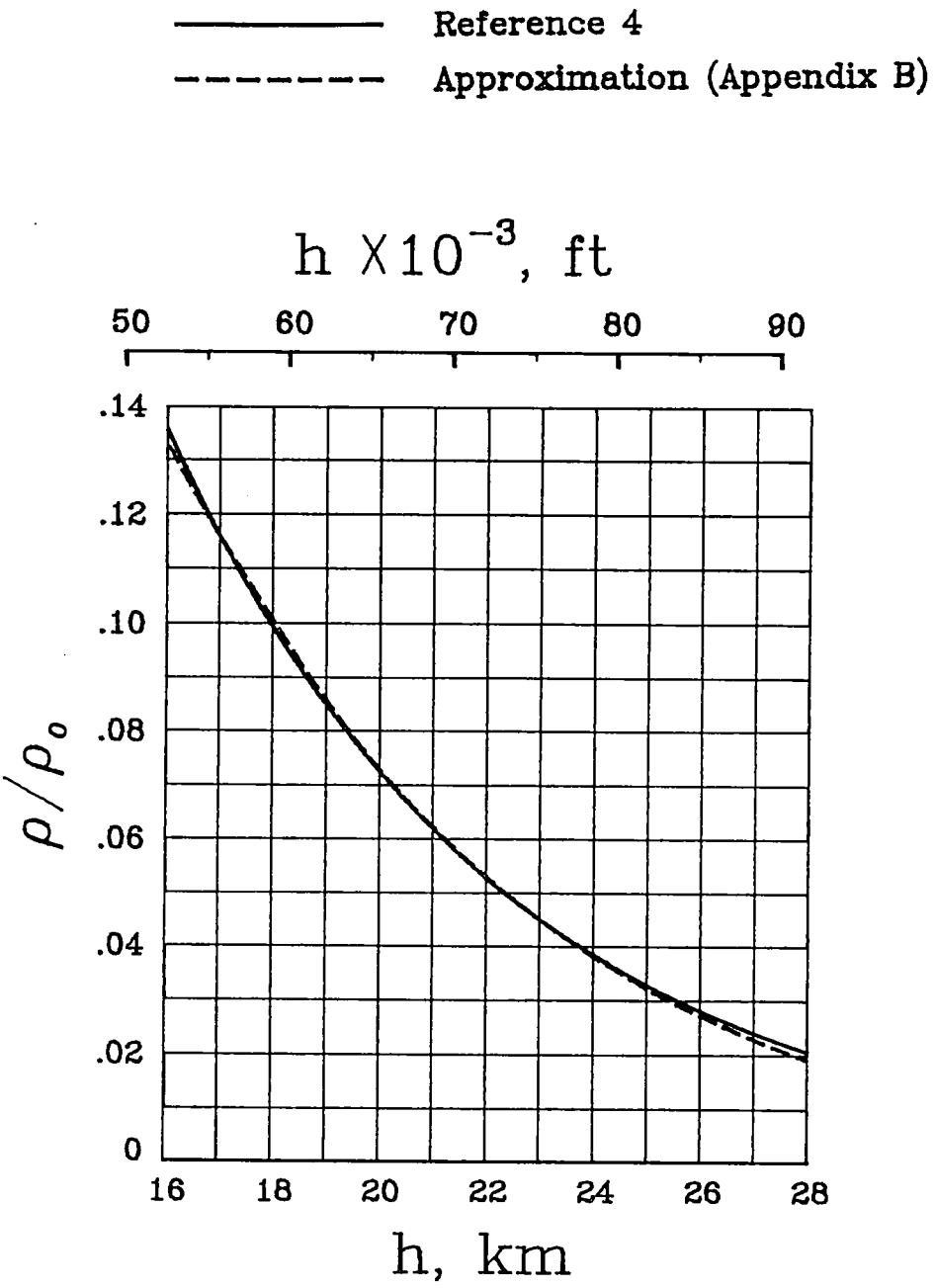

Figure 10. - Comparison of two models of air density variation with altitude.

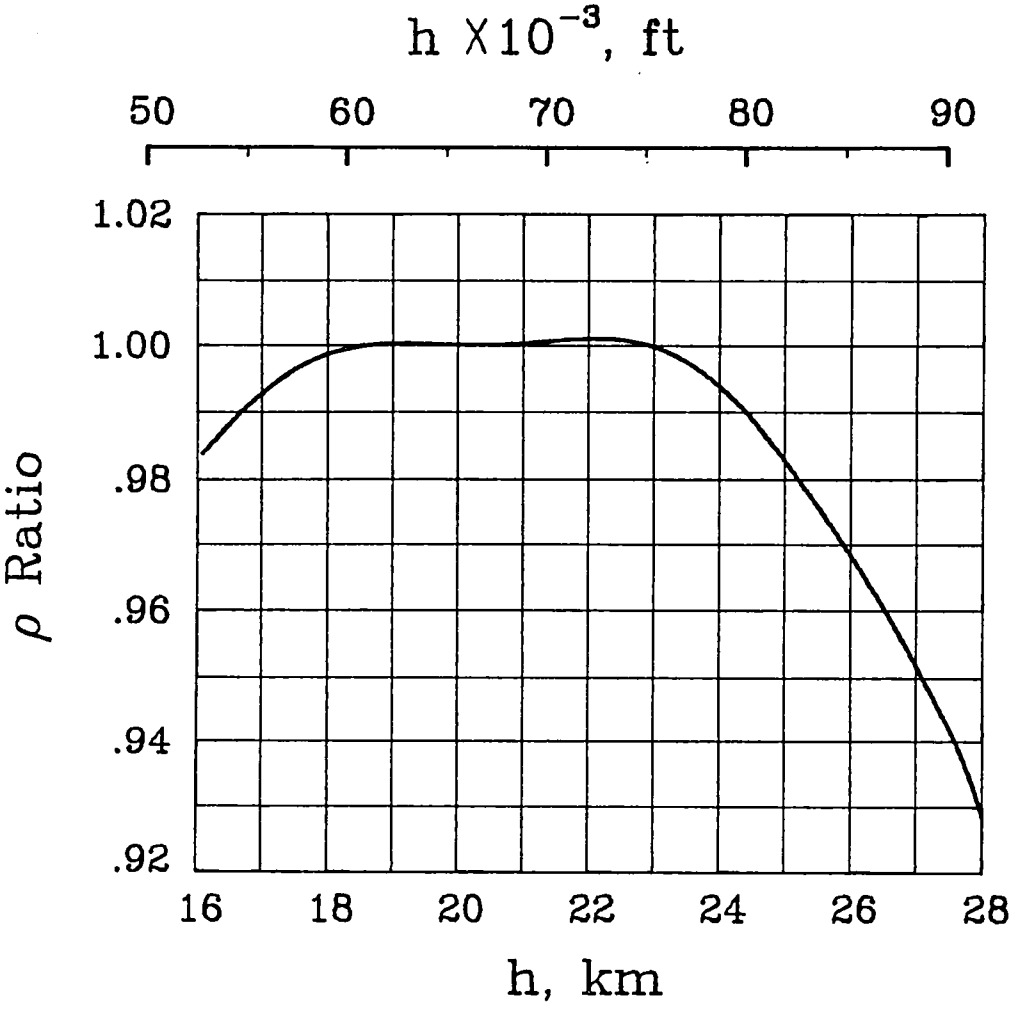

Figure 11. - Ratio of approximate density (Appendix B) to density from reference 4.

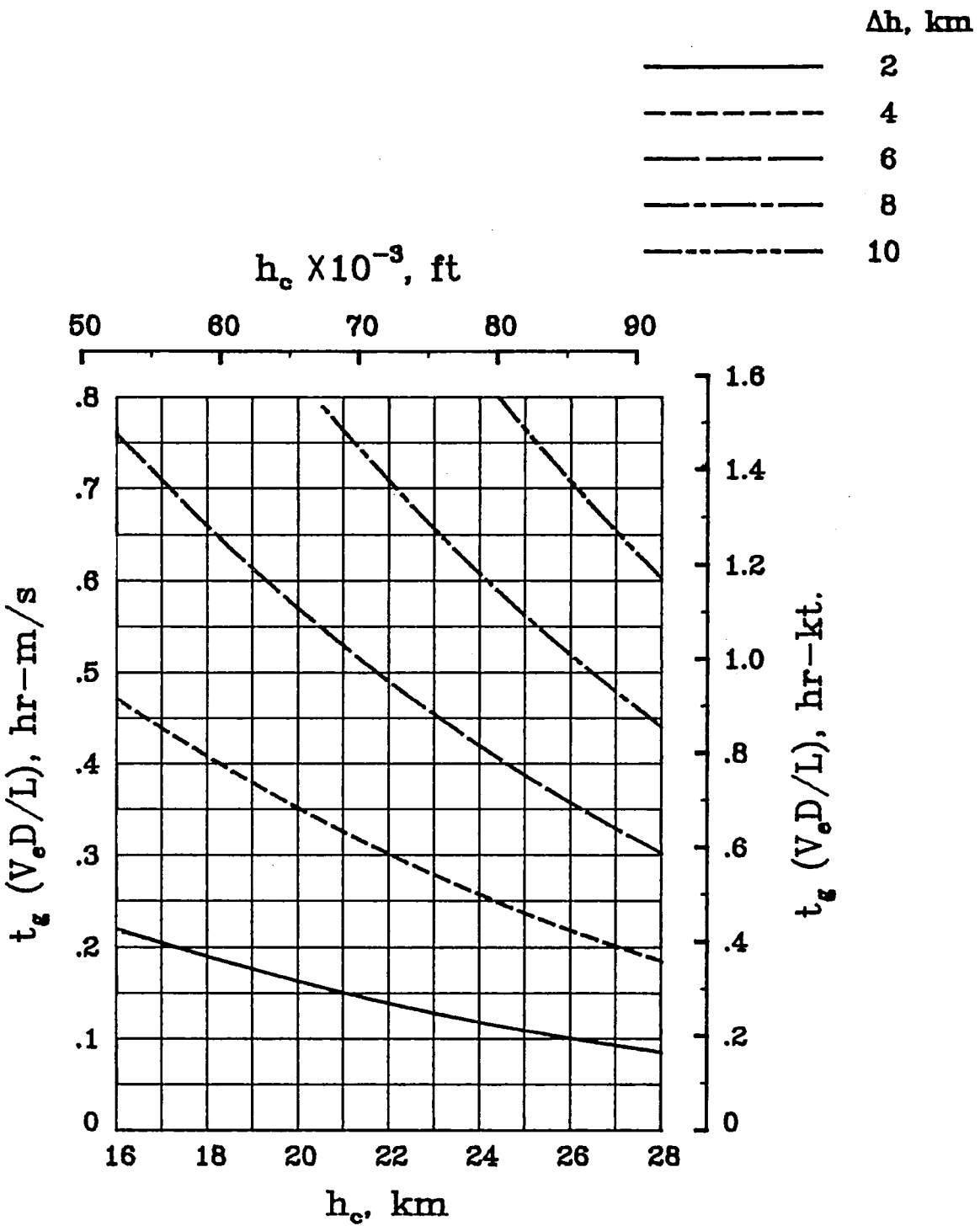

Figure 12. - Variation of glide-time parameter with initial altitude and altitude decrement.

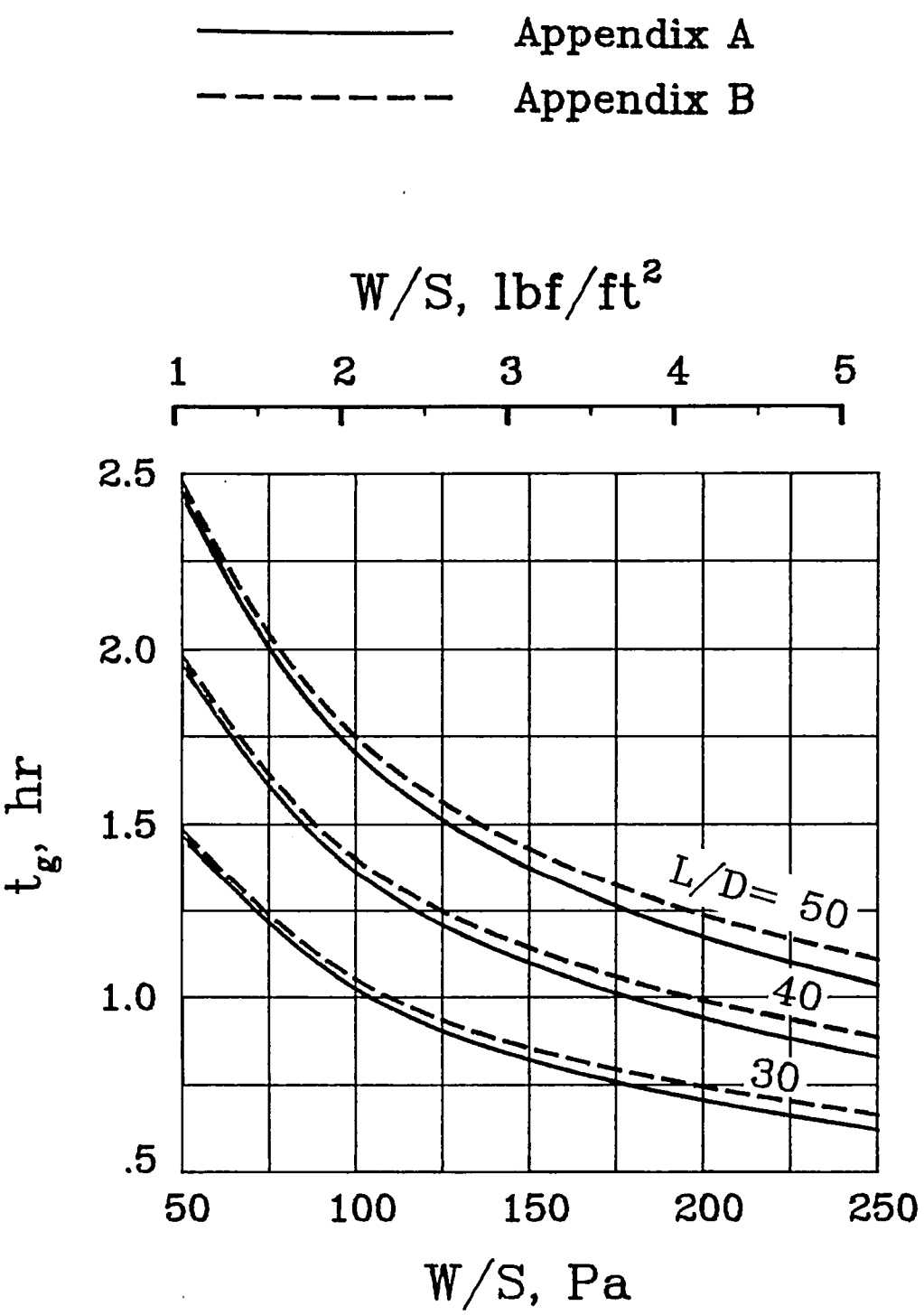

Figure 13. - Variation of time to glide from 25 to 18 km with wing loading and lift-to-drag ratio; CL = 0.9.

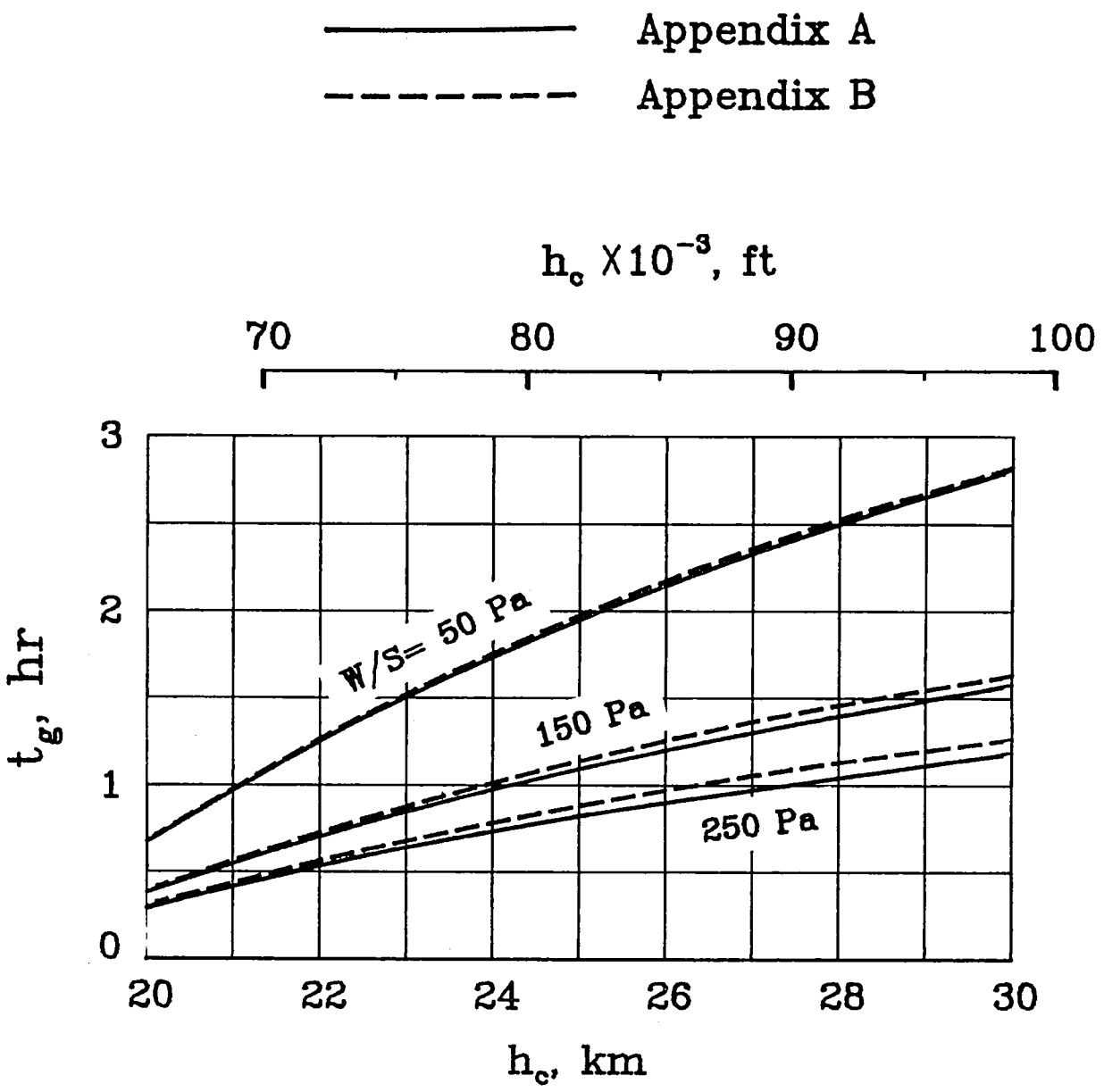

Figure 14. - Variation of glide time with altitude and wing loading; glide termination at 18 km; L/D = 40; CL = 0.9.

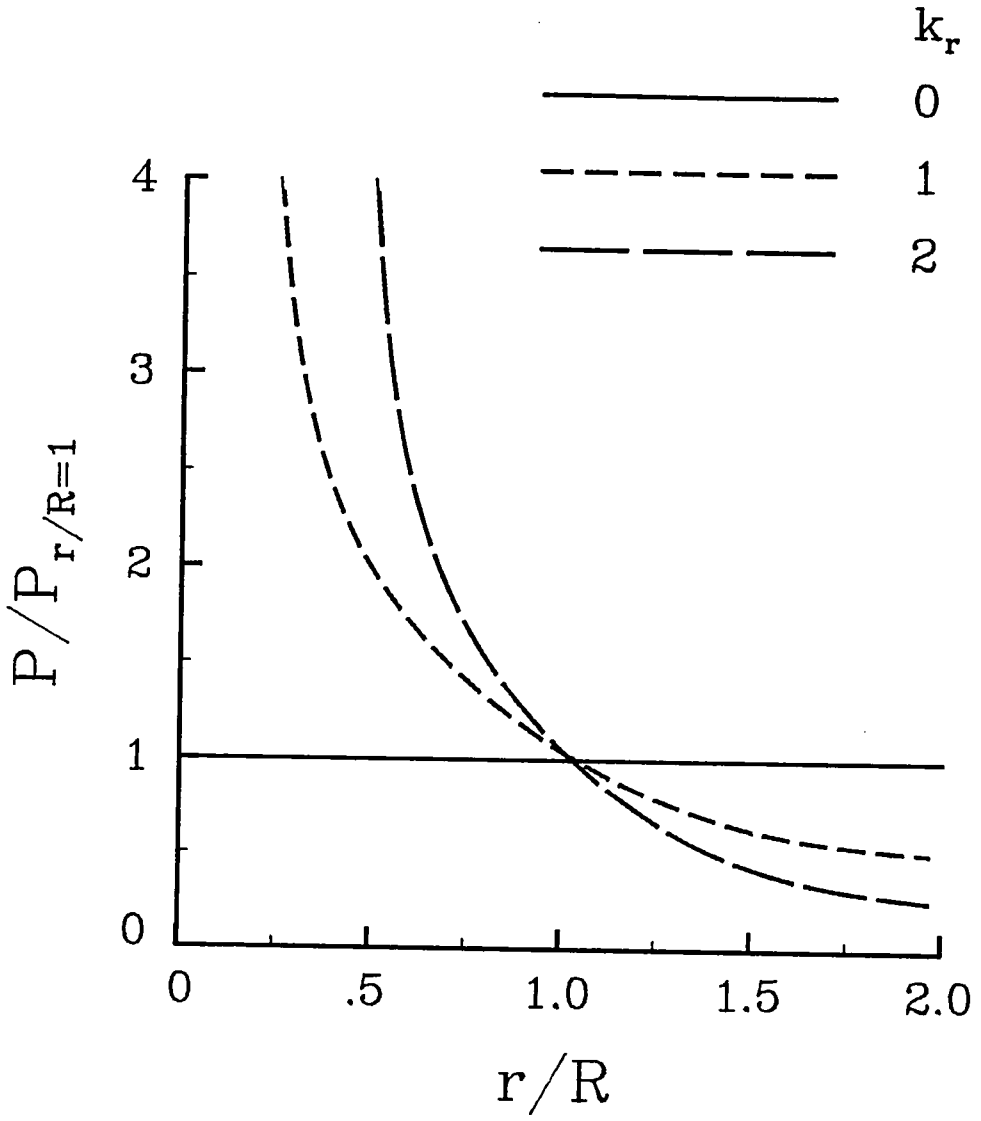

Figure 15. - Relative variation in microwave-beam intensity with range.

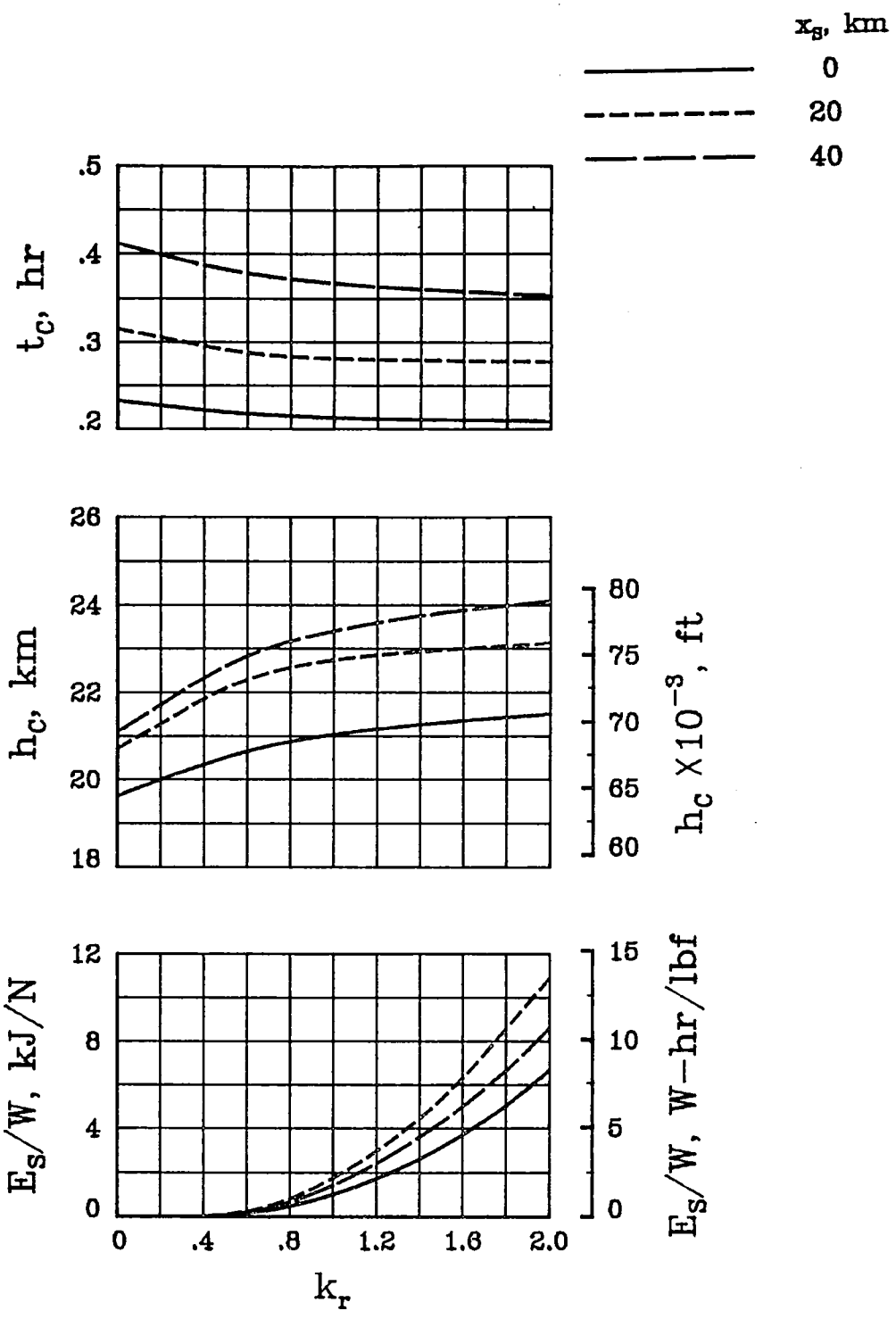

Figure 16. - Variation of baseline configuration performance with microwave-beam intensity factor k_r of equation 15.

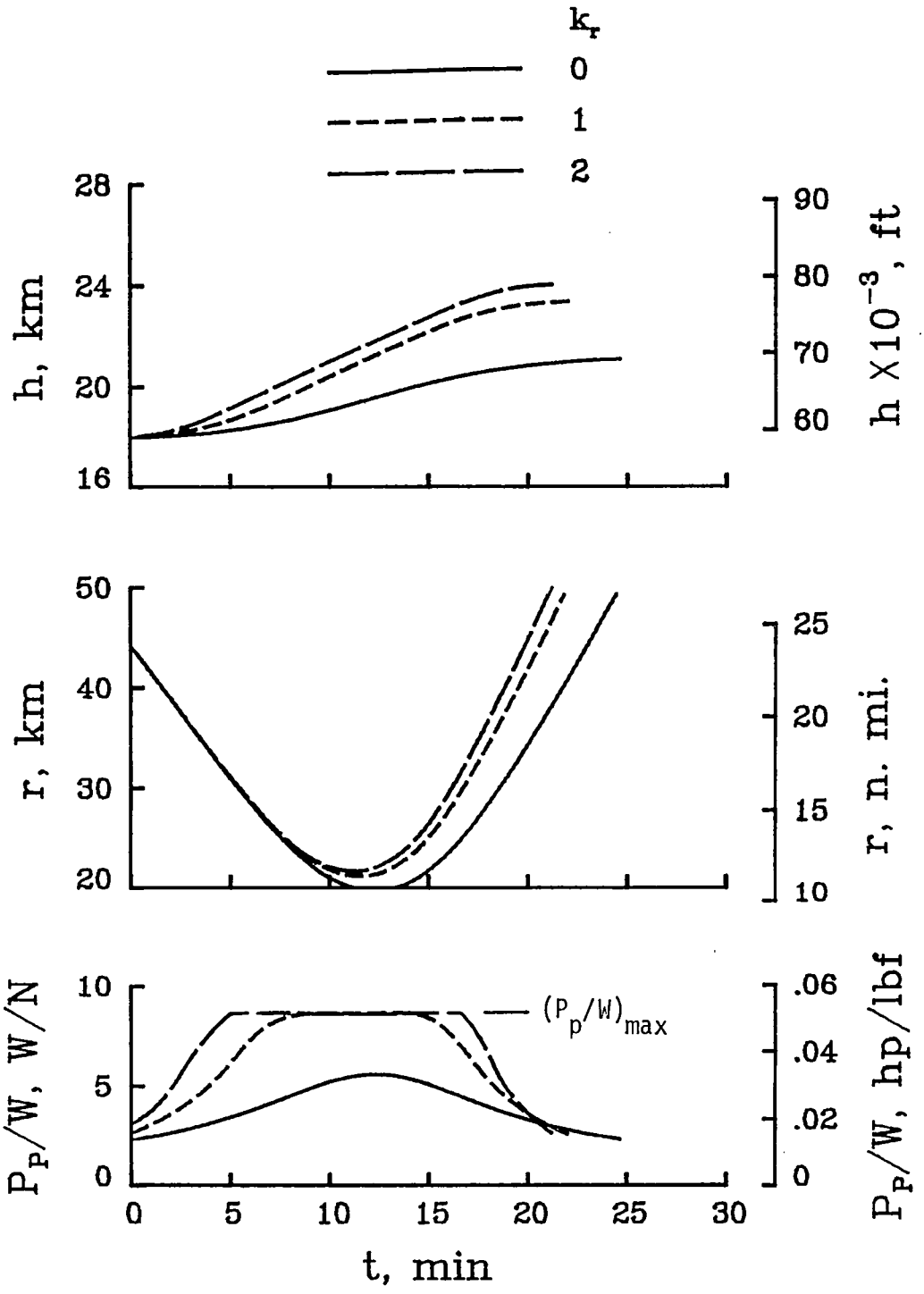

Figure 17. - Climb performance for three values of k_r; baseline configuration; x_s = 40 km.

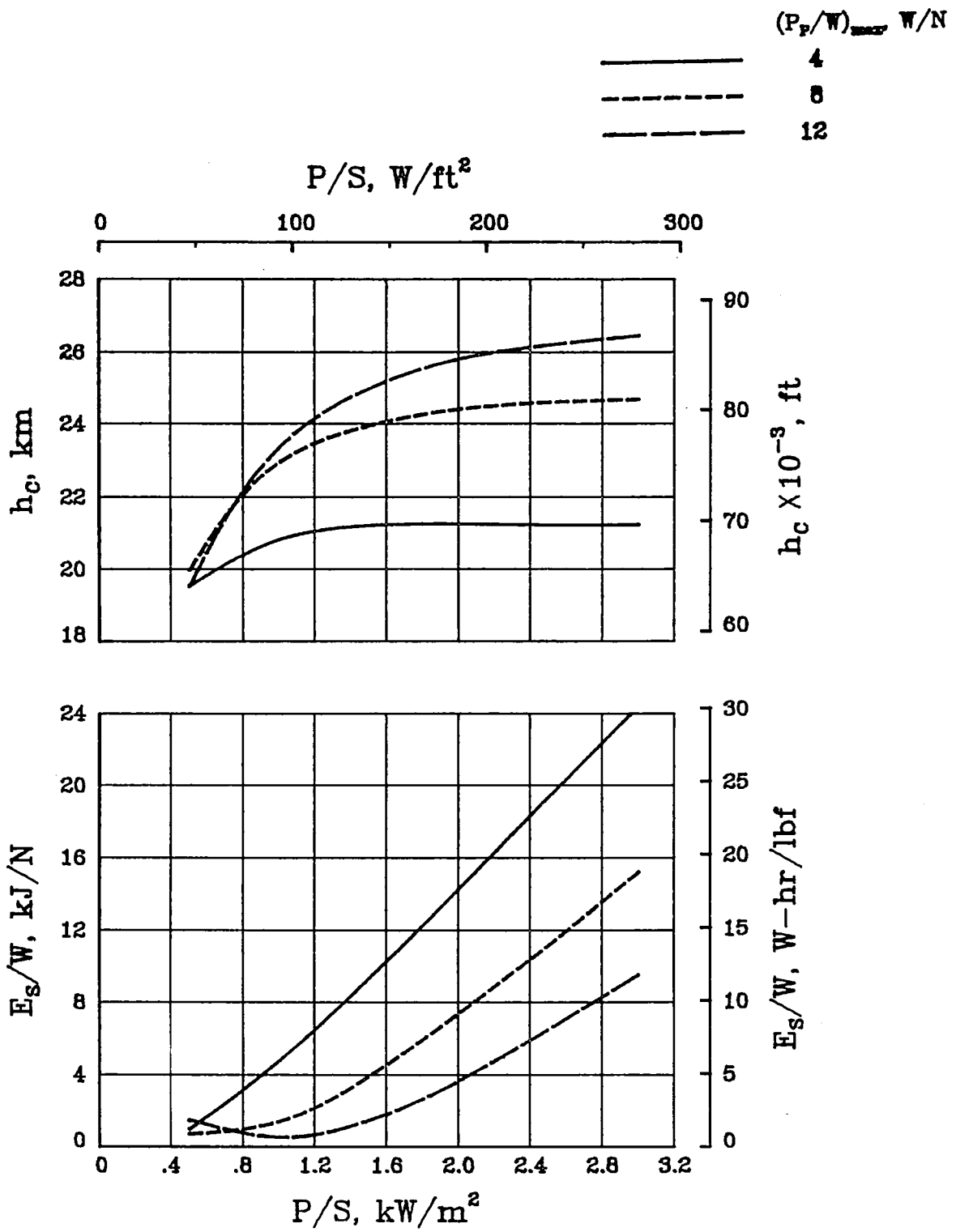

Figure 18. - Effect of beam intensity and motor size on climb performance.

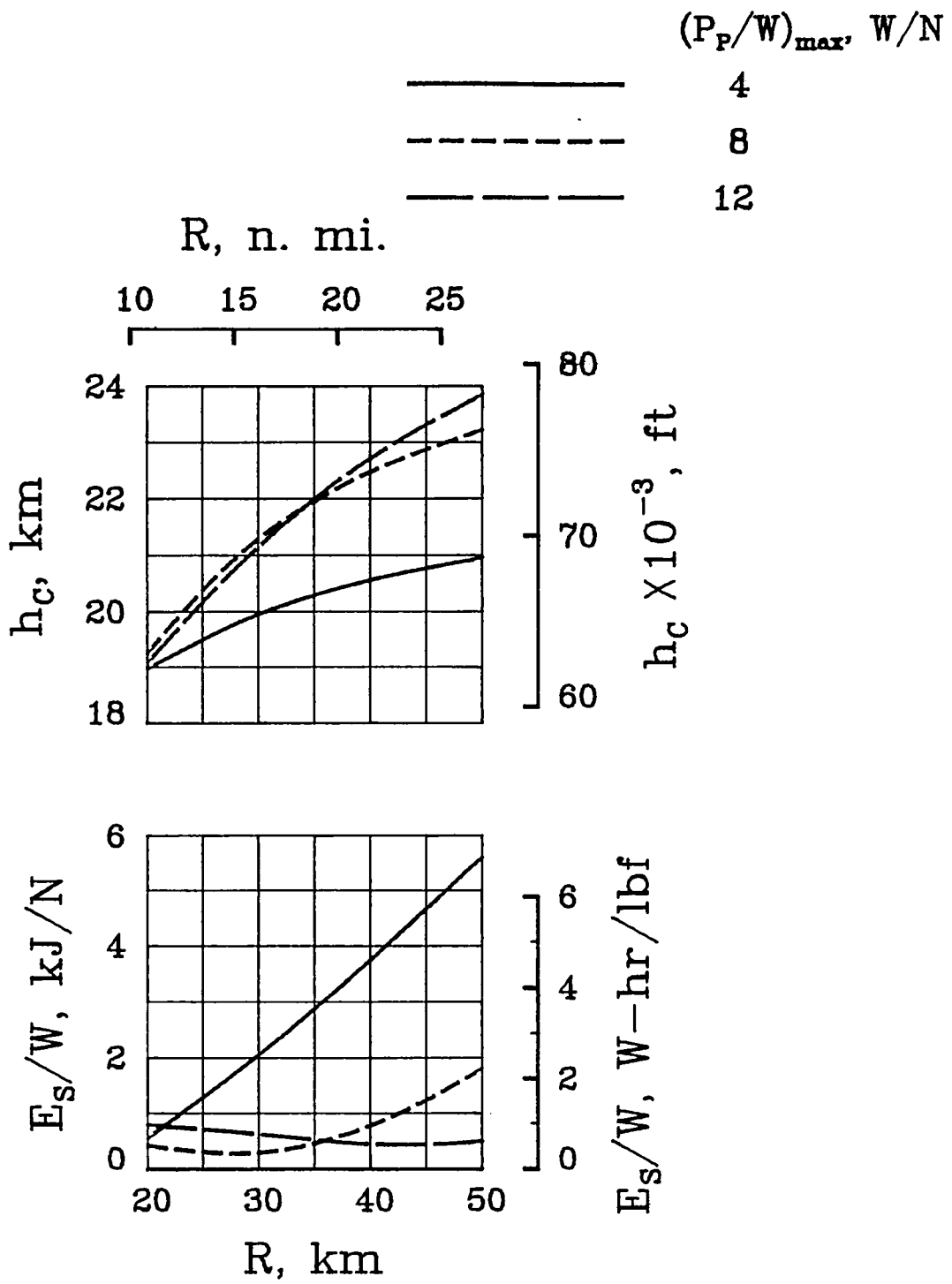

Figure 19. - Effect of variation in reference range and motor size.

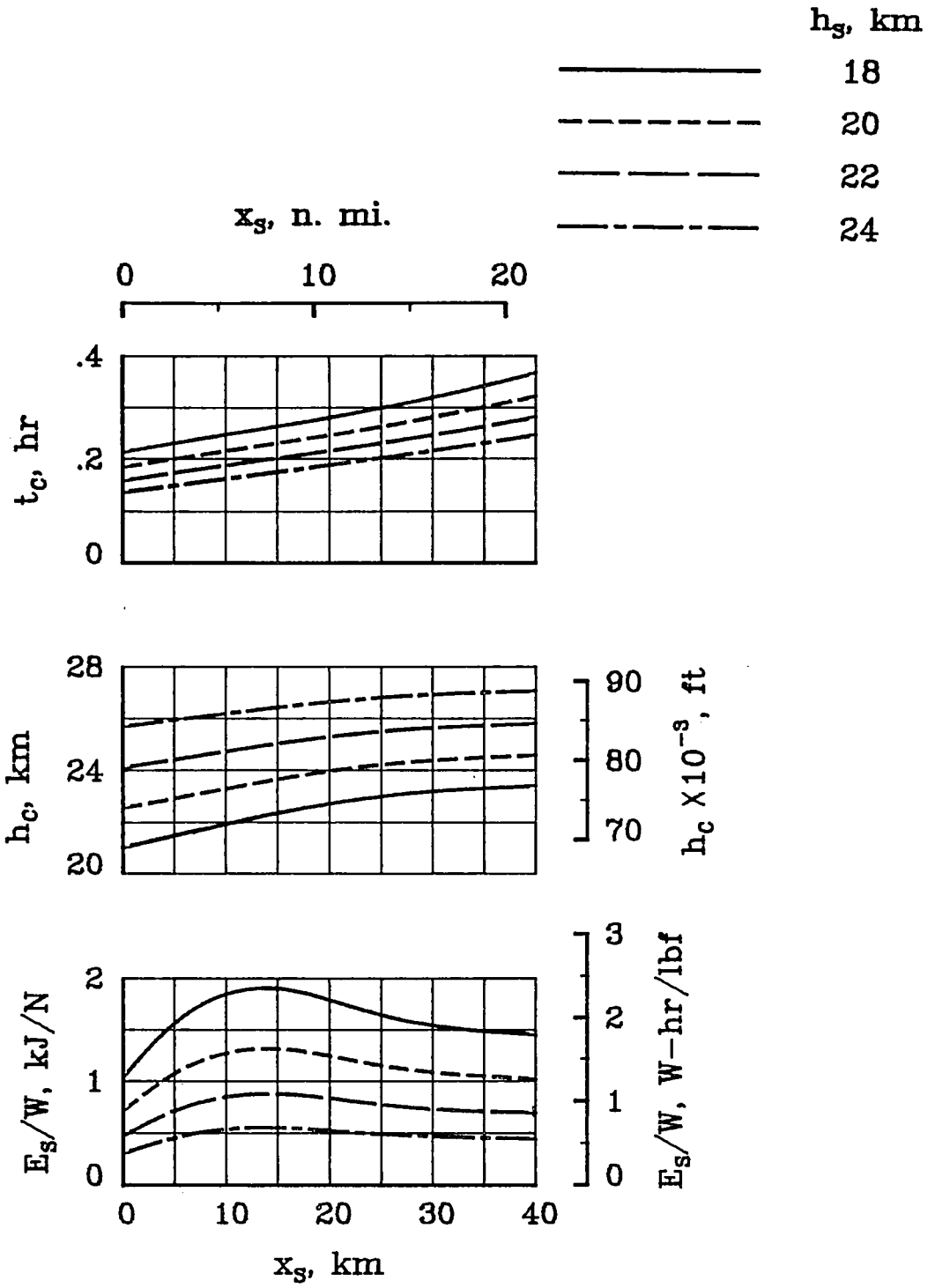

Figure 20. - Effect of initiating climb at different altitudes and horizontal ranges.

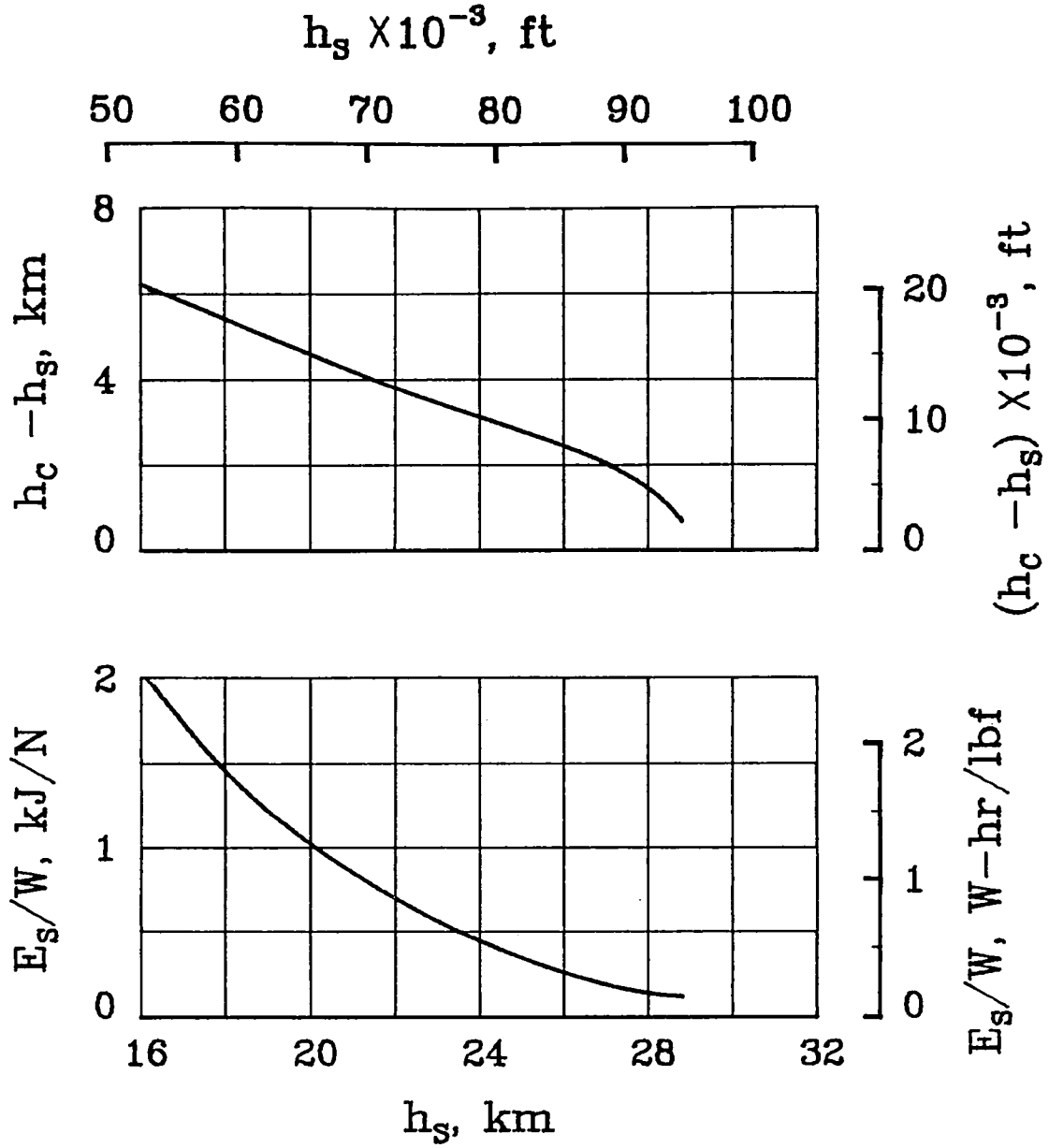

Figure 21. - Effect of variation in initial altitude on climb performance; x_c = 40 km.

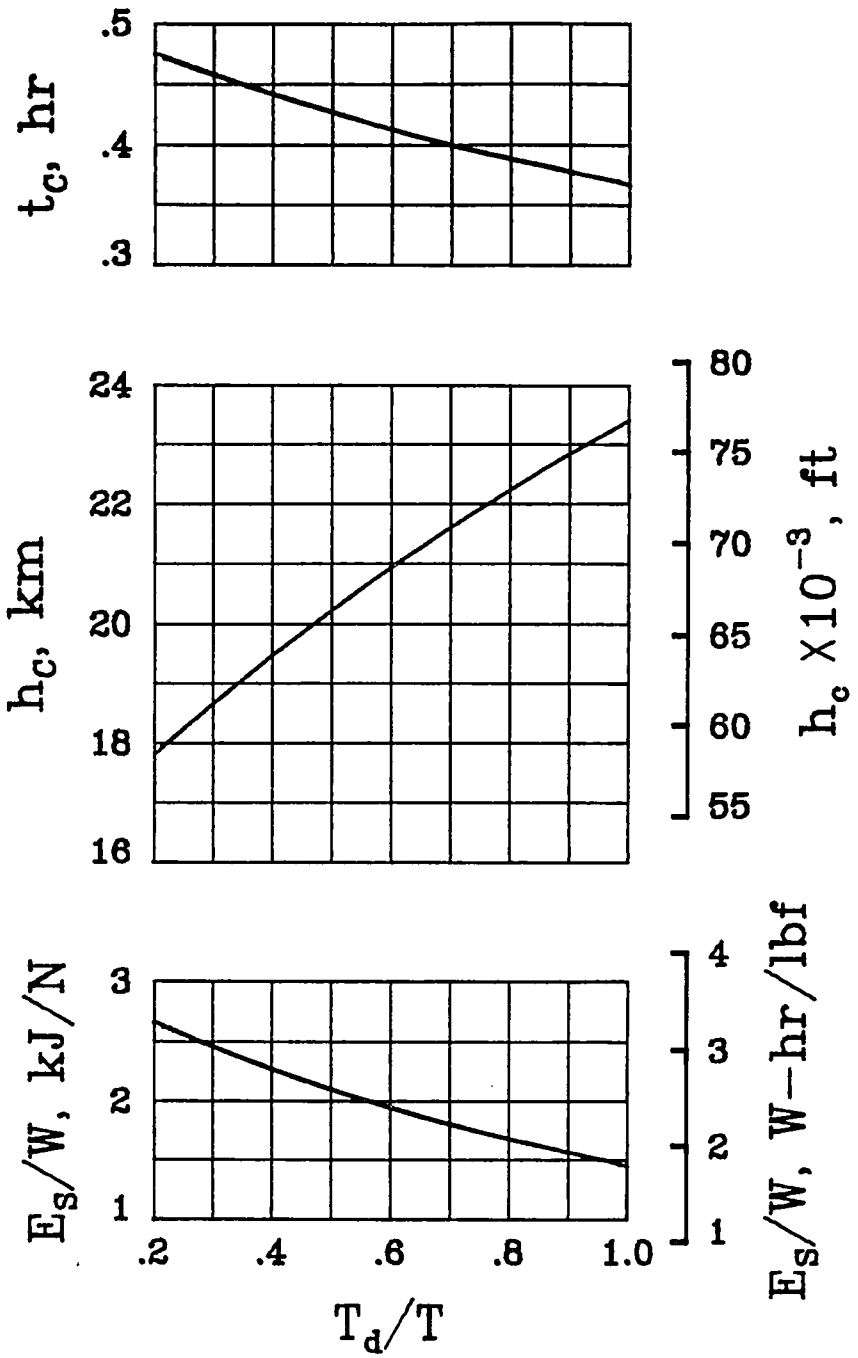

Figure 22. - Effect of propulsion degredation factor on climb performance.

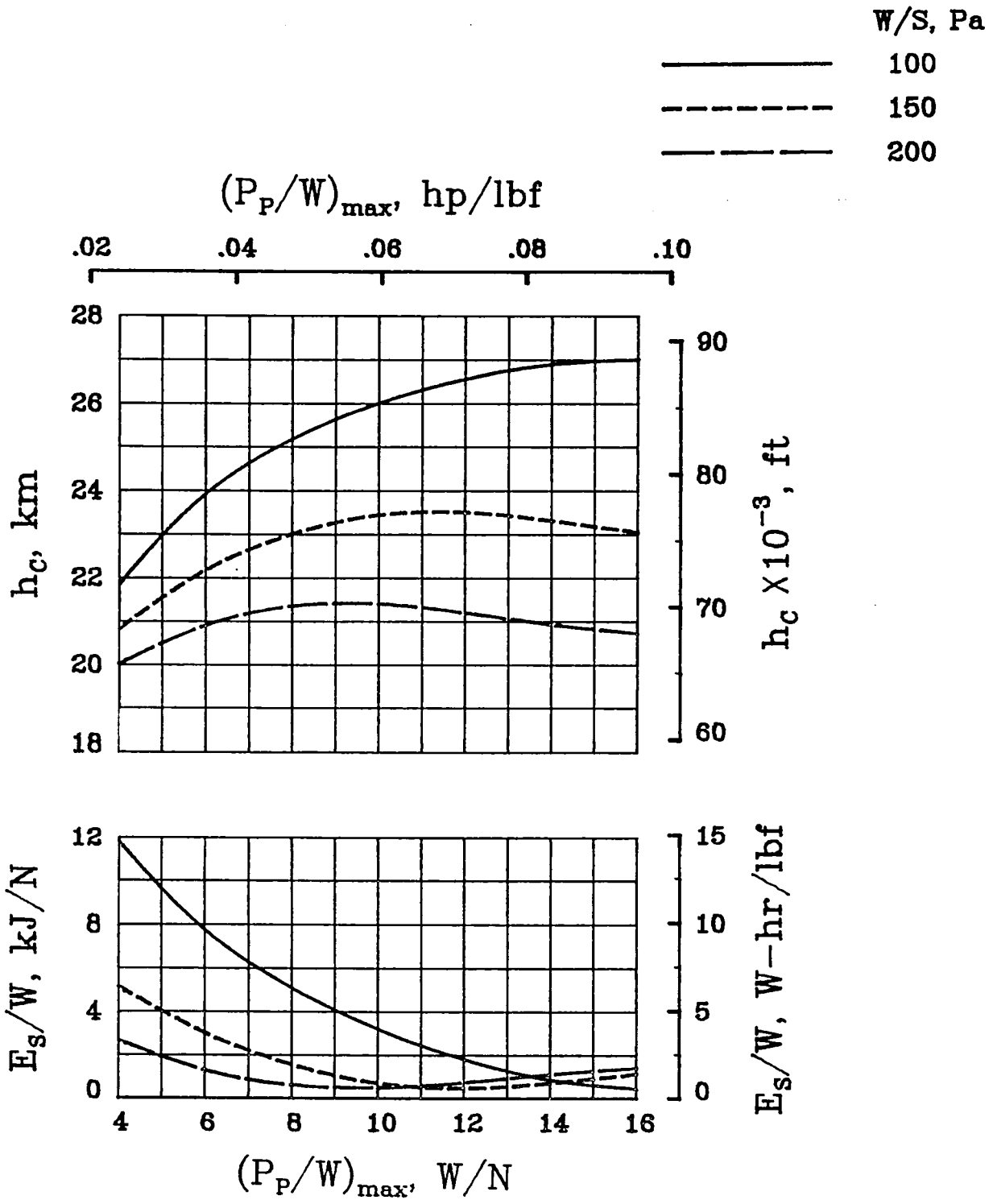

Figure 23. - Effect of motor size and wing loading on climb performance.

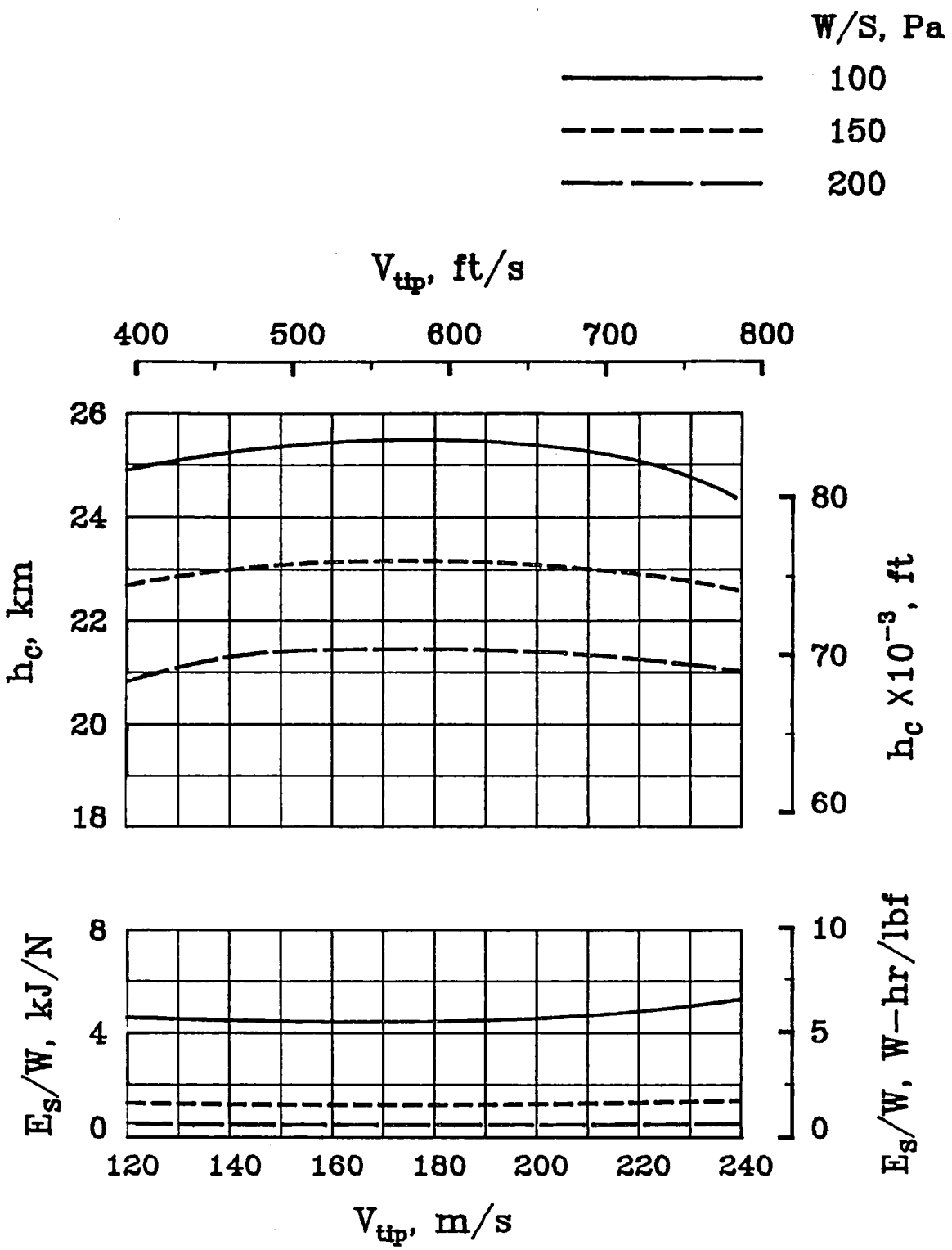

Figure 24. - Effect of propeller tip speed and wing loading on climb performance.

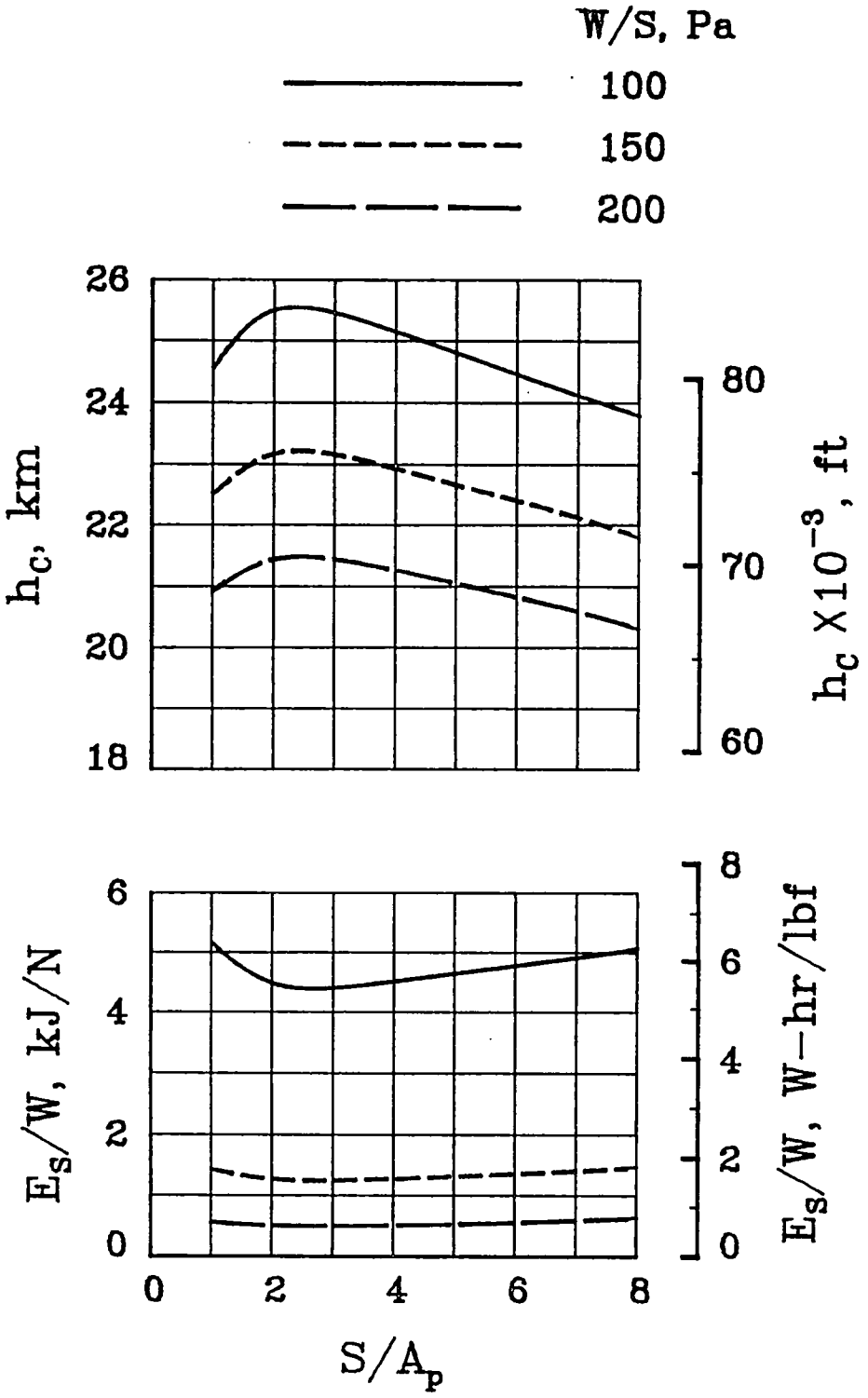

Figure 25. - Effect of propeller size and wing loading on climb performance. V_{tip} = 172 m/s.

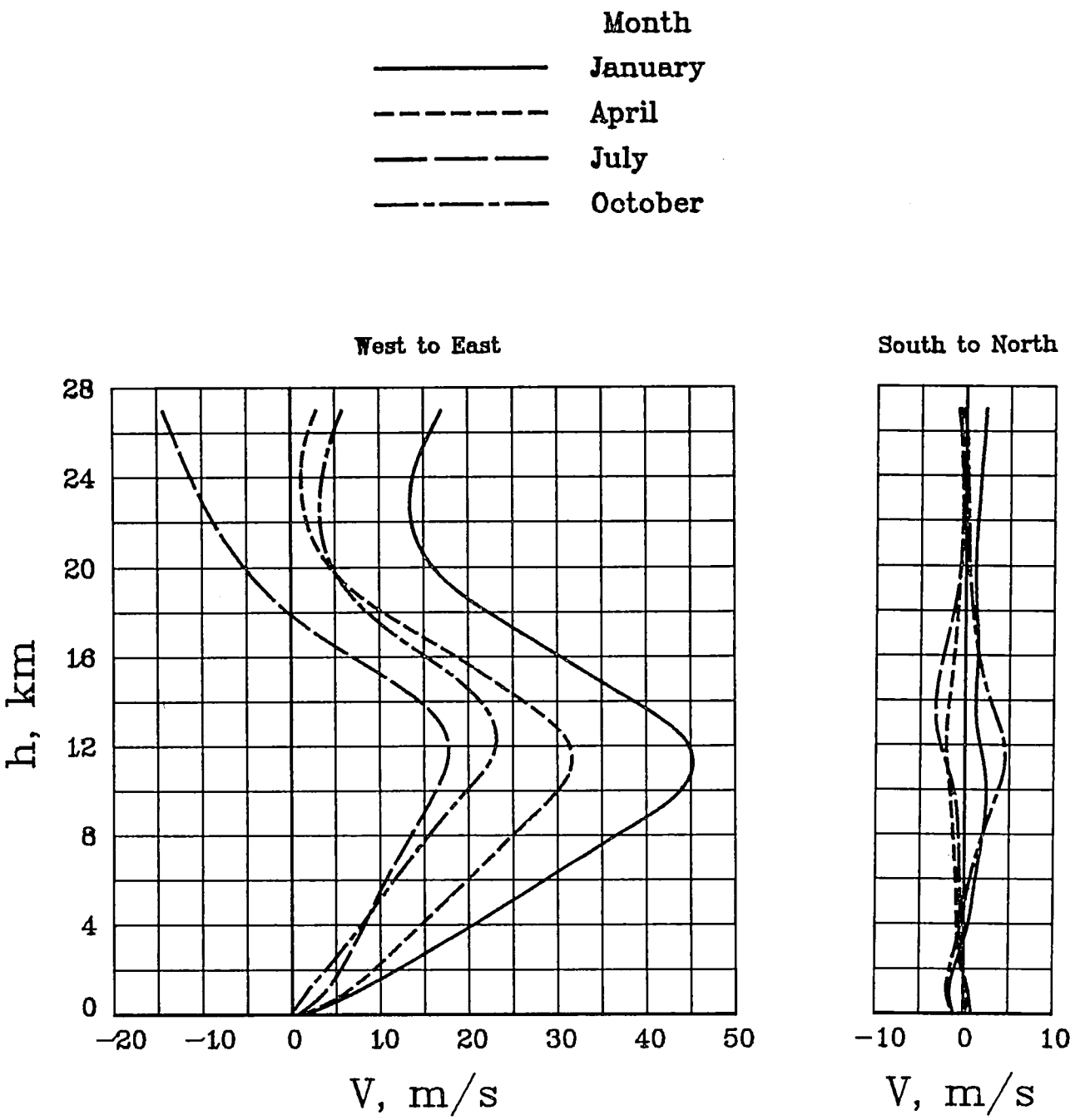

(a) Mean velocities

Figure 26. - Wind profile data (ref. 19).

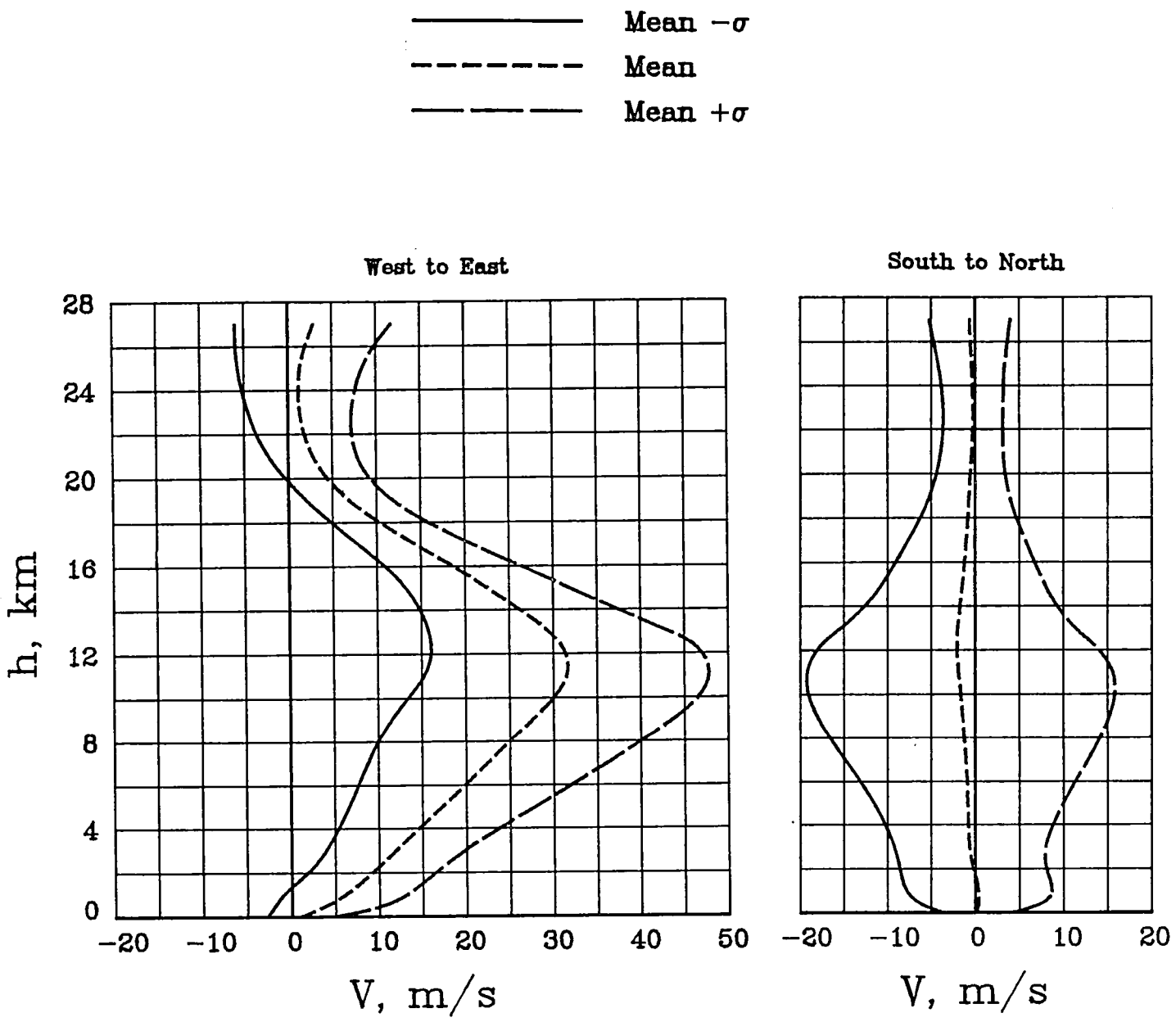

(b) Mean and standard deviation profiles for April.

Figure 26. - Concluded.

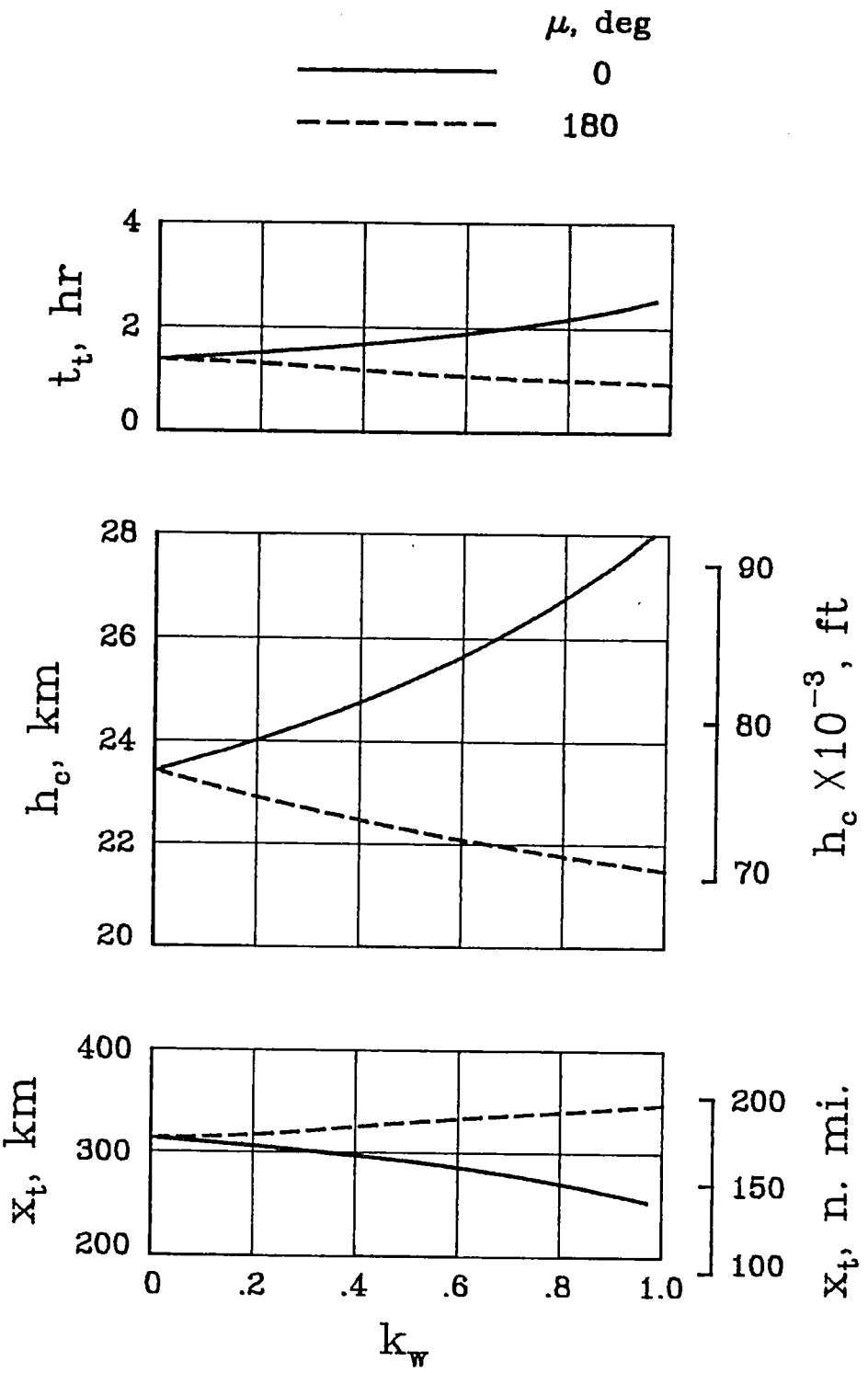

Figure 27. - Effect of headwinds and tailwinds on the performance of the baseline configuration.

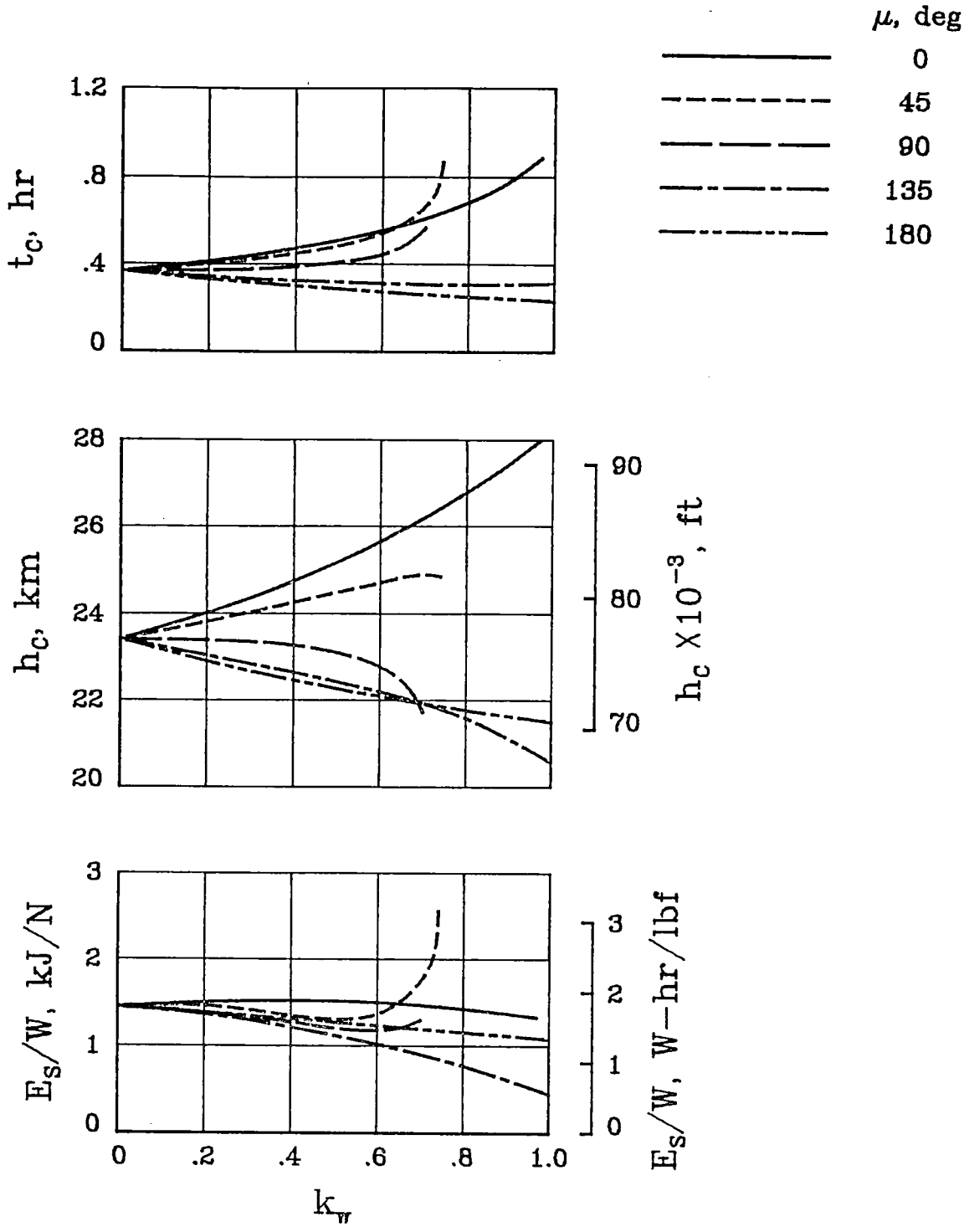

(a) Variation of wind-profile magnitude

Figure 28. - Effect of wind direction and profile amplitude on the performance of the baseline configuration.

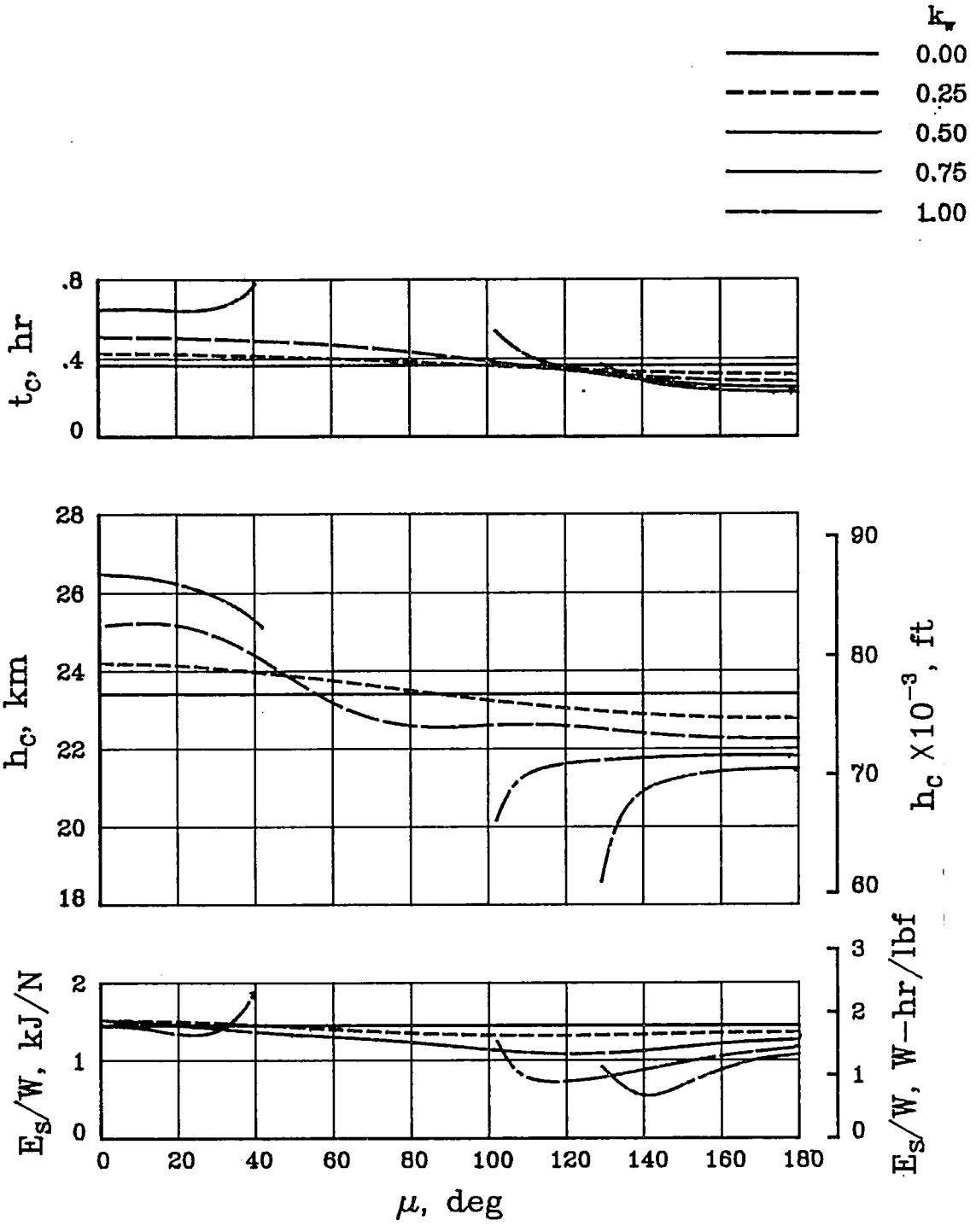

(b) Variation of wind direction.

Figure 28. - Concluded.

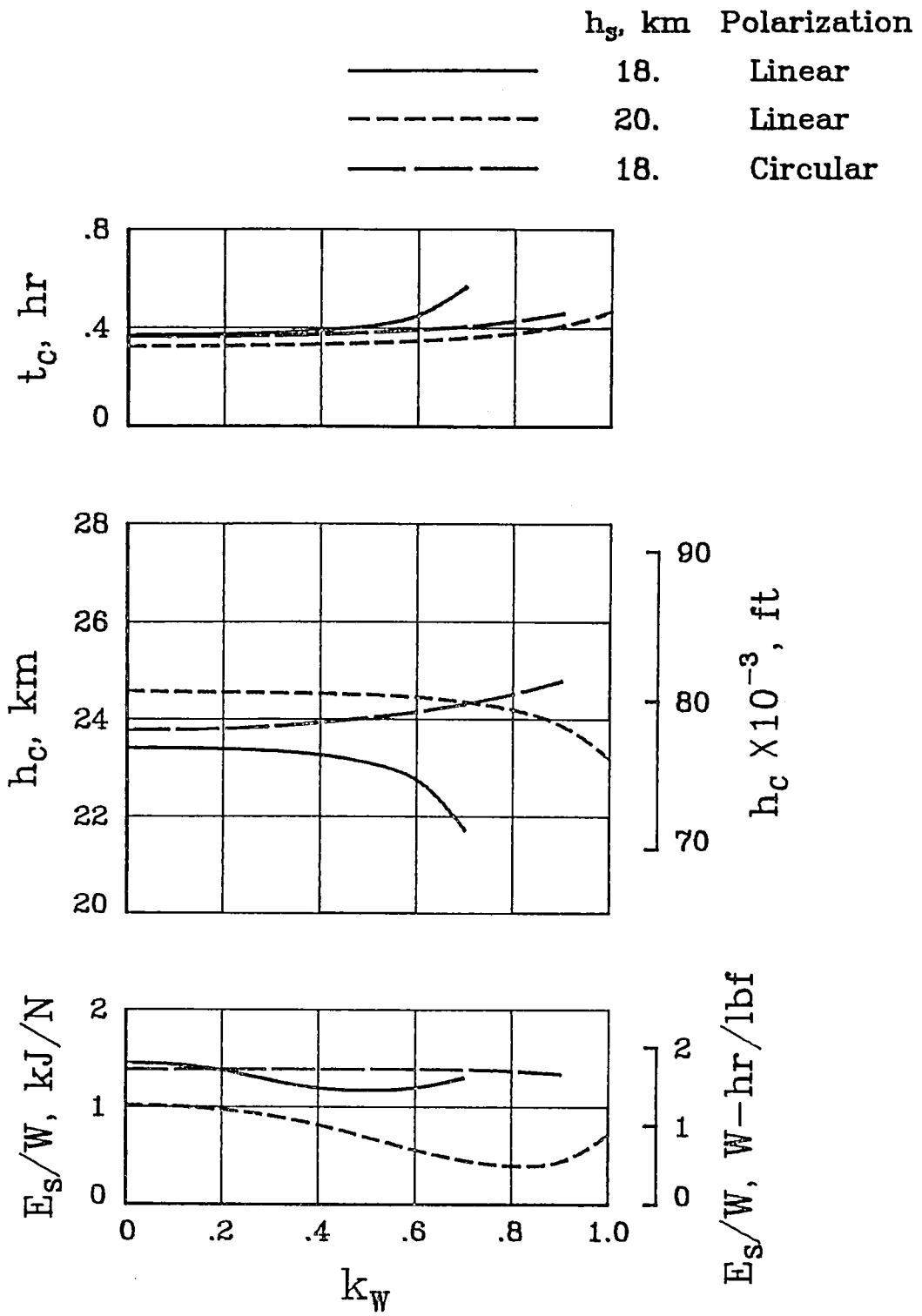

Figure 29. - Climb performance for $\mu = 90^0$ and P/S = 1.1 kW/N^2.

1. Report No.	2. Government Accession No.	3. Recipient's Catalog No.
NASA TM-81969		

4. Title and Subtitle	5. Report Date
ANALYTICAL STUDY OF THE CRUISE PERFORMANCE OF A CLASS OF REMOTELY PILOTED, MICROWAVE-POWERED, HIGH-ALTITUDE AIRPLANE PLATFORMS	April 1981
	6. Performing Organization Code 530-01-13-02
7. Author(s) Charles E. K. Morris, Jr.	8. Performing Organization Report No.
	10. Work Unit No.
9. Performing Organization Name and Address NASA Langley Research Center Hampton, VA 23665	11. Contract or Grant No.
	13. Type of Report and Period Covered Technical Memorandum
12. Sponsoring Agency Name and Address National Aeronautics and Space Administration Washington, DC 20546	14. Sponsoring Agency Code

15. Supplementary Notes

16. Abstract

The performance of a class of remotely-piloted, microwave-powered, high-altitude airplane platforms was studied. Each cycle of the flight profile consists of climb while the vehicle is tracked and powered by a microwave beam, followed by gliding flight back to a minimum altitude. Parameter variations were used to define the effects of changes in the characteristics of the airplane aerodynamics, the power-transmission systems, the propulsion system, and winds.

Results show that wind effects limit the reduction of wing loading and increase of lift coefficient, two effective ways to obtain longer range and endurance for each flight cycle. Calculated climb performance showed strong sensitivity to some power and propulsion parameters. A simplified method of computing gliding endurance was developed.

17. Key Words (Suggested by Author(s))	18. Distribution Statement
Microwave Power High-Altitude Observation Sailplanes	Unclassified - Unlimited Subject Category 05 - Aircraft Design, Testing, and Performance

19. Security Classif. (of this report)	20. Security Classif. (of this page)	21. No. of Pages	22. Price*
Unclassified	Unclassified	76	A05

For sale by the National Technical Information Service, Springfield, Virginia 22161